THE CHEMICAL EFFECTS OF NUCLEAR TRANSFORMATIONS IN SOME TELLURIUM COMPOUNDS

BY

JOHN LAWRENCE WARREN
B.Sc. University of Washington, 1966

A DISSERTATION SUBMITTED IN PARTIAL FULFILLMENT
OF THE REQUIREMENTS FOR THE DEGREE OF
DOCTOR OF PHILOSOPHY

in the Department
of
CHEMISTRY

SIMON FRASER UNIVERSITY

November, 1970

EXAMINING COMMITTEE APPROVAL

.....

Professor C.H.W. Jones
Department of Chemistry
Simon Fraser University
Research Supervisor

.....

Dr. G. Harbottle
Brookhaven National Laboratory
External Examiner

.....

Professor B.D. Pate
Department of Chemistry
Simon Fraser University
Examining Committee

.....

Professor L.K. Peterson
Department of Chemistry
Simon Fraser University
Examining Committee

.....

Professor D.J. Huntley
Department of Physics
Simon Fraser University
Examining Committee

Name: JOHN LAWRENCE WARREN

Degree: DOCTOR OF PHILOSOPHY

Title of Thesis: CHEMICAL EFFECTS OF NUCLEAR TRANSFORMATIONS IN SOME TELLURIUM COMPOUNDS

Date Approved: 20 November 1970

ABSTRACT

The chemical effects of several different nuclear transformations were studied in solid tellurium compounds using both standard radiochemical techniques and Mössbauer spectroscopy with ^{129}I.

In the radiochemical investigation, a comparative study was made in telluric acid, H_6TeO_6, of the molecular fragmentation accompanying the $^{130}Te(n,\gamma)^{131}Te \xrightarrow{\beta^-} {}^{131}I$ process and the β^--decay of ^{131m}Te, ^{131}Te, and ^{132}Te. The chemistry of ^{129}Te recoil atoms formed in the $^{128}Te(n,\gamma)^{129}Te$ nuclear reaction and the decay of ^{129m}Te in telluric acid were also investigated. In each instance the thermal annealing reactions of the recoil fragments in the solid were investigated. The study of the radioactive decay of ^{131m}Te-, ^{131}Te-, ^{132}Te-, and ^{129m}Te-labelled samples was of particular importance. These isotopes differ in the degrees of electronic excitation and ionisation accompanying their decay. Thus it was of interest to see if such differences would lead to different patterns of molecular fragmentation or to differences in the subsequent annealing reactions of the recoil fragments. It was found that the ^{131}I and ^{132}I recoil atoms formed in the decay of the first three isotopes were present in the same chemical forms (I^-, IO_3^-, and IO_4^-) but in differing yields. Differences were also observed in

the thermal annealing reactions in these samples, which may be interpreted in terms of the different processes accompanying the decays. It was found that the ^{129}Te atoms born in the isomeric transition decay of ^{129m}Te are similar in their annealing behaviour to the ^{132}I atoms born in the decay of ^{132}Te. Both of these decay processes are accompanied by large degrees of internal conversion of γ-transitions, which leads to qualitatively similar annealing reactions of the daughter recoil atoms. The trends observed in the recoil product distributions and the annealing reactions are discussed in terms of the difference in the nuclear transformations producing the recoil atoms.

The Mössbauer experiments allowed the study of the recoil atoms in situ in the solid and thus provided a much more detailed picture of the chemical effects of the nuclear transformations. The chemical effects of the decay of $^{129}Te \xrightarrow{\beta^-} {}^{129}I$ were studied in telluric acid, $(H_2TeO_4)_n$, α-TeO_3, tetragonal TeO_2, and H_2TeO_3 using the 27.7 keV, 16.8 nanosecond Mössbauer transition in ^{129}I to provide information about the chemical form of the iodine atom produced. These experiments were performed with a standard $Na^{129}I$ absorber and with the source and absorber at liquid nitrogen or liquid helium temperatures. No chemical effects of the β^--decay were observed in any of the above compounds, the iodine atom remaining bonded to the ligands of the precursor tellurium

molecules. These results are in sharp contrast to the findings of the radiochemical experiments.

Studies were made of the $^{129m}Te \rightarrow {}^{129}Te$ isomeric transition in ^{129m}Te-labelled compounds using the ^{129}I Mössbauer spectrum to provide information about the chemical form of the ^{129}Te atoms formed in the decay. Molecular fragmentation was observed to accompany the decay in a considerable fraction of events in H_6TeO_6 and $(H_2TeO_4)_n$ with the formation of the TeO_3^{2-} ion as the sole decomposition product. The $^{128}Te(n,\gamma)^{129}Te$ nuclear reaction was found to produce the same decomposition in H_6TeO_6. The thermal annealing reactions of the isomeric transition and (n,γ) recoil atoms were also studied and found to lead to a simple, single-step reaction, $TeO_3^{2-} \rightarrow Te(VI)$.

In addition to the above, the Mössbauer work provided several pieces of information concerning bonding and structure in these tellurium compounds and allowed the determination of several constants of general interest in ^{125}Te and ^{129}I Mössbauer studies.

The results of the Mössbauer work are compared and contrasted with those of the radiochemical study.

TABLE OF CONTENTS

CHAPTER PAGE

CHAPTER PAGE

CHAPTER PAGE

CHAPTER PAGE

CHAPTER PAGE

LIST OF TABLES

LIST OF FIGURES

FIGURE PAGE

FIGURE PAGE

ACKNOWLEDGEMENTS

The author wishes to express his most sincere gratitude to Professor C.H.W. Jones for his continued guidance, advice, criticism and encouragement throughout the course of this work.

Sincere thanks are also due to:

Dr. F. Brown at Atomic Energy of Canada, Limited, for his assistance in performing many of the reactor irradiations involved in this work;

Professor A.L. Babb and the staff at the reactor at the University of Washington, Seattle, for their kind assistance in providing laboratory facilities and performing several reactor irradiations;

Dr. A.J. Stone of the University of Cambridge, England, for kindly providing a copy of his Mössbauer computer program;

Dr. P. Vasudev for his assistance in writing and adapting many of the computer programs used in this work;

The Faculty, Staff, and Graduate Students of the Department of Chemistry, and especially the residents of the "Nuclear Suite," for their assistance and friendship;

Mr. T. Bennett for drafting several of the diagrams in this thesis;

Mrs. M. Ellis for her excellent typing of this thesis;

The National Research Council of Canada and the Department of Chemistry for their continuous financial support.

And; my parents, Mr. and Mrs. V.S. Warren, brother Steve and sister Patty, a circle of friends, especially Mr. and Mrs. J.R. McGuinness and Mr. and Mrs. Douglas E. Stillman, who have given a constant supply of encouragement and moral support.

Finally, to my wife Rosana, and our two children, a special note of thanks for all their love and devotion, without whom this work would not have been possible.

I. INTRODUCTION

When an atom which is chemically bound in a molecule undergoes a nuclear transformation, the daughter atom may be observed to have broken some or all of its original chemical bonds. This may occur as a result of several different processes accompanying the nuclear reaction or radioactive decay event. Thus, the emission by the nucleus of a heavy particle, such as an α-particle, or a high energy γ-photon will impart a high recoil kinetic energy to the daughter nucleus as a consequence of momentum conservation. Alternatively, molecular disruption may occur because of electronic excitation and ionisation produced by the nuclear transformation. The latter processes are observed following internal conversion of low-energy γ-quanta, following radioactive decay by electron capture, and, in a small fraction of events, following the β-decay process.

Extensive studies of the chemical effects accompanying nuclear reactions and radioactive decay in solid inorganic compounds have been made in the past[1-8]. The objective of such work has been to clearly define the physical and chemical processes which occur during and following the different transformations in a solid lattice. Generally such studies have been carried out in the following way. A nuclear reaction or radioactive decay is chosen

for which the daughter nucleus is itself radioactive. Following the nuclear transformation the solid is then dissolved in an appropriate solvent, in the presence of carriers for the chemical products suspected to be present, and a chemical separation and radioassay performed. In this way the different radioactively labelled chemical products formed in the solid following the nuclear process may be identified.

If the solid is heated before dissolution, it is generally found that the subsequently observed recoil product distribution has changed markedly, due to the occurrence of solid state chemical reactions involving the recoil products. Studies of these so-called thermal annealing reactions in different solids have pre-occupied many investigators since their discovery by Green and Maddock in 1949.[9] One of the principle objectives of such investigations has been to acquire information about the nature of the chemical environment in which the recoil fragments find themselves in the lattice. By studying the chemical reactions of the recoil atoms in the solid it might be hoped to learn more about the surrounding molecular debris formed in the preceding nuclear transformation. However, the mechanisms of these annealing reactions have been found in many instances to be extremely complex and to reflect properties of the solid other than the local lattice environment of the recoil atom.

A further draw-back of considerable significance to the above type of study is that when the solid is dissolved in the solvent prior to the analysis, chemical reactions may occur during and following dissolution. The final radioactively labelled products observed may not then be the same as those initially present in the solid. While this consideration does not destroy the usefulness of the radiochemical technique for making relative measurements, it obviously raises some questions as to the precise meaning of the results obtained in such investigations.

It would therefore be a considerable advantage to be able to directly identify the chemical form of the recoil atom in situ in the solid. The number of recoil atoms produced in a nuclear reaction or radioactive decay is generally so small as to preclude their study in the solid by most spectroscopic techniques. In recent years, however, such studies have been made possible by advances in electron spin resonance spectroscopy, and by the application of perturbed angular correlation measurements and Mössbauer spectroscopy. Of these three techniques, Mössbauer spectroscopy appears to be the most promising. While it limits the study to certain specific nuclei, nevertheless, in those instances it provides a very powerful tool.

In using Mössbauer spectroscopy in this specific application, a nuclear reaction or radioactive decay is chosen which produces the parent Mössbauer nucleus, or which

directly populates the Mössbauer state of interest. The Mössbauer transition then reflects the chemical effects of the preceding nuclear transformation, since it yields information about the chemical bonding of the atom containing the Mössbauer nucleus.

In the work of this thesis, both the radiochemical and Mössbauer techniques have been used to study tellurium and iodine recoil atoms in solid telluric acid, H_6TeO_6, and several related tellurium oxy-compounds. In the radiochemical study, a detailed comparison of the chemical effects accompanying the (n,γ) reaction, internal conversion, and β^--decay was made, and the thermal annealing reactions of the recoil products observed in each instance compared. Of particular importance in this work was the study of the ^{131}I and ^{132}I recoil atoms formed in the decay of ^{131}Te-, ^{131m}Te-, and ^{132}Te- labelled telluric acid. The decay of each of these isotopes differs in the degree of internal conversion of γ-transitions accompanying the β^--decays, and it was of interest to see if these well-defined differences would lead to different recoil product distributions or differences in the observed thermal annealing reactions. Such a comparative study of the chemical effects of several well-characterised radioactive decay events in the same solid matrix has not previously been reported.

In the Mössbauer work the 27.7 keV, 16.8 nanosecond γ-transition in ^{129}I was used as the probe to investigate

similar nuclear transformations to those studied by radiochemical methods. It was not possible to investigate precisely the same transformations in all instances, however the Mössbauer studies did allow a meaningful comparison with the results of the radiochemical work. The distinct advantages of being able to identify the recoil products directly in the solid by the Mössbauer technique are clearly illustrated in this work. The similarities and differences of the results obtained using the two experimental techniques are discussed toward the end of the thesis.

In order to ensure clarity of presentation, the radiochemical and Mössbauer techniques are treated separately in the introductory review, and in the sections on experimental, results, and discussion.

II. A REVIEW OF THE CHEMICAL EFFECTS ASSOCIATED WITH NUCLEAR TRANSFORMATIONS

A. Sources of Recoil Kinetic Energy and Electronic Charge In Nuclear Transformation Processes

1. Thermal Neutron Capture

In studying the chemical effects of nuclear transformations, the (n,γ) reaction has been the most extensively investigated of all nuclear transformation processes. When an atom undergoes thermal neutron capture, 5-10 MeV in nuclear binding energy is liberated in the form of a complex γ-ray cascade. In most cases several cascades of γ-rays are emitted and the capture γ-ray spectrum is often very complicated. Comprehensive descriptions and listings of capture γ-ray spectra have recently been published by Groshev *et al.*[10]

From the laws of conservation of momentum, an atom emitting a single γ-photon acquires a recoil kinetic energy, E_R, given by the expressions

$$E_R = 1/2\ MV_R^2 = \frac{E_\gamma^2}{2Mc^2} = \frac{536\ E_\gamma^2}{A}\ eV \qquad (I\text{-}1)$$

where E_γ is the energy of the emitted γ-quantum in MeV, and A is the mass number of the emitting nucleus. Where a large number of γ-quanta are emitted, however, vector cancellation

of recoil momenta must be considered, and several theoretical treatments of this problem have appeared in the literature.[11-13] Assuming that the de-excitation of the excited nucleus formed following thermal neutron capture occurs in a time less than ca.10^{-14} second,[14-16] the problem reduces to one of simple vector summation of the many individual recoil events, since chemical bond rupture occurs in times of ca.10^{-12} second. The results of such calculations show that, even allowing for reduction of the recoil momentum because of such self-cancellation effects, the net recoil momentum acquired by the daughter nucleus will exceed chemical bond energies in almost all events.[12,17,18] For example, Cifka[17] has shown that for ^{32}P atoms recoiling from the ^{31}P (n,γ) ^{32}P nuclear reaction (assuming a random distribution of the many γ-quanta emitted), the spectrum of recoil kinetic energies acquired by the ^{32}P recoil atoms extends up to nearly 1000 eV, with only about 1 per cent of the recoil atoms having a recoil energy less than 50 eV. In comparison, chemical bond energies are of the order of 5-10 eV.

A further point of some importance concerning the (n,γ) reaction is the possible existence of long-lived states, having lifetimes of nanoseconds or longer, in the de-exciting γ-ray cascade. Internal conversion of the γ-transitions from these states may lead to extensive electronic excitation and ionisation of the recoiling atom. Internal conversion of low-lying transitions accompanying the (n,γ) reaction

has been directly observed for isotopes of Br,[19] I,[19] Mn,[20] Dy,[20] In,[20,21] and Au[21]. The importance of the timing of the nuclear events occurring in these instances may be understood if a qualitative picture of the recoil event is examined.

Following thermal neutron capture, the prompt emission of many γ-quanta, in a time less than 10^{-14} second, carries off most of the energy of the excited nucleus and the daughter atom may acquire a high recoil kinetic energy. The recoiling atom may break its chemical bonds in the parent molecule, and, considering atoms bound in the solid state, will come to rest in the solid in a time less than ca.10^{-12} second.[22-25] If long-lived excited states of the daughter nucleus exist, then long after the recoiling atom has stopped, considerable electronic excitation and ionisation may occur as a result of internal conversion. This process may significantly influence the chemical form in which the recoil atom is finally stabilised.

A more detailed description of the effects of electronic excitation and ionisation will now be discussed with specific reference to the isomeric transition decay process.

2. Isomeric Transition

Isomeric transition refers to the process in which a nucleus in a metastable excited state makes a transition, generally by emission of a gamma ray or ejection of an orbital electron (internal conversion), to a state of lower energy, often the ground state of the nucleus. Lifetimes for such metastable nuclear states range from ca. 0.1 second to several hundred years.

Where the energy of an emitted γ-quantum in an isomeric transition decay process is very small, chemical effects due to the physical recoil of the atom may be neglected. However, where the isomeric transition is highly internally converted, considerable excitation and ionisation will result from the so-called Auger charging process. This may then result in significant chemical effects accompanying the decay.

The basic theory of Auger charging has been treated by several groups.[26-28] A nucleus may, as an alternative process to γ-ray emission, de-excite with the ejection of an inner-shell atomic electron (usually a K- or L- shell electron), the kinetic energy of which will equal the nuclear transition energy minus the binding energy of the ejected electron. This process leaves an inner-shell hole or vacancy in the atom which is very unstable, and an electron from an outer shell immediately drops into the hole. The difference in binding energy of the electron in the two

shells is either emitted as an x-ray or is given to a second outer-shell electron which is then also ejected from the atom. This latter process is called the Auger process and leads to a multiplication of the number of holes as the initial hole moves out to the periphery of the atom. The end result is the creation of a very high charge on the atom in a time of ca.10^{-14} second following the internal conversion event.

The effects of the above Auger charging process have been extensively studied in atoms in the gas phase using the technique known as charge spectrometry. For example, following the highly internally converted isomeric transition $^{131m}Xe \rightarrow {}^{131}Xe$, in xenon gas at low pressures, Pleasonton and Snell found the xenon ions to be distributed in charge from +1 to +23, with a most probable charge of +8.[29]

When the parent atom is chemically bound in a molecule, the excessively high charge resulting from the Auger process is observed to lead to gross molecular disruption in gas phase experiments at low pressures. Thus, following the production of an initial L - shell vacancy in the iodine atom in CH_3I[30] and CH_3CH_2I[31] (through bombardment of the molecule with monoenergetic x-rays rather than by radioactive decay), the molecule was observed to virtually explode. A wide spectrum of charged fragments was found, and the mass, charge, and kinetic energy distribution of the fragments measured. It was concluded from this work that following

the initial charging of the iodine atom, electron transfer from the other atoms in the molecule takes place, thus spreading the positive charge throughout the molecule. The many charged atoms then Coulomb repel one another, causing the molecule to explode, and the fragments are ejected with appreciable kinetic energy.

It must be emphasised that when the isomeric transition occurs by γ-ray emission, rather than by internal conversion, bond rupture is not likely to occur. Examples which illustrate this point well are the gas phase isomeric transition studies in $^{69m}Zn(C_2H_5)_2$, $^{127m}Te(C_2H_5)_2$, and $^{129m}Te(C_2H_5)_2$.[32,33] The $^{69m}Zn \rightarrow {}^{69}Zn$ isomeric transition is not highly internally converted while the other two processes are. It was found that in the former case 95 per cent of the ^{69}Zn atoms were found in the form of $^{69}Zn(C_2H_5)_2$ following the decay, while $\simeq$0 per cent of the ^{127}Te and ^{129}Te atoms were found chemically bonded to the ethyl groups of the parent molecule.

It is important to discuss what the effects may be of a highly internally converted transition when it occurs in a solid, rather than in a gas. The distinct advantage of gas-phase experiments is that they allow the direct study of the charging process and its immediate chemical effects in molecules. Such direct information is difficult to obtain in solids. However, as will be discussed later, the Mössbauer effect allows the investigation of these processes in solids and permits the study of the chemical state of

the daughter atom in the solid only nanoseconds after its formation in the decay.

It should be anticipated that the extremely high positive charges observed in gases will not be observed in solids. Rapid charge neutralisation will occur as electrons are transferred back to the excited atom from the surrounding lattice. Indeed, high charges as such will probably not be achieved, as electrons will flow back to the atom even as the Auger cascade itself is moving out to the outer shells of the atom. In addition to the above, electronic excitation energy may be readily dissipated to the surrounding medium through the many atomic and molecular vibration modes of the lattice. This will again serve to reduce the amount of molecular disruption accompanying the internal conversion event.

Finally, for atoms bound in solids one must also consider the constraining effects of the surrounding atoms and molecules. This cage effect will prevent the rapid separation of molecular fragments in the event of partial loss of bonding electrons in the charging process. Immediate charge neutralisation and electronic de-excitation may then simply reform chemical bonds, since the recoil fragments will not have been able to separate.

3. Negative Beta Decay

In β^--emission an electron of high kinetic energy and an antineutrino are ejected spontaneously from the nucleus of the radioactive atom. Chemical effects observed for atoms undergoing β^--decay may thus be the result of the kinetic recoil energy acquired by the atom or the electronic excitation and ionisation which may occur as a direct result of the β^--emission process.

In order that momentum be conserved in a β^--decay event, the decaying atom must recoil. The total recoil energy acquired by the atom is determined by vector addition of the recoil momenta imparted by the β^- and antineutrino, and thus the angular correlation between the two should be considered. For a β^--transition in which the energy of the antineutrino approaches zero, the recoil energy acquired by the atom is a maximum and is given by the expression

$$E_R(\max) = \frac{548\ E_{\beta^-}(\max)}{A} + \frac{536\ E_{\beta^-}^2(\max)}{A}\ \text{eV} \qquad \text{(I-2)}$$

where A is the mass number of the emitting nucleus, and $E_{\beta^-}(\max)$ is the maximum energy of the β^--particle in units of MeV. Thus the maximum recoil energy in the β^--decay of ^{132}Te ($E_{\beta^-}(\max) = 0.22$ MeV) is 1.1 eV and for ^{6}He ($E_{\beta^-}(\max) = 3.508$ MeV) is 1418 eV. The average recoil energy acquired by an emitting atom in β^--decay is about one half of the maximum value.

Of perhaps greater importance in β^--decay with regard to chemical effects is the electronic excitation and ionisation resulting from the change in charge of the nucleus. The emission of a β^--particle from the nucleus should give rise to a daughter ion with a single positive charge. However, when the β^--particle leaves the atom in a time short relative to periods of orbital electron motion, the surrounding electron cloud may not have time to adjust to the sudden change in nuclear charge, and may thus be left in an excited state. In most of these cases the electron cloud will contract adiabatically and adjust to the increased nuclear charge. However, in some instances the electron cloud may not contract in this way, and in such a non-adiabatic process the daughter atom is left in an electronically excited state. This excitation energy may result in the process called electron "shake-off" and ionisation of the daughter atom.

The energy, ΔE, available for electronic excitation in β^--decay is given by the difference in kinetic energy acquired by a β^--particle moving through the electrostatic field of the electron cloud of the emitting atom in completely adiabatic and non-adiabatic processes.[34] These expressions are

$$\Delta E = 24.27\ Z^{1/3}(Z'-Z)^2 \text{eV} \quad \text{(for light atoms)} \qquad \text{(I-3a)}$$

and

$$\Delta E = 22.85\ Z^{2/5}(Z'-Z)^2\ \text{eV (for heavy atoms)} \qquad \text{(I-3b)}$$

where Z and Z' in these expressions are the nuclear charges before and after the β^--emission. Thus, for example, in the 1.45 MeV β^--transition $^{129}Te \rightarrow {}^{129}I$, $\Delta E \simeq 160$ eV, assuming the heavy-atom relationship above.

However, experimental evidence, largely that of Carlson and co-workers[35-37], has shown that electron "shake-off" resulting from electronic excitation only occurs in a small fraction of β^--decay events, and that the above theoretical expressions give an upper limit for the excitation energy available in β^--decay. Charge spectra obtained following β^--decay in the rare gases at low pressures show the occurrence of a charge of +1 in 80 to 90 per cent of events, a +2 charge in 10 to 15 per cent of events, and with a maximum charge observed of up to +10.[37] Similar methods of study have been used by a number of groups in investigating the chemical effects of β^--decay in tritium[38,39] and radioactive halogen-containing hydrocarbons[40,41] in the gas phase. The experimental results show that far less excitation and fragmentation occurs than that observed following internal conversion, with singly charged hydrocarbon fragments being the predominant products,

i.e.,

$CH_3T \xrightarrow{\beta^-} (CH_3)^+$ in 82 per cent of events[38]

$CCl_3Br^{82} \xrightarrow{\beta^-} (CCl_3)^+$ in 64 per cent of events.[41]

In these cases the primary decay products $(CH_3\text{-}He)^+$ and $(CCl_3\text{-}Kr)^+$ are unstable and decompose.

It is found that in the few events where the electron "shake-off" process occurs, leading to a high charge on the daughter atom, the mechanism of molecular disruption then observed is similar to that which occurs following internal conversion. It must be emphasised, however, that such processes occur in only a relatively small number of events, and that the principle effects of β^--decay are very mild in comparison with those for internal conversion.

In solids the chemical effects of β^--decay will be far less pronounced than the chemical effects following the (n,γ) reaction or internal conversion. The effects of recoil accompanying most β^--decay events will be small in comparison with the (n,γ) reaction, while the electronic excitation and ionisation are minimal compared with a highly internally converted isomeric transition. The results of chemical investigations of recoil atoms produced by β^--decay in solids support these points in several instances, with little if any bond rupture being observed.[42-45]

B. Models of Recoil-Atom Energy Loss Processes in Solids

In the previous section the origin of recoil kinetic energy and electronic excitation energy was discussed for several different nuclear transformations. Let us now examine in greater detail the specific physical and chemical processes which may occur in a solid lattice following production of the excited recoil atom.

Several models have been proposed which attempt to describe the processes which occur when an atom recoiling with a high kinetic energy loses its energy to the surrounding lattice.

In one such model, the hot-zone model, Harbottle and Sutin[46] and Yankwich[47] have applied the concept of the thermal spike, proposed earlier by Seitz and Koehler.[48] It is visualised that in an (n,γ) nuclear reaction, the recoil atom will, as a result of the kinetic recoil energy acquired in the prompt γ-ray emission cascade, break its original chemical bonds and will move away through the lattice. Such a recoil atom, possessing initially ca.300 eV in recoil kinetic energy, will de-excite in ca.10^{-13}second through a series of displacement and interchange collisions with surrounding substrate atoms. It is proposed that in this process five or six displaced atoms will be produced and that these will lose their kinetic energy in secondary collisions. In so doing, five or six local "hot-spots" will be formed within the lattice, separated by relatively small distances, and these will coalesce in ca.10^{-12} second.

This would produce a hot-zone having a total volume of about 1000 atoms, and in which the crystal would be in an essentially molten state.

Chemical reactions of the recoil atom such as addition, substitution, recombination or exchange-type reactions may take place within this hot-zone with surrounding decomposition fragments or substrate molecules. The hot-zone would then cool to below the melting point of the crystal in ca.10^{-11} second, and in so doing would quench many chemical processes before they had gone to completion. The final recoil site may then be viewed as being in a metastable chemical state. If the solid were then heated following the nuclear transformation it might be expected that some of these reactions could be taken to completion. This latter point will be returned to in the following section.

A second model of considerable significance is the disorder model[49,50] which is based largely on Vineyard's computer calculations of the changes occurring when highly energetic atoms de-excite in a metal lattice.[51,52] Here, an atom acquiring a recoil energy of several hundred eV in an (n,γ) nuclear reaction is visualised as losing its kinetic energy very quickly in coming to rest in the lattice only a few interatomic distances away from its starting point. It is proposed that the general damage to the lattice is quite small, with only a few atoms changing places or becoming interstitial atoms. The majority of the recoil energy is

considered to be carried off through the lattice in focussing collisions and in the production of dynamic crowd-ions, i.e., where each atom of a collision chain moves into the position of its nearest neighbour leaving a vacancy at the origin of the chain. The net effect of these processes is to transport the excess energy away from the recoil atom site and to deposit it in the lattice some considerable distance from the initial event.

Cairns and Thompson[53] have found some tentative evidence for these phenomena occurring in solids following the (n,γ) reaction. In their experiments surfaces of single crystals of potassium iodide were labelled with ^{131}I, and were then irradiated with thermal neutrons. They observed that the ^{131}I atoms were ejected from the crystal surfaces in certain preferred directions, indicating that focussing collisions were occurring within the KI crystal.

The best experimental support for the disorder model is found in the work of Müller with mixed crystal systems.[49,50] Müller investigated the chemical effects of the $^{185}Re(n,\gamma)^{186}Re$ nuclear reaction in homogeneous mixed crystals of K_2ReBr_6/K_2SnCl_6 and K_2ReBr_6/K_2OsCl_6 containing 1 to 28 and 6 to 20 mole per cent of K_2ReBr_6, respectively. Subsequent radiochemical analysis showed a spectrum of recoil products of the type $ReCl_{6-x}Br_x^{2-}$, and from the observed product distribution several conclusions were drawn. Thus, the observed distribution was interpreted as being inconsistent

with the formation of a melt in the recoil zone, since the distribution, taking account of the numbers of halogen atoms in the reaction zone, was not statistical. From the distribution of Cl and Br ligands on the ^{186}Re daughter nucleus at the lowest K_2ReBr_6 concentrations the reaction zone was calculated to be 1/10th the size of that predicted by the hot-zone model. Hahn and Willard[54] have reported a similar finding in experiments on the $^{80m}Br \rightarrow {}^{80}Br$ isomeric transition in alkyl bromides, their results indicating the presence of a reaction zone of one or two molecular diameters in size. In this latter case, however, the ^{80}Br atom produced is not a highly energetic recoil.

The final model to be discussed here is Walton's "hot-electron" model[55], in which chemical effects of nuclear transformations are described primarily from the point of view of electronic excitation and consequent loss of valence (bonding) electrons. Thus, in a nuclear reaction or radioactive decay, energy may be made available as electronic excitation energy. For atoms in the solid state this may be sufficient to remove bonding electrons from valence orbitals into the conduction band of the crystal. It is then pictured that in some events bonds are broken through loss of electrons, while in others the bonds may reform as electrons from the conduction band re-populate the bonding orbitals. The actual physical disruption at the recoil site may be minimal, if any occurs at all.

This model raises several interesting points. Thus, such a model may be used, for example, to explain how stereochemical configuration may be retained following nuclear transformations. Following thermal neutron capture in d-$[^{59}Co(en)_3](NO_3)_3$, the only $[^{60}Co(en)_3](NO_3)_3$ labelled product observed is the d-form.[6] If the crystals are heated following the transformation some of the ^{60}Co decomposition products present react to produce $[^{60}Co(en)_3](NO_3)_3$, again exclusively in the d-form. Similar observations have been made on cis- and trans- $[Co(en)_2Br_2](NO_3)_3$.[6] Thus, there is some tentative evidence to support the idea of simple electron loss and bond reformation at the recoil site, with no real physical disruption taking place.

While the validity of Walton's model may be questioned where the atom produced in the transformation possesses translational energy as a result of recoil, the model may well describe in a simple qualitative way the results of electronic excitation following an isomeric transition or β^--decay. Thus, as discussed in Section I-A(2), following an Auger cascade or electron "shake-off" in a solid, the final chemical effects may be quite different from those in isolated gas molecules. In a solid, electron loss through excitation to the conduction band will be balanced in many events by the reverse process and the molecule may then remain intact. On the other hand, in some events bonding electrons may be completely lost and bond rupture will then result. Certainly it is most

unlikely that the large charges generated in isolated molecules in gases, and the attendant Coulomb explosion, will be observed in solids.

C. Annealing Reactions

One aspect of radiochemical studies of recoil atoms in the solid state which has attracted much attention in the past is the so-called thermal annealing process. When the solid containing the recoil fragments is heated following the nuclear transformation, chemical reactions of the radioactively-labelled molecular fragments produced in the preceding transformation take place. These reactions generally lead to the reformation of the parent molecule, as observed on subsequent radiochemical analysis. Moreover, these same annealing reactions can be initiated by several methods other than by heating; for example, by irradiating the solid with light or ionising radiation, by the application of pressure, and by crushing or grinding the crystals.

1. Mechanisms of Annealing Reactions

The thermal annealing reactions may be viewed as simple chemical reactions involving the recoil atom and surrounding molecular debris formed in the preceding nuclear event or surrounding parent substrate molecules. It is possible to visualise several mechanisms for the annealing reaction.

Thus the annealing reaction may occur through what may be described as the recombination of initially correlated fragment pairs.[6,57,58] In a monoatomic lattice or simple alkali halide lattice, this reaction may involve the return of the recoil atom, from where it was stopped in the lattice following the nuclear event, back to the vacant position in the lattice from which it originated. This process is a simple vacancy - interstitial pair recombination.[56] Alternatively, for a lattice containing molecular ions, the reaction may involve the recombination of the recoil atom, which underwent bond rupture in the recoil event, with its original ligand groups. In this instance the recoil atom may undergo a single recombination with a fragment species, or may undergo a sequential recombination with groups in a step-wise process.[58]

An alternative mechanism to the above is the recombination of initially randomly distributed fragment pairs.[6,56,59] In this reaction it is proposed that the recoil atom and the lattice vacancy, or molecular ligand groups, that recombine may not have originated in the same event, and that diffusion occurs in the lattice leading to the reactions observed. This reaction mechanism would lead to at least second order kinetics, i.e., the probability of a reaction occurring would be dependent on both reactants being present.

A third annealing reaction mechanism is that of the recrystallisation of the hot-zone, which was mentioned in

the preceding section. Here it is proposed that within the metastable recoil site the previously quenched chemical reactions may now continue to completion on heating.

Yet another mechanism which has been invoked to explain annealing reactions is that of isotope exchange between the recoil atom and surrounding substrate molecules. This mechanism was first proposed to explain annealing in organic halides[58]

$$RX + X^{*} \quad RX^{*} + X$$

where RX is the parent molecule and X^{*} the recoil atom. Recent experiments with doped inorganic crystals have found further evidence of such exchange reactions. Thus, so-called transfer annealing reactions in doped chromates ($^{51}Cr^{3+} \rightarrow {}^{51}CrO_4^{2-}$)[60,61], iodates ($^{131}I^{-} \rightarrow {}^{131}IO_3^{-}$)[62,63] and bromates ($^{82}Br^{-} \rightarrow {}^{82}BrO_3^{-}$)[64] have been observed and explained by a simple exchange model. Moreover these processes bear a striking resemblance in temperature dependence and kinetics to recoil fragment thermal annealing in these systems. It must be noted that in the exchange experiments no nuclear event is involved in producing the radioactive dopant atom in the crystal, and thus there is no fragment structure of the recoil site as created by a "hot" atom present. The dopant atom is surrounded only by intact molecules with which it may react.

2. The Role of Crystal Defects in Recoil Fragment Annealing

Although the previously described mechanisms appear to be quite straightforward, detailed studies of annealing reactions have disclosed considerable complexity. Thus it has been found in many different chemical systems, that defects present in the crystal are intimately involved with the recoil annealing reactions that occur.

The past work of Andersen clearly illustrates this point. Andersen et al.[65-67] have compared thermoluminescence glow curves, conductivity measurements, and recoil fragment annealing curves in thermal neutron irradiated chromates and bromates, and following β^--decay in tin compounds. In each instance, distinct correlations were observed in the data for all three processes. The experiments showed that crystals containing recoil fragments were found to exhibit increases in their conductivity and to luminesce at the same temperatures that recoil-fragment annealing reactions were found to occur. From this Andersen concluded that the release of electrons or positive holes from γ-induced defects must be involved in the thermal annealing of the recoil fragments, since they are certainly involved in the other two processes.

Collins[68] has proposed a model which may well describe the way in which crystal defects can promote recoil product annealing. He proposes that within the

crystal there exist many trap sites of varying depth (energy) which are filled by free electrons and positive holes in the order of their depth. On heating the crystal, mobile defects (the electrons or positive holes) are released to the conduction band of the crystal where they are free to move. When such a free defect reaches a recoil site, the annealing reaction itself may then take place through one of several different mechanisms. Thus the recoil atom may be oxidised or reduced depending on whether an electron or positive hole is involved, and this will lead to a change in the chemical form of the recoil atom. Alternatively, the recombination of an electron-positive hole pair may lead to the deposition of energy within the recoil site. This may then be followed by fragment recombination or by an exchange process as described earlier.

Realising that annealing reactions are in some way "triggered" by electronic crystal defects, several groups have attempted to determine the origin and type of defect-sites involved. Thus, treatments such as crushing,[69] irradiating the crystals with electrons before and following the nuclear event,[70,71] and doping with cations[69] have all been found to cause an increase in the susceptibility of recoil fragments in crystals to undergo thermal annealing reactions. On the other hand, Machado et al.[72] have found that if Co(III)- and Cr(III)- trisacetylacetonate crystals are

heated prior to (n,γ) activation, subsequent recoil fragment thermal annealing produces a much smaller chemical change than that found without the pre-heat treatment. Machado explained this latter phenomenon as being the result of the production of trap sites by the pre-heating, which can compete with the recoil defect sites in the annealing reaction. Harbottle,[3] on the other hand, has suggested that the pre-heating removes defects which might otherwise trap positive holes or electrons produced during the neutron bombardment, and which afterwards could be released to promote recoil product annealing.

The above processes are related in that they appear to show the influence on the thermal annealing reaction of crystal defects present throughout the crystal lattice. As such, these annealing reactions have been described as extrinsic annealing reactions, or annealing reactions triggered in some way by extrinsic crystal defects. The existence of a second type of annealing reaction has been shown by the work of Collins and Harbottle,[73] and more recently by the work of Andersen[74] and Jones.[75] This reaction was found to be an intrinsic annealing reaction, i.e., an annealing reaction involving only fragments or defects produced by the isolated nuclear event. The characteristic of intrinsic annealing reactions is that they can be shown to be independent of the bulk properties of the crystal lattice and appear to arise solely as a

consequence of fragments and crystal defects formed in the nuclear transformation event itself.

It can be concluded from the above that recoil fragment annealing reactions are most complex, both in the events that initiate these reactions and in the actual reaction mechanisms themselves. In a further effort to clarify the meaning of the observed annealing reactions, quantitative kinetic analyses have been made for many systems.

3. Kinetic Analysis of Recoil Fragment Annealing

The kinetic analysis of recoil fragment annealing data appears, however, to be equally complicated. From quantitative kinetic treatments of annealing data, investigators have attempted to determine the relative effects of diffusion and electronic processes in the annealing reaction. Thus far, however, this has not been accomplished.

Recoil fragment annealing curves are found to exhibit zero,[58] first,[76-78] and second order kinetics,[79] while in other cases, a simple kinetic analysis has not been found possible.[57,80] Activation energies determined from these procedures generally range from 0.5 - 2.0 eV.

The Vand-Primak analysis[81,82] is a more general form of kinetic treatment which is based on the concept that, rather than having a discrete energy of activation, an annealing reaction of a given order may be governed

by a distribution of activation energies. Such an analysis has been applied successfully in several systems.[76,77,79,83,84] In addition, using a computer method of analysis, Harbottle[85] has shown that by assuming a block or Gaussian distribution of activation energies, one can derive hypothetical annealing curves much like those experimentally observed. Finally, Andersen[65-67] has shown the data in some of his work to be best described by assuming a combination of discrete first-order processes, each having a discrete activation energy.

It is again obvious that the interpretation of the kinetic analyses of thermal annealing data has been able to provide very little information as to the nature of recoil atom annealing processes occurring in solids. For example, one can question the significance of activation energies obtained by these methods,since in almost every instance there is more than one method of kinetic analysis which may yield fits to the experimental data. Moreover, since it is known that the annealing reactions proceed through quite complex mechanisms, involving the de-trapping of electrons and positive holes in the crystal, diffusion of these defects to the recoil site, and finally the annealing step itself, it is not clear precisely what the activation energy corresponds to. The theory of Collins and the experimental work of Andersen appears to show that in those instances at least, the activation energy is determined by the de-trapping of the electronic defect rather than by the chemical reaction occurring at the recoil site.

4. Conclusions

Several conclusions may be drawn from this discussion. The annealing reactions of recoil atoms in solids are triggered in some way by electronic processes occurring in the crystal, and these processes may be initiated by heating or crushing the crystals, or by γ-irradiation. These electronic processes give rise to the annealing reaction itself, which may involve fragment recombination, exchange, or electronic oxidation or reduction. The net effect of such annealing reactions in many instances is to restore the recoil atom to its original chemical form.

In these annealing reactions two processes may be distinguished, those involving extrinsic crystal defects and those involving intrinsic defects created in the nuclear transformation itself. The former processes often serve only to confuse and complicate the interpretation of annealing experiments. Thus, in studying (n,γ) recoil atoms in solids, one must consider the effects of the γ-radiation absorbed by the sample during the reactor irradiation, which will serve to produce defects throughout the bulk of the crystal. It is also necessary to consider the effects of thermal and γ-ray annealing which may occur at ambient temperature during the irradiation itself. In an ideal situation, in studying the chemical environment of a recoil atom in a solid, it would be desirable to be able to identify only the intrinsic component of the annealing reaction.

III. DECAY CHARACTERISTICS FOR THE TELLURIUM - IODINE SYSTEMS INVESTIGATED IN THIS WORK

From the preceding review it can be seen that while the origins of kinetic recoil energy and electronic excitation energy in nuclear transformations are well understood, descriptions of the processes which occur in solids during and following these transformations are not clearly defined. In the present work it was felt that a detailed comparative study of several different well-characterised nuclear transformations in the same isotopic system would add significantly to an understanding of recoil chemistry in solids. The principle objective of the present work then was to study the comparative chemical effects accompanying β^--decay, internal conversion of a γ-transition, and thermal neutron capture, all in the same solid matrix. The thermal annealing reactions observed following each of these transformations were also of interest, since again a comparative study would hopefully provide useful information about the relative chemical effects of the different transformations.

Few isotopic systems allow such a comprehensive study of the several different transformations which it was intended to investigate. One such isotope system, however, is that of tellurium - iodine. This is clearly

shown in the decay schemes for ^{131}Te, ^{132}Te, and ^{129}Te as seen in Figures 1 and 2. Table I summarises most of the relevant decay characteristics for these tellurium-iodine isotopes. Moreover, as will be discussed in Section V there are several Mössbauer nuclei which may be studied in this system.

In the present work telluric acid was chosen as the parent compound in which to study the different transformations. Telluric acid has been used by several investigators in the past, since it is readily prepared, chemically stable, and very soluble in aqueous solvents, which allows for convenient radiochemical separations.

A. Decay Sequences Studied in the Chemical Analysis of Iodine Recoil Atoms

Using radiochemical methods of analysis, ^{131}I and ^{132}I recoil species may be investigated following four different transformation sequences. These include, in telluric acid

		Radioactive Recoil Studied
1.	$H_6{}^{130}TeO_6(n,\gamma)^{131}Te(^{131m}Te) \xrightarrow{\bar{\beta}\ (\gamma)}$	^{131}I
2.	$H_6{}^{131m}TeO_6 \xrightarrow[18\%\ \text{isomeric transition}]{\beta^-(\gamma)}$	^{131}I

3. $H_6{}^{131}TeO_6 \xrightarrow[\text{ca. 18\% internal conversion}]{\beta^-(\gamma)} {}^{131}I$

4. $H_6{}^{132}TeO_6 \xrightarrow[\text{ca. 85\% internal conversion}]{\beta^-(\gamma)} {}^{132}I$

In the (n,γ) activation process, (1) above, ca. 5.9 MeV of binding energy is liberated in the prompt γ-cascade of ^{131}Te which, assuming that only one γ-quantum is emitted, imparts ca. 142 eV in kinetic recoil energy to the daughter ^{131}Te atom. Unfortunately, a detailed description of the prompt γ-ray spectrum is not available for ^{131}Te, thus a more precise calculation of this recoil energy is not possible. It is also not known at present if delayed states are populated in the (n,γ) reaction. The ratio of ^{131}I activities produced from the decay of ^{131}Te and ^{131m}Te is given approximately by the respective thermal neutron capture cross sections for the two tellurium isotopes, giving a ratio of about 5 to 1.

For the purposes of the present work, the studies of the recoil iodine atoms produced in the radioactive decay of ^{131m}Te, ^{131}Te, and ^{132}Te, as shown in (2), (3), and (4) above, were of principle interest. The decay schemes of these isotopes are in many ways quite similar, but more importantly, several differences exist. Thus in the decay of ^{131m}Te, in 82 per cent of events decay occurs through $\beta^-(\gamma)$ transitions directly to ^{131}I, while in 18 per cent of

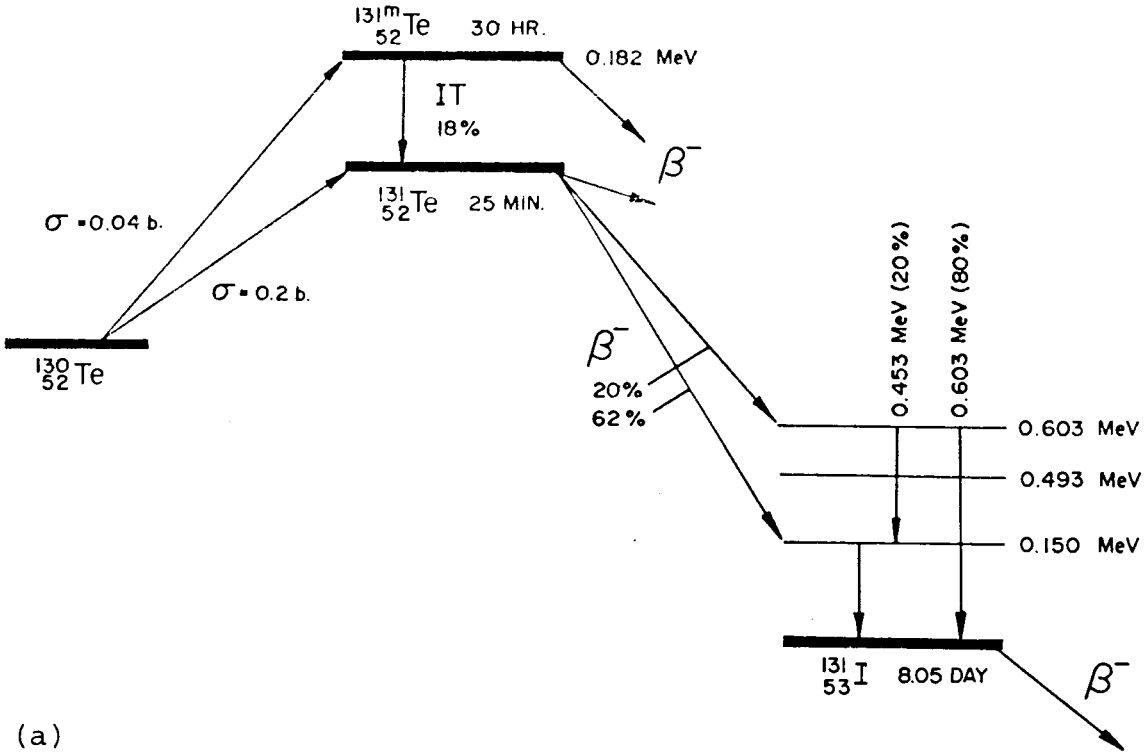

(a)

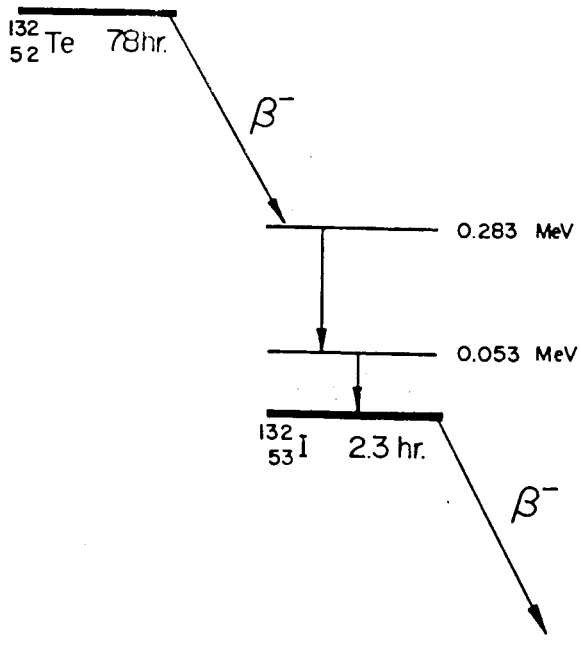

(b)

Figure 1 Decay Scheme for (a) ^{131m}Te and ^{131}Te and (b) ^{132}Te [86].

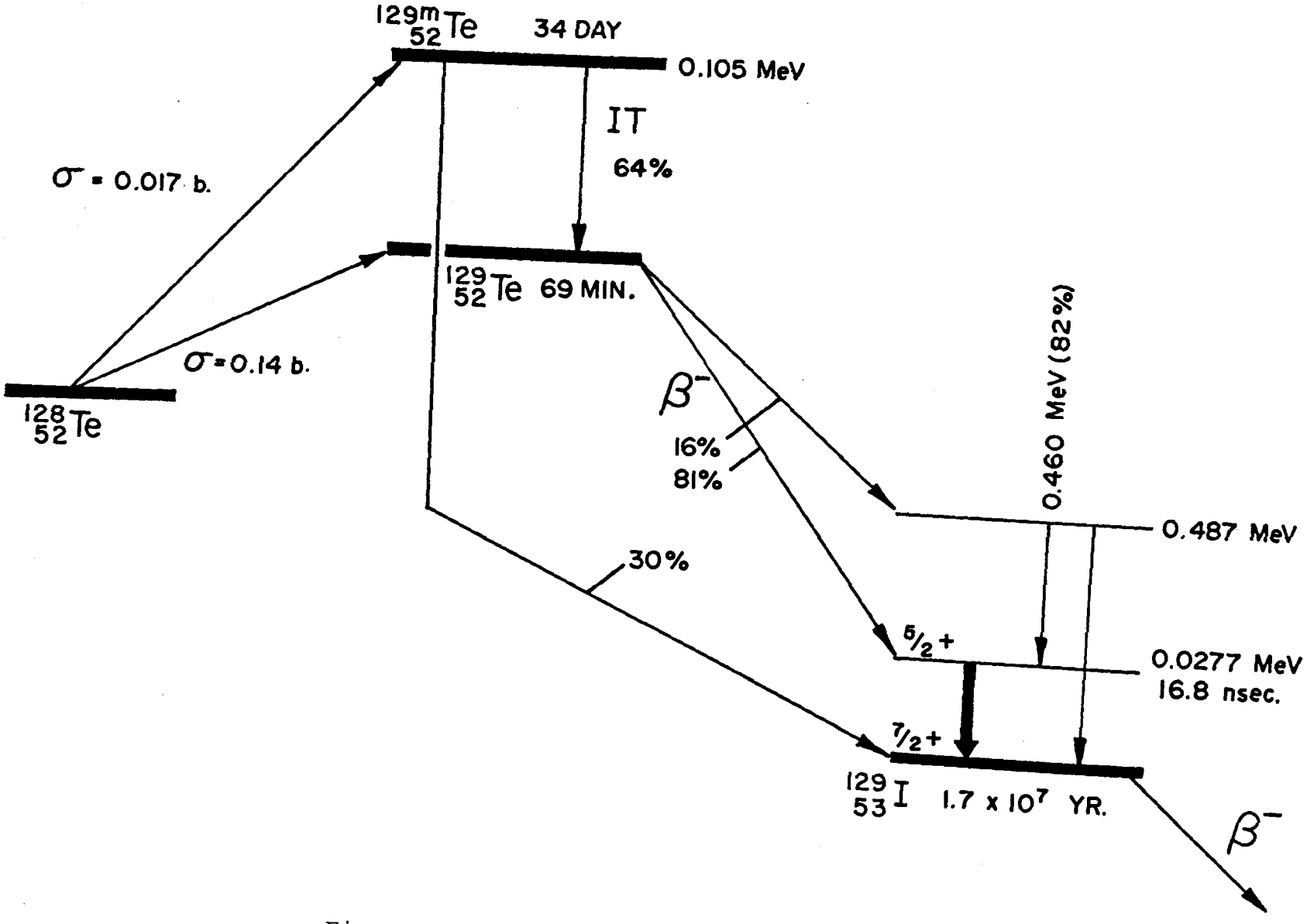

Figure 2 Decay Scheme for ^{129m}Te and ^{129}Te [86].

TABLE I

PRINCIPLE DECAY CHARACTERISTICS FOR THE TELLURIUM-IODINE ISOTOPES INVESTIGATED

Isotope	σ^{th} for its Production (Barns)	$t_{1/2}$	Daughter Isotope Produced	Principal Decay Radiations (MeV) (Where Relevant Maximum Recoil Energies Available in the Transition, Are Shown in Parentheses, in eV)		
				β^{-1}	γ	Internal Conversion Coefficient
^{131}Te	.2	25 min	^{131}I	2.14(27.7) 1.69(18.5)	.150(.09) .453(.90)	αK = .26
^{131m}Te	.04	30 hr	18% IT to ^{131}Te 82% β^- to ^{131}I	.42(1.76) .57(3.71)	IT. .182(0.14) .115(2.50) .854(2.88) 1.145(5.30)	αK = V.Large
^{131}I		8.03d	^{131}Xe		0.364	
^{132}Te		78 hr	^{132}I	.22(1.1)	.283(.33) .053(.01)	α = .05 αK = 5.3
^{132}I		2.3 hr	^{132}Xe		.668 .773	
^{129m}Te	.017	34d	64% IT to ^{129}Te 36% β^- to ^{129}I	1.60(17.4)	IT .1056	αK = V.Large
^{129}Te	.14	69 min	^{129}I	1.45(14.9) 1.00(8.4)	.027(Mössbauer Transition) .460(.88)	αK = 4.5

• Calculated assuming simple momentum conservation

events the highly internally converted isomeric transition precedes the $\beta^-(\gamma)$ decay. On the other hand, the decay of ^{131}Te occurs in 100 per cent of events by $\beta^-(\gamma)$ decay to ^{131}I. However, in ca. 80 per cent of events the decay proceeds through the .150 MeV level in ^{131}I, which has a K-shell internal conversion coefficient of $\alpha_K=0.26$. Thus, for ^{131}I produced from ^{131}Te, internal conversion occurs following the β^- transition in ca. 18 per cent of events. The decay schemes of these two isotopes thus exhibit only minimal differences, and it was of some interest to see if such differences would be reflected in the chemical effects accompanying the decay.

For ^{132}Te, the decay occurs in every event through the .053 MeV transition in ^{132}I which has $\alpha_K=5.3$. In this instance internal conversion and the accompanying extensive electronic excitation will occur in ca. 83 per cent of decay events and the effects of this on chemical bonding should be readily observable. Moreover, in this latter case the parent ^{132}Te and daughter ^{132}I exist in radioactive transient equilibrium. This equilibrium is important in that it allows a very detailed study of the thermal annealing reactions of the ^{132}I recoil atoms, as will be subsequently shown.

B. Decay Sequences Studied in the Chemical Analysis of Tellurium Recoil Atoms

Chemical investigations of the chemical states of tellurium recoil atoms in telluric acid could also be carried out following the transformation sequences shown below

		Radioactive Recoil Studied
5.	$H_6{}^{128}TeO_6(n,\gamma)^{129m}Te \xrightarrow[\text{transition}]{\text{isomeric}}$	^{129}Te
6.	$H_6{}^{129m}TeO_6 \xrightarrow[\text{transition}]{\text{isomeric}}$	^{129}Te
7.	$H_6{}^{128}TeO_6(n,\gamma) \longrightarrow$	^{129}Te

It can be seen that these experiments allow a comparison of the chemical effects for isotopic (Te) and nonisotopic (I) recoil atoms within the telluric acid lattice.

In the thermal neutron capture reaction $^{128}Te(n,\gamma)^{129}Te$, about 6.1 MeV of binding energy is liberated in the prompt γ-ray cascade which, if only one γ-ray were emitted, would give the daughter ^{129}Te nucleus ca. 155 eV in kinetic recoil energy. Again, the significant details of the prompt γ-ray spectrum for ^{129}Te have not been reported.

The nuclear transformation of prime importance in this study is that of (6) above, where the isomeric transition decay of ^{129m}Te is $\simeq$ 100 per cent internally converted. Although only 64 per cent of all ^{129m}Te decays

proceed via the isomeric transition process, of the remaining 36 per cent of events, none go through the .46 MeV γ-ray in ^{129}Te used in the radiochemical assay. As in the case of the $^{132}Te \rightarrow {}^{132}I$ system, a transient equilibrium is present in the $^{129m}Te \rightarrow {}^{129}Te$ decay scheme, which again is of prime importance when the annealing reactions of the ^{129}Te recoil atoms are investigated.

It is of interest to now briefly review previous investigations of iodine and tellurium recoil atoms in solids.

IV. PREVIOUS RADIOCHEMICAL INVESTIGATIONS OF IODINE AND TELLURIUM RECOIL FRAGMENTS IN SOLIDS

A. Iodine Recoil Atoms Produced in Tellurium Compounds

In general, only ^{131}I recoil atoms produced by thermal neutron activation followed by β^--decay have been investigated in tellurium compounds.[87-95] Some representative results of these studies are shown in Table II.

An examination of these and other results shows that in each case ^{131}I activity is found in the same three chemical forms of I^-, IO_3^-, and IO_4^-, in comparable yields. Moreover, the distribution of radioiodine recoil products observed in each instance is found to depend on the pH and the carriers present during dissolution, and on the method of chemical analysis employed.

The dependence of the product distribution on the pH of the solution clearly shows that oxidation-reduction or exchange reactions must occur in aqueous solution under certain conditions. These processes will clearly mask the true chemical identity of the recoil atoms formed in the nuclear transformation. Bertet, Chanut, and Muxart[90] have investigated the effects of varying the dissolution conditions in detail. It can be concluded from their work that in order to minimise any possible chemical reactions following dissolution, the crystals should be dissolved in basic media.

TABLE II

IODINE RECOIL ATOMS PRODUCED IN PARENT TELLURIUM COMPOUNDS. IN ALL INSTANCES ANALYSIS WAS CARRIED OUT FOLLOWING DISSOLUTION IN BASIC SOLUTION

COMPOUND AND TRANSFORMATION SEQUENCE	YIELDS OF IODINE RECOIL ATOMS AS			REFERENCE
	I^- (%)	IO_3^- (%)	IO_4^- (%)	
$H_6{}^{130}TeO_6$ (n,γ) $^{131}Te+{}^{131m}Te$ $\xrightarrow{\beta^-}$ ^{131}I	44.2	52.9	2.9	90
$(H_2{}^{130}TeO_4)_n$ (n,γ) $^{131}Te+{}^{131m}Te$ $\xrightarrow{\beta^-}$ ^{131}I	34	66		93
$^{130}TeO_2$ (n,γ) ^{131}Te + ^{131m}Te $\xrightarrow{\beta^-}$ ^{131}I	54	36.8	9.2	91
$^{130}TeO_2$ (n,γ) ^{131}Te $\xrightarrow{\beta^-}$ ^{131}I	45	42.5	12.5	90
$^{132}TeO_2$ $\xrightarrow{\beta^-(\gamma)}$ ^{132}I	41	54	5	89

In recent experiments of a similar nature, Hashimoto *et al.* studied the ^{131}I recoil product distribution following $^{130}Te(n,\gamma)^{131,131m}Te \xrightarrow{\beta^-} {}^{131}I$ in several tellurium compounds. It was found that varying the carriers present during dissolution of the solid influenced the product distribution observed on electrophoretic analysis. These workers tentatively identified the formation of $^{131}IO_2^-$, as well as $^{131}I^-$, $^{131}IO_3^-$, and $^{131}IO_4^-$. However, the reproducibility in this work was poor and the carriers were present in such very large concentrations in several of the experiments as to place some doubt on the significance of the results obtained.

Other experiments reported in the literature include investigations of the gross ^{131}I activity formed by $^{130}Te(n,\gamma)^{131,131m}Te \xrightarrow{\beta^-} {}^{131}I$ in $(H_2TeO_4)_n$,[93] α-TeO_3[91] and TeO_2.[92] In these studies it was again found that $^{131}I^-$, $^{131}IO_3^-$, and $^{131}IO_4^-$ products were formed. On thermal annealing the $^{131}I^-$ yield was observed to decrease in $(H_2TeO_4)_n$, and to increase in α-TeO_3 and TeO_2.

In none of the previous studies have any attempts been made to study in a comparative way the chemical effects of decay in ^{131}Te, ^{131m}Te, and ^{132}Te-labelled compounds.

B. Iodine Recoil Atoms Produced in Iodine Compounds

Chemical effects, primarily resulting from high energy nuclear reactions, have been studied for radioiodine recoil atoms produced in iodate and periodate lattices.[96-105]

The results of a representative portion of this work are shown in Table III for comparison with the results presented in the previous discussion.

Several general comments can be made. Where the chemical analysis has permitted their identification, three iodine fractions have always been observed. In a periodate lattice or an iodate lattice, very different nuclear transformations are observed to produce quite similar product distributions. This similarity in results following the different nuclear transformations points to the difficulty in obtaining meaningful information using radiochemical methods of analysis. Additional factors, such as chemical reactions during and following dissolution, may have a marked effect on the observed product distributions.

Finally, studies of recoil fragment thermal annealing in iodates and periodates have shown only the presence of oxidative annealing reactions, i.e., $*I^-$ and $*IO_3^-$ → $*IO_4^-$ in periodates, and $*I^-$ → $*IO_3^-$ in iodates, where *I is the radioactive recoil atom.

C. Tellurium Recoil Atoms Produced in Tellurium Compounds

Previous investigations of the chemical effects observed for tellurium recoil atoms produced in tellurium (VI) compounds have been carried out for the nuclear transformation occurring in aqueous solutions[106-108] as well as in solids.[74,108-113]

TABLE III

IODINE RECOIL ATOMS PRODUCED IN PARENT IODINE COMPOUNDS

COMPOUND AND TRANSFORMATION SEQUENCE	YIELDS OF IODINE RECOIL ATOMS AS			REFERENCE
	I^-(%)	IO_3^-(%)	IO_4^-(%)	
$KIO_4(p,pxn)I$	8	92		[98]
$^{133}CsIO_4(n,\alpha)\ ^{130}I$	6.3	87.3	6.4	[103]
$^{127}CsIO_4(n,\gamma)\ ^{128}I$	6.2	86.7	7.0	
$^{127}CsIO_4(n,2n)\ ^{126}I$	4.8	89.4	5.7	
$^{127}NaIO_3(n,\gamma)\ ^{128}I$	32.4	65.7	1.9	[101]
$^{129}NaIO_3(n,\gamma)\ ^{130}I$	55.8	42.5	1.7	
$^{133}CsIO_3(n,\alpha)\ ^{130}I$	40.6	59.4		[102]
$^{127}CsIO_3(n,\gamma)\ ^{128}I$	30.2	69.8		
$^{127}CsIO_3(n,2n)\ ^{126}I$	39.6	60.4		

The chemical effects of the highly internally converted isomeric transition decay in ^{127m}Te- and ^{129m}Te-labelled telluric acid were studied by Hahn[108] over a wide range of pH in aqueous solution. Bond rupture, yielding ^{127}Te(IV) and ^{129}Te(IV) was observed in ca. 100 per cent of events in acid media, and slightly less in basic media, thus clearly showing the effect of the extensive electronic excitation and ionisation accompanying every decay event.

The isomeric transition decay process was studied by Seaborg[106] in frozen aqueous solutions of telluric acid. Bond rupture was again found to give Te(IV) in 100 per cent of events. This result is perhaps surprising when one considers that the parent molecule is now encased in an ice matrix which might be expected to both constrain the positions of the recoil fragments and to permit rapid charge neutralisation processes to occur, thus preventing molecular fragmentation.

Several experimenters have made cursory examinations of the ^{127m}Te and ^{129m}Te isomeric transitions in solid telluric acid and tellurate lattices. Thus Hahn[108] was the first to look at the chemical effects of the isomeric transition in ^{129m}Te-labelled telluric acid. He found that, after allowing the ^{129m}Te (33 day) → ^{129}Te (69 minute) decay to reach radioactive equilibrium in the solid state, 76.4 per cent of the ^{129}Te atoms were observed on subsequent

radiochemical analysis to be in the parent molecular form. Similar findings have since been reported following the isomeric transition of ^{127m}Te occurring at room temperature in sodium tellurate (83.5 per cent as ^{127}Te(VI)),[109,112] and for ^{127m}Te-labelled telluric acid (66 per cent as ^{127}Te(VI)).[74] Kirin et al.[111] have also reported high retentions in the parent chemical form following isomeric transition for a large number of ^{127m}Te-labelled tellurates. Obviously,in all of these instances, the crystal lattice is capable of dissipating the electronic excitation energy in addition to neutralising any high positive charge formed, in most cases well before bond rupture can occur.

Dancewicz and Halpern have briefly reported the thermal annealing observed when $Na_2{}^{127m}TeO_4$ is heated following the isomeric transition.[109] They found that the ^{127}Te(IV) molecular fragment annealed back to the parent ^{127}Te(VI) chemical form. While the work of the present thesis was in progress Andersen[74] and Halpern[113] published detailed investigations of the thermal annealing reactions of ^{127}Te recoil products in telluric acid and tellurates, respectively. They again found that the decomposition products formed in the isomeric transition thermally anneal back to the parent Te(VI) form.

Looking briefly at the chemical effects of thermal neutron capture, one might now expect to see the chemical effects of physical recoil as well as effects of electronic excitation or ionisation. Bertet and Muxart[110]

and Stevovic and Muxart[112] have reported studies of the (n,γ) reaction in telluric acid. They observed that bond rupture occurs in a slightly higher percentage of events than is found following isomeric transition. Depending upon the irradiation conditions, 39 to 55 per cent of the ^{127}Te, ^{129}Te and ^{131}Te recoil atoms were found to remain in the parent chemical form. The thermal annealing of the (n,γ) recoil atoms was not investigated.

The results for the (n,γ) and isomeric transition experiments are thus quite similar in that an appreciable fraction of the recoil atoms survive in the parent molecular form in each instance. The chemical analyses used only allowed the separation of the daughter activity into two fractions; the Te(IV) form which is the molecular decomposition product, and the Te(VI) form which is indistinguishable from the parent chemical form.

In conclusion it must be noted that, where comparisons can be made, quite consistent chemical results have been obtained by the different experimenters in investigating tellurium recoil atoms in telluric acid and tellurates, even though quite different analytical methods have been used. This is in marked contrast to the case of iodine recoil atoms in tellurium compounds, where the observed experimental results are greatly dependent on the pH of the solution in which the crystals are dissolved, the nature of the carriers present, and the type of chemical separation used.

The past studies of iodine recoil atoms in tellurium compounds and in iodine compounds serve to clearly illustrate the uncertainty of using radiochemical methods of analysis in such investigations. The probable occurrence of chemical reactions in solution before the analysis is performed means that the results of such radiochemical investigations must be treated with some reservation.

V. THE MÖSSBAUER EFFECT

It is apparent from the preceding discussion that a method for observing recoil atoms as they come to rest in the solid lattice would be a much more valuable tool in the study of chemical effects rather than the standard radiochemical methods which have been generally used in the past. Such a tool is now available with the development of Mössbauer spectroscopy. Through the use of the technique of Mössbauer resonance absorption, one can observe the recoil species as it exists in the solid, in many cases within nanoseconds following its production in the lattice in a nuclear reaction or radioactive decay. Moreover, from the several parameters which can be obtained from Mössbauer absorption spectra, it is possible to describe in detail the chemical bonding of the recoil atom (the Mössbauer nucleus).

A. Basic Principles

The basic theory of the Mössbauer effect has been described by Mössbauer,[114] Lustig,[115] Shapiro,[116] Frauenfelder,[117] and more recently by Goldanskii and Herber.[118] Applications of the Mössbauer effect in chemistry and solid state physics have been reviewed in several books.[118-120]

The Mössbauer effect arises from the recoilless emission and resonant re-absorption of low-energy γ-rays in the solid state. Resonance occurs if a γ-ray which is emitted by a nucleus in decaying from an excited state to the ground state is then absorbed by an identical nucleus in its ground state and which is then excited to the corresponding excited state. Such a resonance process is not usually observed for a free nucleus because of accompanying recoil energy loss arising from momentum conservation in the radioactive decay event. Thus, for a nuclear transition of energy E_o, the energy of the emitted γ-ray, E_γ, is given by

$$E_\gamma = E_o - E_R \qquad \text{(V-1a)}$$

where E_R is the kinetic recoil energy acquired by the decaying atom. Moreover, since the energy required in the absorption process is, for similar reasons, given by

$$E_\gamma = E_o + E_R \qquad \text{(V-1b)}$$

the γ-ray emission and absorption lines will be separated by $2E_R$, or by about .01 - .1 eV for $E_o \leq 100$ keV.

The finite lifetime of the nuclear excited state gives rise to a Lorentzian distribution of energies for the γ-transition, described by a line width, Γ,

$$\Gamma = \hbar/\tau \qquad \text{(V-2)}$$

where τ is the mean lifetime of the state. Thus for nuclear states whose lifetimes range from 10^{-9}- 10^{-8} second, Γ will correspondingly range from 10^{-6} to 10^{-7} eV. Therefore it is found that since $E_R >> \Gamma$, resonant absorption generally does not occur for free nuclei.

In 1958 Mössbauer discovered that, for nuclei held strongly in a solid lattice, in a fraction of events the emission and absorption processes can occur without recoil energy loss. In such instances the recoil momentum is taken up by the lattice as a whole, the lattice acting as a body of infinite mass, and $E_R = 0$ and thus $E_\gamma = E_o$.

The probability, f, of a transition being a recoilless process is given, using the Debye approximation for the vibrational energy spectrum of the solid,[119] by

$$f = \exp(-2W) \qquad \text{(V-3)}$$

where W, the Debye-Waller temperature factor, is given as

$$W = \frac{3E_R}{k\theta_D}\left[\frac{1}{4} + \left(\frac{T}{\theta_D}\right)^2 \int_0^{\theta/T} \frac{x}{e^x - 1}\, dx\right]. \qquad \text{(V-4)}$$

Here E_R is the recoil energy of the free nucleus, and T is the temperature of the Mössbauer source or absorber. θ_D is the Debye temperature, which is defined in terms of the maximum vibrational frequency of the solid ω_{max},

$$k\theta_D = \hbar\, \omega_{max}. \qquad \text{(V-5)}$$

At low temperatures, i.e., for $T << \theta_D$, expression (V-4) simplifies to

$$W = 3/4 \frac{E_R}{k\theta_D} \qquad (V-6)$$

which, for $E_R < 2k\theta_D$, gives f values approaching unity. At high temperatures, i.e., for $T >> \theta_D$, the expression reduces to

$$W = 3/4 \frac{E_R}{k\theta_D} 4 \frac{T}{\theta_D} \qquad (V-7)$$

In this case $W >> 1$ and f becomes very small.

In theory, the line width of a Mössbauer absorption spectrum is given by the sum of the source and absorber line widths, $\Gamma_{expt} = \Gamma_s + \Gamma_a = 2\Gamma$, where Γ is the theoretical line width calculated from the Heisenberg uncertainty principle. However, several factors lead to the phenomenon of line broadening, and the theoretical value of 2Γ is seldom observed.

The principle factor which leads to line broadening is the thickness of the absorber. The variation of line width with absorber thickness is given by the relationship[121]

$$\Gamma_{expt} = \Gamma_s + \Gamma_a + 0.27\ \Gamma_a\ T_a \qquad (V-8)$$

where T_a is the effective absorber thickness given by

$$T_a = f_a \, n \, \sigma_o \, t_a \qquad \text{(V-9)}$$

and f_a is the absorber f value, n is the number of resonantly absorbing atoms per cubic centimeter, and σ_o is the resonance cross section and t_a is the thickness in centimeters.

Another source of line broadening is the diffusional motion of atoms in the source or absorber. For atoms strongly bound in their normal positions in a solid lattice, the effect of diffusional motion is negligible. However, an atom which is present, for example, as an interstitial in the solid lattice may have sufficient mobility to lead to diffusional line broadening.

B. Chemical Applications of Mössbauer Spectroscopy

Applications of Mössbauer spectroscopy to chemical studies are based on the fact that the energy levels of a nucleus are perturbed by interactions of the nucleus with orbital electrons. These interactions give rise to the phenomena of isomer shift, quadrupole splitting, and magnetic hyperfine splitting. The magnitude of these effects is of the order of 10^{-6} - 10^{-7} eV, and thus they are sufficient to displace the emission and absorption lines from one another, destroying resonance. However, resonance may be restored by moving the emitting atom relative to the

absorbing atom at velocities usually in the range of 1-10 mm. sec^{-1}. The doppler shift in the photon energy, E_D, is given by

$$E_D = E_o \left(\frac{v}{c}\right) \qquad \text{(V-10)}$$

where E_o is the transition energy, c is the speed of light, and v is the velocity at which the atom is moved.

The origin of the Mössbauer isomer shift and quadrupole splitting will now be discussed in detail since these are the parameters used in the present work.

1. The Isomer Shift

The isomer shift arises from the interaction of the s-electron density at the nucleus with the nuclear charge, and has its origin in the change in nuclear radius which occurs when the nucleus goes from the excited state to the ground state. The effect of this interaction may be shown by a non-relativistic perturbation calculation to yield an excited state-ground state transition energy difference, δ, between the source and absorber of[117]

$$\delta = \frac{4\pi}{5} Ze^2R^2 \left[|\psi s(0)|_a^2 - |\psi s(0)|_s^2\right] \left(\frac{\delta R}{R}\right). \qquad \text{(V-11)}$$

In this expression $\delta R = Rex - Rgnd$ and $R = \frac{Rex + Rgnd}{2}$, where Rex and Rgnd are the nuclear radii of the Mössbauer

nucleus in its ground and excited nuclear states. $|\psi s(0)|_a^2$ and $|\psi s(0)|_s^2$ are the s-electron densities at the nucleus for the Mössbauer atom in the absorber and source compounds.

From this expression it can be seen that if a Mössbauer nucleus is present in different chemical environments in the source and absorber compounds, the different s-electron densities at the nucleus, which arise from the different chemical bonding in the two compounds, will give rise to slightly different nuclear transition energies in each case. Their respective emission and absorption lines will then no longer overlap, and resonance will be lost. The doppler velocity (energy) shift that is required to restore resonance is the isomer shift δ.

The relationship between the direction of an observed isomer shift, the change in nuclear radius of the ground and excited states, and the change in s-electron density at the nucleus for any given Mössbauer source-absorber combination is shown below.

				e.g.
$\delta>0$	Rex-Rgnd>0	$\|\psi s(0)\|_a > \|\psi s(0)\|_s$	s → a	^{129}I, ^{125}Te
	Rex-Rgnd<0	$\|\psi s(0)\|_a < \|\psi s(0)\|_s$		^{127}I
$\delta<0$	Rex-Rgnd>0	$\|\psi s(0)\|_a < \|\psi s(0)\|_s$	s ← a	^{129}I, ^{125}Te
	Rex-Rgnd<0	$\|\psi s(0)\|_a > \|\psi s(0)\|_s$		^{127}I

2. Quadrupole Splitting

The phenomenon of quadrupole splitting is the splitting of a resonance line into two or more lines as a result of the interaction of an electric field gradient with the electric quadrupole moment of the Mössbauer nucleus. The Hamiltonian for this interaction can be written as[122]

$$H_Q = \frac{e^2qQ}{4I(2I-1)} \left[3I_z^2 - I(I+1) + \frac{\eta}{2}(I_+^2 + I_-^2)\right] \qquad \text{(V-12)}$$

where Q is the electric quadrupole moment of the nucleus, eq is the electric field gradient along the principle axis (z), and I_z, I_+, and I_- are the spin projection, and raising and lowering operators, respectively. η in the above expression is the asymmetry parameter, which reflects the overall symmetry of the electric field gradient about the nucleus.

The eigenvalues of H_Q for the excited state-ground state spin combination of 5/2 - 7/2, characteristic of the ^{129}I and ^{127}I Mössbauer transitions, are

$$E_{m,I} = \frac{e^2qQ}{4I(2I-1)} (Co - C_2\eta^2) \qquad \text{(V-13)}$$

where

$$Co = 3m^2 - I(I+1) \qquad \text{(V-14)}$$

$$C_2 = 1/12 \left[\frac{f(I,m-1)}{m-1} - \frac{f(I,m+1)}{m+1}\right] \qquad \text{(V-15)}$$

and

$$f(I,m) = 1/4\ (I^2-m^2)\ [(I+1)^2 - m^2] \qquad \text{(V-16)}$$

where m refers to the z component of nuclear spin.

Thus, for an M1-type transition as in the case of the ^{129}I and ^{127}I Mössbauer nuclei, we find that there exist eight allowed transitions in the quadrupole split spectrum whose energies are given by equation (V-13). These are shown in Figure 3. The relative intensities of the resonance lines in a quadrupole split spectrum are given by the square of the Clebsch-Gordon coefficients.[123] The theoretical intensities of the eight lines are also shown in Figure 3.

For the ^{125}Te Mössbauer nucleus on the other hand, having a ground state spin of 1/2 and excited state spin of 3/2, the solution is much simpler. The eigenvalues obtained from equation (V-12) are now found to be

$$E_m = \frac{e^2qQ}{4I(2I-1)}\ [3m^2 - I(I+1)]\left(1 + \frac{\eta^2}{3}\right)^{1/2} . \qquad \text{(V-17)}$$

In this instance, only two lines are observed in the quadrupole split spectrum, corresponding to the transitions $1/2 \rightarrow 3/2$ and $1/2 \rightarrow 1/2$. The absorption lines in this case will generally be expected to have equal intensities.

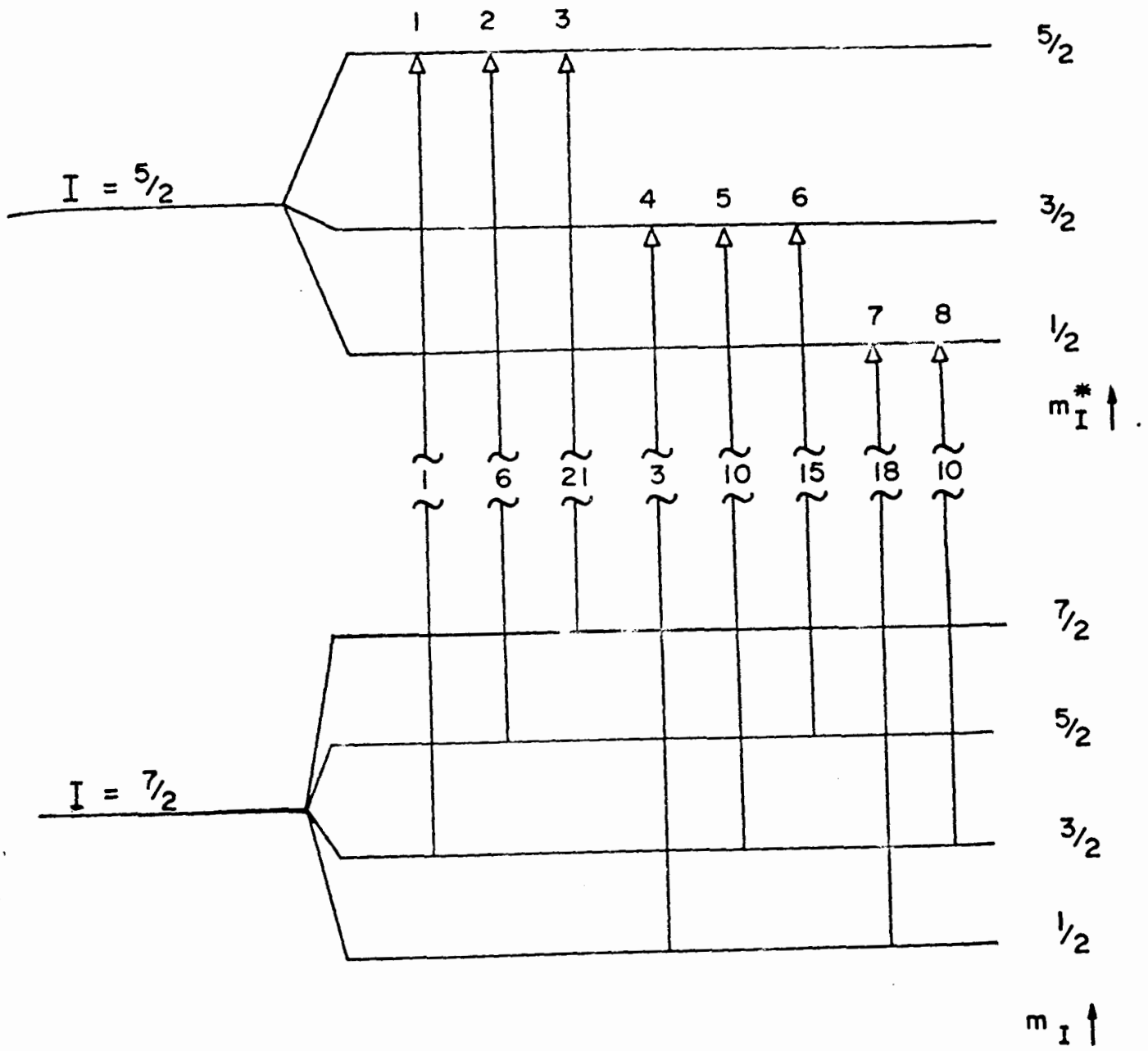

Figure 3 ^{129}I Quadrupole Splitting for e^2qQ_{gnd} Positive Clebsch-Gordon Coefficients, $\widetilde{CG}^2$, are Given Showing the Relative Transition Probabilities.

VI. THE MÖSSBAUER EFFECT FOR ^{129}I

A. Choice of the Mössbauer Nucleus

There are three Mössbauer nuclei found among the isotopes of tellurium and iodine, namely ^{125}Te, ^{127}I and ^{129}I. Of these, ^{129}I exhibits the most favorable characteristics for the study of the chemical effects of nuclear transformations in tellurium compounds.

Thus the 35.5 keV, 1.6 nanosecond Mössbauer transition in ^{125}Te (Figure 4(a)), is characterised by a very large natural line width, $2\Gamma = 5.32$ mm. sec^{-1}., while the observed isomer shifts are relatively small as a consequence of a small ΔR value. These two factors together lead to complex irresolved spectra when more than one tellurium chemical species is present.[124-126] Moreover, the quadrupole coupling constants, e^2qQ, observed for tellurium nuclei in an electrostatic field gradient, q, are relatively small in comparison with those observed in analogous iodine compounds, because of the small value of the quadrupole moment Q.

The 57.6 keV, 1.9 nanosecond Mössbauer transition in ^{127}I (Figure 4(b)) again has a broad natural line width, $2\Gamma = 2.54$ mm. $sec.^{-1}$, while the isomer shifts are again observed to be small. The quadrupole coupling

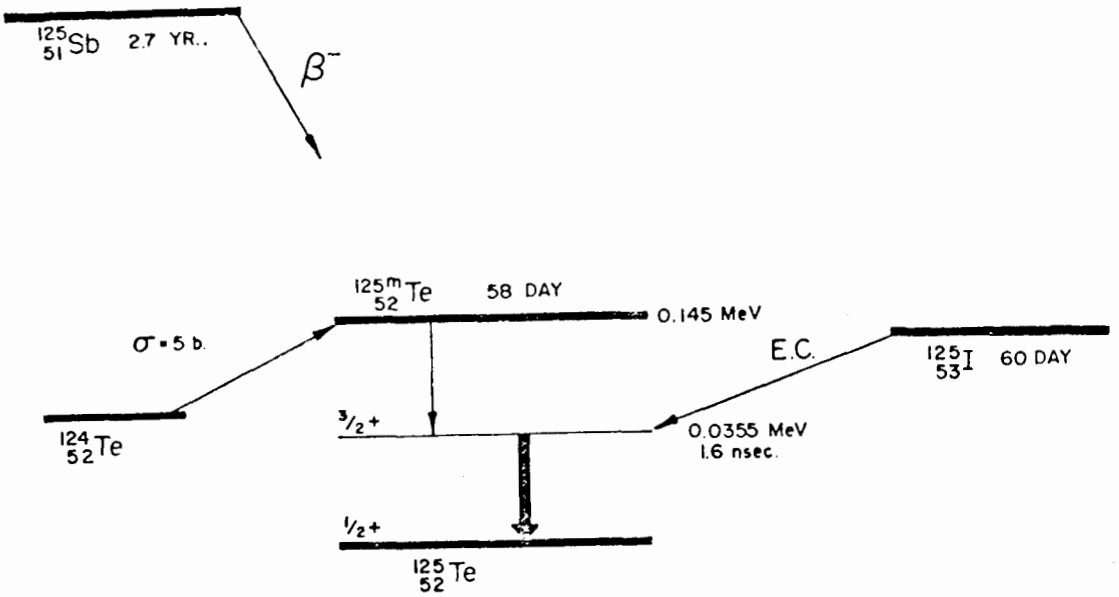

(a)

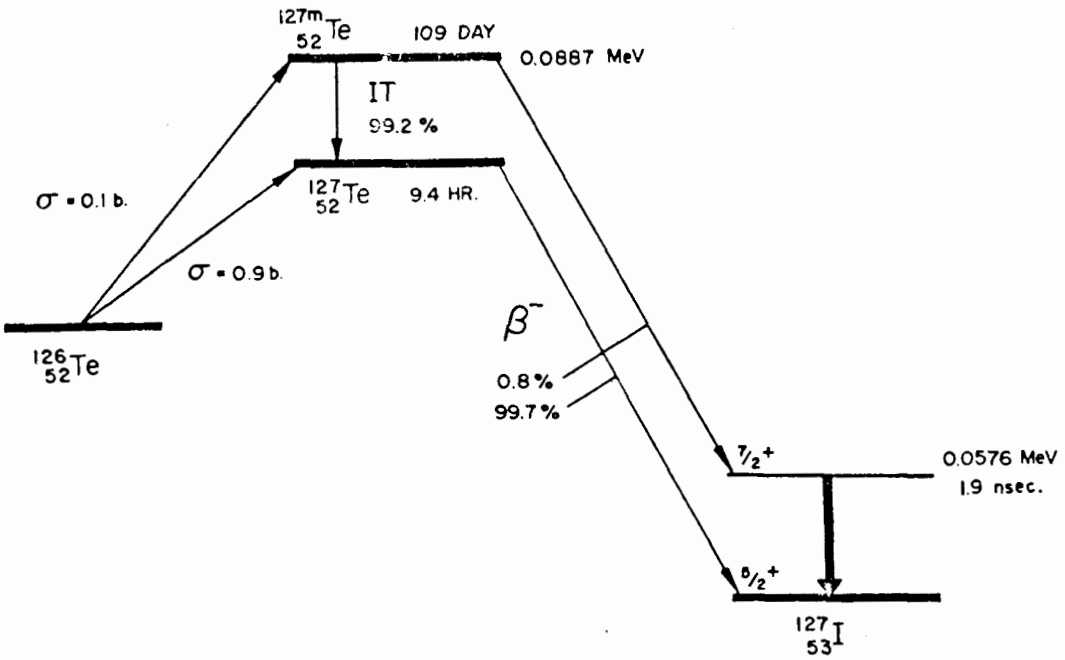

(b)

Figure 4 Decay Scheme Showing the Population of the Mössbauer Transitions in (a) ^{125}Te and (b) ^{127}I [86].

constants for the ^{127}I nuclei are slightly greater than those for ^{129}I in the same chemical environment. However, this factor is outwayed by the large value of 2Γ. Finally, the high energy, 57.6 keV, of the ^{127}I transition demands that the source and absorber be held at liquid helium temperatures in order to obtain measurable resonance absorptions, and such experiments are not only costly but difficult to perform.

In comparison with the above, the 27.7 keV, 16.8 nanosecond ^{129}I Mössbauer transition[127] yields a narrow natural line width, 2Γ = .59 mm. sec.$^{-1}$ with relatively large isomer shifts and quadrupole coupling constants. This may be illustrated by reference to the experimentally measured isomer shift ratios and quadrupole coupling constant ratios previously reported in the literature.

$$\frac{\delta(^{129}I)}{\delta(^{125}Te)} = 3.15\,[128] \qquad \frac{\delta(^{129}I)}{\delta(^{127}I)} = -2.67\,[129]$$

$$\frac{e^2qQ\ (^{125}Te)(1 + \frac{\eta^2}{3})^{1/2}}{e^2qQ\ (^{129}I)} = .40\,[130]$$

and

$$\frac{e^2qQ\ (^{129}I)}{e^2qQ\ (^{127}I)} = .70121\,[131] \quad .$$

While the ^{129}I nucleus has the favourable characteristics outlined above, experiments with this Mössbauer

nucleus are complicated by several factors. Thus, as shown in Figure 3, the transition is a 5/2 (excited) - 7/2 (ground) transition and this leads to 8 lines in a quadrupole split spectrum. It must be anticipated that this may result in quite complex spectra in some instances. Furthermore, the 27.7 keV transition has a K-shell internal conversion coefficient of 5.3[127] and thus in only about one in six transitions is the Mössbauer γ-ray emitted.

In performing a Mössbauer experiment with this isotope, a radioactive ^{129}Te or ^{129m}Te source is used to populate the 27.7 keV transition, leading to the emission of the Mössbauer γ-ray (see Figure 2), and an ^{129}I-labelled compound is used as the absorber. Where ^{129}Te is used as the source very rapid experimental manipulations are required because the half-life of this isotope is only 69 minutes. Alternatively, when ^{129m}Te ($t_{1/2}$ = 34 days) is used as the parent isotope, a very high background radiation is encountered, because the $^{129m}Te \rightarrow {}^{129}Te$ isomeric transition is totally internally converted and the resulting Te Kα x-rays (27.4 keV) overlap the Mössbauer transition.

A further point concerns the ^{129}I absorber. Iodine has a natural isotopic abundance of 100 per cent ^{127}I. The isotope ^{129}I is radioactive with a half-life of 1.7×10^7 years, and in its decay produces 29.4 keV xenon x-rays. This adds to the background radiation but may be reduced by placing an indium or tin critical absorber between the

^{129}I absorber and the detector.

Finally, all Mössbauer experiments with ^{129}I must be carried out at or below liquid nitrogen temperatures. The Debye temperature, θ_D, for most tellurium compounds is about 150°K., giving $k\theta_D \simeq 13 \times 10^{-3}$ eV. To obtain a significant recoilless fraction $k\theta_D$ must be greater than E_R and T must be less than θ_D, as was shown previously in expressions (V-5), (V-6), and (V-7). For ^{129}I, $E_R = 3.2 \times 10^{-3}$ eV which meets the first requirement, while the second requires that $T \lesssim 150°K$.

B. Nuclear Transformations Available for Study With ^{129}I

As can be seen from Figure 2, the chemical states of ^{129}I produced by β^--decay from ^{129}Te can be studied using Mössbauer spectroscopy following four different transformation sequences. These are, in telluric acid,

1. $H_6{}^{129}TeO_6 \xrightarrow{\beta^-} {}^{129}I$
2. $H_6{}^{129m}TeO_6 \xrightarrow[\text{transition}]{\text{isomeric}} {}^{129}Te \xrightarrow{\beta^-} {}^{129}I$
3. $H_6{}^{128}TeO_6(n,\gamma){}^{129m}Te \xrightarrow[\text{transition}]{\text{isomeric}} {}^{129}Te \xrightarrow{\beta^-} {}^{129}I$
4. $H_6{}^{128}TeO_6(n,\gamma){}^{129}Te \xrightarrow{\beta^-} {}^{129}I$

In these experiments the ^{129}Te-or ^{129m}Te-labelled compound is used as the source in the Mössbauer experiment and the resonance spectrum recorded against a standard $Na^{129}I$

absorber. The Mössbauer spectrum should then reflect the chemical effects accompanying the various transformations.

The results of the above Mössbauer experiments may be directly compared with similar radiochemical studies. Thus, the transformation sequences of (2), (3) and (4) above are basically the same as sequences (5), (6) and (7) discussed previously in Section III-B concerning the radiochemical investigation of tellurium recoil atoms. The only difference that exists is that in the above Mössbauer studies there is an additional β^--decay, which populates the ^{129}I Mössbauer transition.

The thermal annealing of the ^{129}Te recoil atoms produced following (n,γ) activation and isomeric transition may also be investigated using Mössbauer spectroscopy, and the results again compared to those for the radiochemical investigation. In addition, we can now study the chemical effects of β^--decay and isomeric transition occurring in crystals maintained at very low temperatures, for example at liquid nitrogen or liquid helium temperatures. This is a very important point because it allows the study of these processes under conditions where little or no thermal annealing will occur. Such studies cannot be made using radiochemical methods of analysis because some annealing must certainly occur as the crystals are warmed to ambient temperature during dissolution.

Let us now examine the previous work in which the Mössbauer effect with ^{129}I has been applied as a probe to study the ^{129}I atom in iodine compounds. This will illustrate how the measurable parameters in a Mössbauer spectrum can be used to obtain meaningful information about the chemical environment of the iodine Mössbauer nucleus.

C. Analysis of the Mössbauer Effect with ^{129}I in Iodine Compounds

The Mössbauer effect using ^{129}I was first observed by Jha et al.[132] and, because of the favorable Mössbauer effect properties found for the ^{129}I nucleus, much work has been carried out recently with a variety of iodine compounds. Groups of iodine compounds which have now been extensively investigated include the iodine oxides,[133-136] alkali halides,[134,137,138] mixed iodine-halogen compounds,[139,140] and molecular iodine.[141,142]

Iodine compounds have been extensively studied in the past by nuclear quadrupole resonance spectroscopy, from which accurate quadrupole coupling constants (e^2qQ), and asymmetry parameter constants(η) have been obtained.[131,143] However Mössbauer spectroscopy allows not only the measurement of these parameters, but also the determination of the sign of the electric field gradient and the isomer shift, and provides detailed information about chemical bonding and lattice dynamics.

1. Analysis of Isomer Shift Data

Where the Mössbauer spectrum is a single absorption line, the isomer shift may be obtained directly. However, in order to obtain the isomer shift for a quadrupole split spectrum, the centroid of the eight line spectrum must be found. Bershon[144] has derived an expression for the position of each line in a quadrupole split spectrum as a function of the isomer shift, assuming that only terms up to η^2 need be considered.

$$\delta_{ij} = \frac{ce^2qQgnd}{4E_\gamma}\left[\frac{Qex}{Qgnd}\frac{(Co^* + C_2^*\eta^2)}{I^*(2I^* - 1)} - \frac{(Co + C_2\eta^2)}{I(2I - 1)}\right] + \delta \qquad \text{(VI-1)}$$

where δ_{ij} is the position of the line corresponding to the $m_i \rightarrow m_j$ transition, δ is the isomer shift, and the remaining constants are as defined in expressions (V-14), (V-15), and (V-16). $\frac{Qex}{Qgnd}$, the ratio of the quadrupole moments of the excited and ground states, is 1.231 ± 0.001.[134,141]

Cohen[145] has calculated the line positions in the eight-line spectrum for intervals of η and has shown that only the positions of lines 4 and 8 are in fact sensitive to η. The above expression can therefore be used to determine values for δ, e^2qQgnd, and η in the following way. The observed positions of the lines other than 4 and 8 are used to determine δ and e^2qQgnd by neglecting the terms in η^2. Then, by iteration, η can be obtained from the positions of lines 4 and 8.

The relationship between the isomer shift and the s-electron density of the Mössbauer nucleus was given in expression (V-11), which for ^{129}I becomes

$$\delta = 2.23 \times 10^{-23} \frac{\Delta R}{R} [|\psi s(0)|_a^2 - |\psi s(0)|_s^2] \qquad \text{(VI-2)}$$

where

$$\frac{\Delta R}{R} = \frac{Rex - Rgnd}{Rgnd} = + 3 \times 10^{-5} \text{[134]} \qquad \text{(VI-3)}$$

The positive value for $\frac{\Delta R}{R}$ for ^{129}I indicates that if the s-electron density at the absorbing nucleus is greater than that at the source nucleus, the isomer shift will be positive in sign. The ^{129}I isomer shifts for a variety of iodine absorbers are shown in Figure 5. All of the isomer shifts are reported relative to ^{129}I as produced by β^--decay in a standard ZnTe source.

Some of the important features of the ^{129}I isomer shifts may be best illustrated by considering the specific cases of IO_6^{5-}, IO_4^-, IO_3^- and I^-. The δ value for IO_6^{5-} is large and negative, while that for IO_4^- is also negative but smaller in magnitude. These isomer shifts correspond to a low s-electron density at the iodine nucleus, in

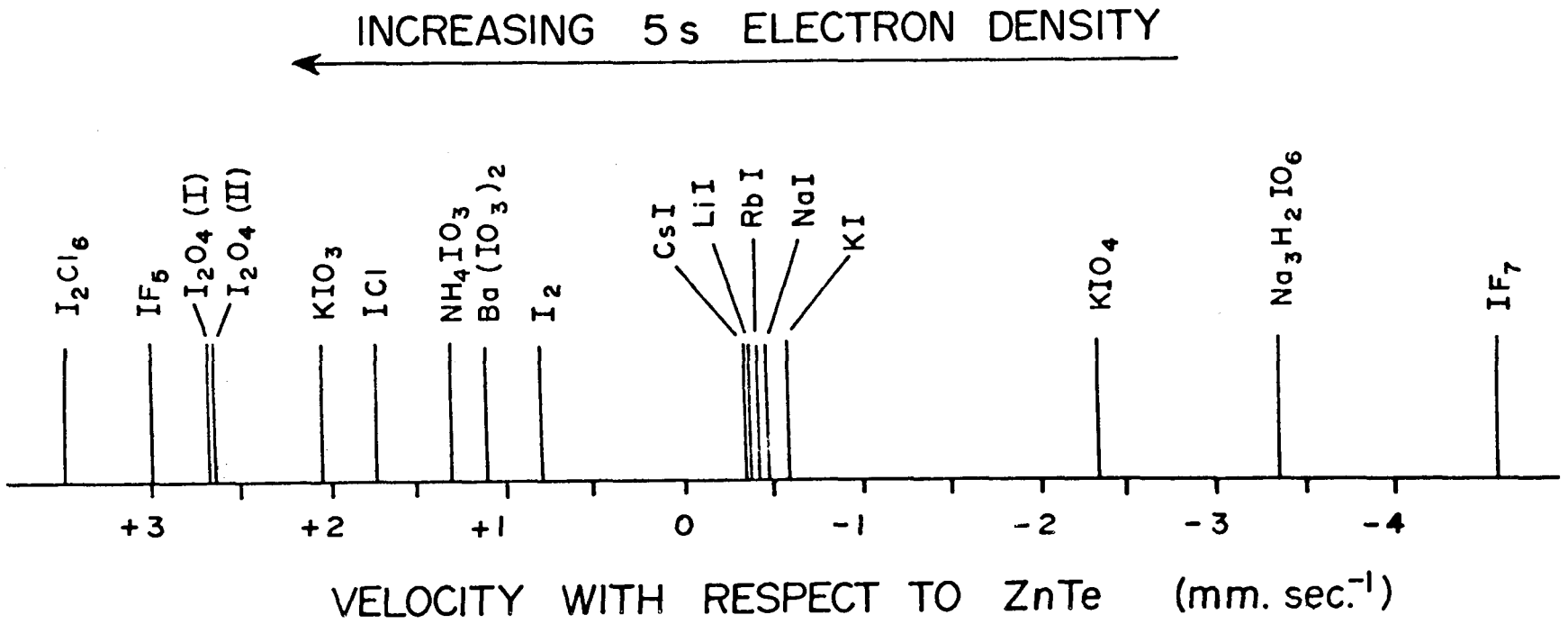

Figure 5 A Comparison of Isomer Shifts for ^{129}I-Labelled Iodine Compounds. A Positive Velocity Corresponds to the ZnTe Source Moving Towards the Absorber.

comparison with that in the I^- ion in the ZnTe source, and may be explained by the presence of sp^3d^2 hybridisation in IO_6^{5-} and sp^3 hybridisation in IO_4^-. The 5s electrons on the iodine are thus delocalised into the bonding orbitals in these compounds leading to a low $|\psi_s(0)|^2$.

The isomer shift values for the iodides are clustered near to $\delta=0$. This means that in the various iodide lattices the I^- ion is very similar in electronic configuration to the I^- ion formed in the radioactive decay of the Te^{2-} ion in the $Zn^{129}Te$ source ($^{129}Te^{2-} \xrightarrow{\beta^-} {}^{129}I^-$). The fact that all the iodides do not have exactly the same δ, however, is of interest. The formal electronic configuration in the valence shell of the I^- ion is $5s^2\ 5p^6$. The 5p electrons are effective in screening the 5s electrons from the nucleus. The small differences in δ in going from KI through to CsI (Figure 5) may be explained by invoking a small loss of 5p electrons from the I^- ion in CsI, this leading to decreased shielding of the $5s^2$ electrons from the nucleus, a higher value of $|\psi s\ (0)|^2$, and thus a more positive isomer shift. It must be noted that this proposal concerning the removal of 5p electrons from the iodine in the alkali iodides was made prior to the Mössbauer experiments, to explain the nuclear magnetic resonance chemical shifts[146] in these compounds, and appears to fit in well with the Mössbauer δ data.

The isomer shifts for the iodates are positive in marked contrast with IO_6^{5-} and IO_4^-. The explanation for

this is that in the iodate ion the iodine does not employ hybrid orbitals, but that it uses pure p-orbital electrons in bonding to the oxygens. This is born out by the fact that the O-I-O bond angles are ca. 90° in iodates. The removal of 5p electrons from the iodine into the bonding orbitals leads to decreased shielding of $5s^2$ electrons from the nucleus, again with an increase in $|\psi s(0)|^2$ as reflected in large positive values for the isomer shifts. The same explanation has been proposed to explain the bonding in the mixed iodine halogen compounds such as ICl and I_2Cl_6.[139]

In describing the bonding in iodates and I-Cl compounds a simple relationship has been derived which relates the isomer shift, δ, to the number of p electrons transferred from the central iodine to the ligands[142]

$$\delta = 1.5\ hp - 0.54 \qquad \text{(VI-4)}$$

where hp is the number of p-electron holes in the $5s^2\ 5p^6$ configuration of the I^- ion and δ is in mm. $sec.^{-1}$ measured relative to ZnTe. Thus, the iodate ion is considered to be formed from the I^- ion and three O ligands. The isomer shift for KIO_3 is +1.6 mm. $sec.^{-1}$ and thus 0.47 5p electrons are transferred from the iodine to each oxygen in the iodate ion in this compound. This value is in good agreement with that obtained from N.Q.R. measurements by Dailey and Townes (0.5),[147] and Gordy and Thomas (0.44).[148]

In examining the isomer shifts for IF_5 and IF_7 it is apparent that a simple picture of pure p - bonding, analogous to that in I_2Cl_6, breaks down.[140] It appears that the very high electronegativity of the fluorine leads to the removal of 5s electrons as well as 5p electrons from the iodine. These two factors work in opposition in influencing δ. In these cases δ can be related to the number of s and p electrons taken from the iodine in forming the bonds [142]

$$\delta = -8.2\ hs + 1.5\ hp - 0.54 \qquad \text{(VI-5)}$$

where hs is the number of electron holes in the 5s shell of the closed configuration $5s^2\ 5p^6$. The above description of the bonding in IF_5 and IF_7 is obviously a simplistic one since some hybridisation is almost certainly involved.

2. Analysis of Quadrupole Splitting Data

Only those iodine compounds possessing nearly perfect cubic (I^-), tetrahedral (IO_4^-), or octahedral (IO_6^{5-}) symmetry about the iodine atom are observed to give a single Mössbauer absorption line. The quadrupole splitting observed for other iodine compounds provides detailed information about chemical bonding which is complementary to the information obtained from isomer shifts. It was shown earlier in reference to equation (VI-1) how the quadrupole coupling

constant e^2qQ and the asymmetry parameter η may be calculated from a quadrupole split spectrum.

The electrostatic field gradient (e.f.g.) q, and thus the quadrupole coupling constant e^2qQ, is determined by the spatial distribution of electrons around the nucleus. The relative distribution of p-electrons in the x, y and z directions will be directly reflected in the e.f.g., while s electrons, which have spherical symmetry, do not contribute directly to the e.f.g., but may make a second-order contribution in the case of hybrid orbitals. If we consider only the case of pure p-bonding, the description of e^2qQ and η in terms of the p-electron distribution is quite simple. In such an analysis the principal axis of the molecule is defined as the z-axis. Then $e^2q_{mol}Q$, the quadrupole constant for the molecule of interest is defined as [149]

$$e^2q_{mol}Q = -U_p e^2q_{at}Q \qquad \text{(VI-6)}$$

where $e^2q_{at}Q$ is the quadrupole coupling constant for one P_z electron, and the value for ^{129}I deduced from nuclear quadrupole resonance studies is -1607 Mc. $sec.^{-1}$ U_p is defined as the p electron deficit or excess along the z-axis and is given by

$$Up = -U_z + \frac{(Ux + Uy)}{2} \qquad \text{(VI-7)}$$

where Ux, Uy and Uz are the electron populations in x, y and z directions respectively.

The asymmetry parameter, which defines the divergence from axial symmetry in the molecule, is then given by[150]

$$\eta = \frac{3}{2} \frac{Ux-Uy}{U_z} \qquad \text{(VI-8)}$$

The experimental measurement of e^2q_{mol} Q and η do not alone allow the determination of Ux, Uy and Uz. However, for the case of pure p bonding:

$$hp = 6 - (Ux + Uy + Uz) \qquad \text{(VI-9)}$$

where hp can be obtained from δ as previously described. Thus it is possible to determine values for Ux, Uy and Uz, this then providing a fairly detailed picture of the distribution of p electrons in the molecule. Such analyses have been carried out with varying degrees of success for several ^{129}I compounds in the past.[135,139,142]

VII. PREVIOUS APPLICATIONS OF MÖSSBAUER SPECTROSCOPY TO THE STUDY OF CHEMICAL EFFECTS

In studying the chemical effects of nuclear transformations, using Mössbauer spectroscopy as a solid-state probe, the experiments take the following form. The solid containing the radioactive recoil atoms is used as the Mössbauer source and a standard single-line absorber is employed. The Mössbauer spectrum then reflects the different chemical forms of the atoms in the source as produced in the preceding nuclear transformation. Such studies have been carried out with the following Mössbauer nuclei: ^{57}Fe[23,151-175], ^{119}Sn[173,176-183], ^{40}K[184,185], ^{61}Ni[186], ^{125}Te[124-126,187-189], ^{127}I[190], ^{129}Xe[191], ^{129}I[192,193], $^{156,158}Gd$[194], $^{177,178,180}Hf$[195], ^{193}Ir[196], and ^{237}Np[22]. The next section is a brief review of the previous investigations of the chemical effects for Mössbauer nuclei other than tellurium or iodine.

A. Studies With Mössbauer Nuclei Other than Tellurium and Iodine

The greatest portion of this work has been carried out with ^{57}Fe and a further sizable portion with ^{119}Sn.

1. ^{57}Fe

The 14.4 keV, 98 nanosecond ^{57}Fe Mössbauer transition is populated in the electron capture decay of ^{57}Co. In this decay event Auger charging occurs and the resulting ^{57}Fe Mössbauer spectrum might be expected to show a distribution of charge states for the ^{57}Fe atoms stabilised in the solid. Indeed, in ^{57}Co-labelled or doped compounds, the daughter ^{57}Fe atoms are often found to be in several oxidation states. Thus for example in $^{57}Co(II)$ doped Cu_2O, Fe^{+}, Fe^{2+}, Fe^{3+}, and Fe^{4+} have been observed following the decay.[171]

The origin of the charge states observed in such studies is, however, open to several interpretations. In ^{57}Co doped metal oxides and alkali metal halides the several oxidation states of iron observed may in some instances arise from the association of mobile crystal defects, such as cation vacancies, with the daughter ^{57}Fe ion.[175] Herber and Hazony[196] have proposed that pressure effects may play some part in explaining the distribution of charge states. Thus, when $^{57}Co(III)$ decays to ^{57}Fe, the increase in nuclear radius in the daughter ^{57}Fe ion may give rise to an internal pressure effect which may then manifest itself as anomolous charge states in the resulting ^{57}Fe Mössbauer spectrum. This theory has some support in that $^{57}Fe(III)$ absorbers placed under high pressure give Mössbauer spectra which show an apparent reduction of $Fe(III) \rightarrow Fe(II)$.[197,198]

These spectra are very similar to those observed following the decay of ^{57}Co in similar compounds.

Bhida and Shenoy[176] proposed in some early work that the ^{57}Fe charge states formed in the decay of ^{57}Co may be changing during the lifetime of the Mössbauer nucleus, i.e., that metastable states are formed following the decay with lifetimes comparable with the 98 nanosecond half-life of the 14.4 keV state. More recent experiments have been reported by Triftshauser et al.[23,171] in which the time differential Mössbauer spectrum was recorded for selected variable survival times of the Mössbauer state in ^{57}Fe, ranging from 4 to 140 nanoseconds following the electron capture event. These spectra were interpreted as showing only a relativistic "time-filtering" effect, with no evidence of any change in the distribution of ^{57}Fe recoil fragments. This indicates that the Auger charging process and resulting electronic rearrangements and charge neutralisation processes are all complete in a time less then ca. 10^{-8} second.

While many investigations of chemical effects have been made using ^{57}Fe Mössbauer spectrosopy , this system does not readily allow for a direct comparison between radiochemical and Mössbauer studies because ^{57}Fe is a stable nucleus. Fenger and Siekierska[168] have recently compared the chemical effects of electron capture, observed using Mössbauer spectroscopy, in $^{57}Co\ C_2O_4 \cdot 2H_2O$ with radiochemical

studies of the neutron capture reaction $^{58}Fe\ (n,\gamma)\ ^{59}Fe$ in $FeC_2O_4 \cdot 2H_2O$. Similar results were obtained in the two experiments in terms of the distribution of the iron recoil atoms between the Fe^{2+} and Fe^{3+} oxidation states. However, the significance of these findings is questionable since here one is comparing the chemical effects of two different nuclear transformations in two different compounds.

2. ^{119}Sn

The 23.7 keV, 19 nanosecond Mössbauer transition in ^{119}Sn is populated in the highly internally converted isomeric transition of ^{119m}Sn. In compounds labelled with ^{119m}Sn the effects of the Auger cascade in the isomeric transition may thus be studied. The effects of thermal neutron capture may also be investigated for the reaction $^{118}Sn\ (n,\gamma)\ ^{119m}Sn$, using the irradiated solid as the source in the Mössbauer experiment. The results of such experiments have shown the formation of both oxidised and reduced states of the daughter ^{119}Sn recoil atom in many compounds.

Hannaford, Howard, and Wignal[178] were the first to compare the results of Mössbauer and chemical methods of analysis for tin compounds. They observed that following the nuclear reaction $^{118}Sn\ (n,\gamma)\ ^{119m}Sn$ in $Mg_2{}^{118}SnO_4$, that the Mössbauer spectrum for ^{119}Sn contained a weak secondary absorbtion line attributable to $^{119}Sn(II)$. Thermal

annealing of this sample removed the ^{119}Sn(II) line, with the line of the parent compound Sn(IV) increasing in intensity. Chemical analysis of this same sample upon dissolution, however, showed only ^{119m}Sn(IV) following thermal neutron capture.

This was the first instance in which chemical and Mössbauer methods of analysis of the effects of the same nuclear reaction in the same compound, were found to give different results. This work has since been repeated by Andersen,[181] who observed exactly the same effects.

3. Other Systems

In the present context it is relevant to discuss two other Mössbauer experiments. Perlow and Perlow[191] studied the effects of the β^--decay $^{129}I \xrightarrow{\beta^-} {}^{129}Xe$ in a variety of parent iodine compounds, using the 39.6 keV, 1.0 nanosecond Mössbauer transition in ^{129}Xe. They found that in every decay event the daughter molecule remained intact, the ^{129}Xe remaining bonded to the ligands of the parent iodine molecule. In this study the synthesis, and chemical bonding and structure, of several new xenon compounds was studied.

Rother, Wagner, and Zahn[195] have examined the chemical consequences of the ^{192}Os (n,γ) ^{193}Os nuclear reaction and subsequent β^--decay of ^{193}Os in several osmium compounds using the 73 keV, 6 nanosecond Mössbauer transition

in ^{193}Ir. They observed extensive molecular decomposition accompanying the (n,γ) reaction in osmium oxides and halides. Moreover, they identified several iridium compounds in the Mössbauer spectrum which had not previously been observed, namely IrO_4^- and IrO_4^+. Indeed, the highest oxidation state of iridium in compounds previously prepared is +6, while compounds of the type $[IrO_4]^{n-}$ have not previously been reported.

B. Studies with Isotopes of Tellurium and Iodine

1. ^{125}Te

The 35.5 keV, 1.6 nanosecond Mössbauer transition in ^{125}Te may be populated in the isomeric transition decay of ^{125m}Te, the electron capture decay of ^{125}I, and the β^--decay of ^{125}Sb. The $^{124}Te(n,\gamma)\ ^{125m}Te$ reaction may also be studied using this Mössbauer state (see Figure 4(a)). The chemical effects of these transformations have been extensively studied in recent years, much of this work being reported while the present thesis work was in progress.

Violet and Booth[124] investigated the effects of electron capture and Auger charging in $Na^{125}IO_3$. They observed a broad irresolved absorption which they interpreted in terms of the presence of two tellurium fragments, Te(V) and Te(VI), formed in the decay, with each giving a quadrupole split spectrum. Subsequently, Jung and

Triftshauser[125] repeated the experiment, observing identical spectra which they interpreted in a quite different way. They concluded that following electron capture in $Na^{125}IO_3$, $^{125}TeO_3^{2-}$ and $^{125}TeO_3$ (or $^{125}TeO_4^{2-}$) are formed. In $Na^{125}IO_4$ they identified the presence of $^{125}TeO_3^{2-}$ and $^{125}TeO_4^{2-}$, while in $Na_3H_2\ ^{125}IO_6$ the tellurium appeared to remain bonded in the parent chemical form, yielding $Na_3H_2\ ^{125}TeO_6$. The different interpretations arrived at by the two groups for the results in $Na\ ^{125}IO_3$ clearly illustrate the problems which arise because of the very broad line widths for the ^{125}Te transition (2Γ = 5.32 mm. sec^{-1}.).

Studies of the ^{125}Te spectrum following β^--decay in ^{125}Sb-labelled antimony (III) and (V) oxide and halide compounds show no chemical effects accompanying this decay, consistent with the low electronic excitation and kinetic recoil energy expected in the decay event.[125]

Several reports have appeared of studies of the $^{125m}Te \rightarrow {}^{125}Te$ isomeric transition in ^{125m}Te-labelled compounds, although details of the work have yet to be published. Levedev *et al.*[187] observed a broadened asymmetric line in the emission spectra for the sources $H_6\ ^{125m}TeO_6$ and $Na_2H_4\ ^{125m}TeO_6$, which they interpreted as evidence for molecular fragmentation accompanying the isomeric transition. Maddock[189] has studied the Mössbauer emission spectrum of $Na_2\ ^{125m}TeO_4$ and observed no effects of the isomeric transition.

The chemical effects accompanying the ^{124}Te (n,γ) ^{125m}Te nuclear reaction were studied by Ullrich[188] in tellurium metal, PbTe, and tetragonal TeO_2. In none of these solids was there any evidence of atomic displacement occurring as a result of recoil. Annealing studies were also attempted in this work, although again no statistically significant effects were observed.

2. ^{127}I and ^{129}I

Neither of these Mössbauer nuclei has been extensively used to study the chemical effects of radioactive decay, although several isolated experiments of some interest have been reported. In the initial work of Perlow and Perlow,[190] the ^{127}I emission spectrum of $H_6\,^{127m}TeO_6$ was studied. In this experiment the observed spectrum was an unsplit, though somewhat broadened, single line whose isomer shift corresponded to that for an IO_6^{5-} ion. Here, the decay of ^{127m}Te proceeds directly to the 57.6 keV Mössbauer transition in ^{127}I by β^--decay (see Figure 4(b)) and it was concluded that the β^--decay did not result in observable molecular disruption.

The above experiment was subsequently repeated by Pasternak[192], only now using the ^{129}I Mössbauer transition as a probe. For a pure monoclinic $H_6\,^{129}TeO_6$ source the spectrum exhibited a small, but clearly defined, quadrupole splitting, attributable to the distorted lattice environment

in monoclinic H_6TeO_6. Indeed, this small quadrupole splitting was most probably the cause of the broadened single line in the ^{127}I spectrum, where the much broader ^{127}I Mössbauer lines would completely destroy the resolution in the quadrupole split spectrum. Again the isomer shift of the ^{129}I quadrupole split spectrum corresponded to that of the IO_6^{5-}.

The ^{129}I emission spectra of ^{129}Te-labelled tellurium metal, $Te(NO_3)_4$, and orthorhombic TeO_2 have also been reported following neutron irradiation of these materials.[193] The objective of this work was to study bonding and structure in these tellurium lattices rather than to study chemical effects associated with the nuclear transformation. However, it can be concluded from this work that there were no observable effects associated with the (n,γ) reaction in these compounds.

VIII. EXPERIMENTAL TECHNIQUES

A. General Preparation of Telluric Acid

The telluric acid used in this work was routinely prepared by the oxidation of tellurite ion in 8N HNO_3 with potassium permanganate.[200] The material was precipitated from solution by the addition of concentrated HNO_3, and was filtered and washed with a further portion of concentrated HNO_3. The material was then usually recrystallised from water or dilute HNO_3, and finally dried over P_2O_5 in a vacuum dessicator.

Samples of telluric acid prepared in this way were analysed by potentiometric titration and were found to be >99 per cent H_6TeO_6.[201] The melting points of many different samples, measured in sealed tubes, were in the range 132.5 to 135.5°C., compared with the literature value of 136°C.[202] Thermogravimetric analysis gave decomposition curves identical to those reported in the literature.[202-204]

Telluric acid is reported to have two crystal modifications, the cubic or α-form which is obtained by slow crystallisation from concentrated HNO_3 solution, and the more stable monoclinic or β - form which is obtained from water or dilute nitric acid. The x-ray powder photographs [202-207] and the I.R. spectral data[207,208] have been

reported for these two modifications. It is known that in the cubic form the geometry of the six -OH groups around the central Te is octahedral while in the monoclinic form there is considerable distortion from regular octahedral geometry and that strong Te-O-H $\cdots\cdot$ O-Te hydrogen bonding between adjacent molecules is present. The samples of telluric acid prepared as described above were found to give x-ray powder patterns identical with that for the pure monoclinic structure. The I.R. spectra showed absorptions at 1120, 1180, and 1218 $cm.^{-1}$, characteristic of the Te-O-H distortion modes in the monoclinic form. It is concluded that the samples were in the pure monoclinic form. Attempts to prepare the cubic modification by slow evaporation of concentrated HNO_3 solutions yielded a mixture of the two forms. Since the preparation of labelled samples had to be performed very rapidly in many instances, the crystals were always precipitated from aqueous solution with HNO_3, this always yielding the monoclinic product.

B. Sample Preparations for the Chemical Investigation of Iodine Recoil Atoms in Telluric Acid

1. H_6TeO_6 for Thermal Neutron Irradiation

In studying the $^{130}Te(n,\gamma)^{131,131m}Te \xrightarrow{\beta^-} {}^{131}I$ process samples of telluric acid prepared with naturally isotopic abundant tellurium (34.49 per cent ^{130}Te) were irradiated in milligram amounts in the rabbit-facility of the

University of Washington, Seattle reactor. The thermal neutron flux ranged from 10^{11} to 10^{12} n.cm.$^{-2}$ sec.$^{-1}$ in different irradiations, with a concurrent γ-dose rate of 1 to 10 Mrd. hr.$^{-1}$

2. H_6TeO_6 Prepared Labelled with ^{130}Te and ^{131m}Te

The method of preparation used in each case was essentially the same.

For labelling telluric acid specifically with ^{131}Te, ca. 3 grams of telluric acid were reactor irradiated for 25 minutes. The sample then contained telluric acid molecules labelled with ^{131}Te ($t_{1/2}$=25 minutes), decomposition products formed in the (n,γ) recoil event labelled with ^{131}Te, a similar distribution of products labelled with contaminating ^{131m}Te ($t_{1/2}$=30 hours), and ^{131}I in a variety of chemical forms produced in the decay of ^{131}Te and ^{131m}Te during the irradiation.

The sample was immediately dissolved in 6N HCl containing Te(IV) carrier. Stoichiometric milligram amounts of I^- and IO_3^- carriers were added and the molecular $^{131}I_2$ formed was extracted into chloroform. This gross iodine extraction was repeated three times and was shown to remove all ^{131}I activity from the solution. The ^{131}Te(IV) and ^{131m}Te(IV) present as a consequence of the chemical effects of the (n,γ) reaction were then removed by extraction into 25 per

cent tri-butyl phosphate (T.B.P.) in kerosene. This separation was also shown to be >99 per cent efficient. The gross iodine extraction was then rapidly repeated and the telluric acid crystals immediately precipitated by the addition of 16N HNO_3, and dried over P_2O_5. The time from the end of the reactor irradiation to filtering the precipitated $H_6{}^{131}TeO_6$ was no more than 20 minutes. Following this sample preparation, ^{131}I activity was observed to grow in with a 25 minute half-life.

Samples prepared in this way contained principally $H_6{}^{131}TeO_6$. However, the longer-lived ^{131m}Te isomer is also produced in the neutron irradiation. The relative cross-sections of these two isotopes together with their half-lives leads to the presence of ca. 26 per cent ^{131}I from the decay of ^{131m}Te 48 hours after the sample preparation. This value rises to ca. 36 per cent after 10 to 12 days.

Telluric acid was also prepared labelled with ^{131m}Te in a similar way. Following a 2 hour reactor irradiation, the sample was left overnight to allow the decay of ^{131}Te. The $^{131m}Te(IV)$ and ^{131}I were then removed as described above, and the $H_6{}^{131m}TeO_6$ precipitated from solution. The ^{131}I activity was observed to grow into the sample with the 30 hour half-life of the parent ^{131m}Te.

3. H_6TeO_6 Prepared Labelled Specifically with ^{132}Te

Carrier free ^{132}Te was obtained from the Oak Ridge National Laboratory as $Na_2{}^{132}TeO_3$ in NaOH. This was found to contain ^{131}I, ^{103}Ru, and other unidentified long-lived radioactive contaminants. The ^{131}I was removed via the previously described gross iodine extraction. Te(IV) carrier was added and the usual preparation of telluric acid carried out.

C. Sample Preparations for the Chemical Investigation of Tellurium Recoil Atoms in Telluric Acid

1. H_6TeO_6 for Thermal Neutron Activation

The chemical effects of the $^{128}Te(n,\gamma)\ ^{129}Te$ reaction in telluric acid were investigated by irradiating telluric acid prepared from naturally isotopic abundant tellurium (31.79 per cent ^{128}Te) in the Seattle reactor for one hour and immediately analysing the sample.

The $^{128}Te(n,\gamma)\ ^{129}Te$ reaction was investigated by irradiating ^{128}Te enriched (99.46 per cent ^{128}Te) H_6TeO_6 in the N.R.U. reactor at Chalk River at a thermal neutron flux of 2.1×10^{14} n. cm.$^{-2}$ sec.$^{-1}$ with a concomitant γ- dose rate of 100 Mrd. hr.$^{-1}$ The sample was kept at ca. 36°C. by flowing water through holes in an aluminium block in which the sample was mounted. In these latter irradiations the samples were sealed in quartz ampoules.

2. H_6TeO_6 Prepared Labelled with ^{129m}Te for Studies of the Chemical Effects of Isomeric Transition

The samples of ^{128}Te enriched H_6TeO_6 reactor irradiated at Chalk River were used to prepare samples of $H_6{}^{129m}TeO_6$ using the methods outlined in Section B(2) above.

D. Chemical Separations and Analysis of Recoil Fragments

1. Analysis for the Oxidation States of ^{131}I

Both electrophoretic and solvent extraction methods of analysis were employed. The electrophoretic separation could only be used where the specific activity of the samples was high and where the time available for the separation and counting was of the order of hours rather than minutes.

In the electrophoretic separation[209] milligram samples of telluric acid containing the ^{131}I recoil species were dissolved in a basic solution containing I^-, IO_3^-, and IO_4^- carriers, each in ca. 0.0015M concentration. A 5 microliter portion of this solution was spotted near to the end of a strip of Whatmann 3MM paper cut 2 cm. wide and 56 cm. long, which had previously been wetted with a solution 0.005N in NaCl and NaOH. The paper strip was then mounted in an electrophoretic apparatus, the paper being supported between two glass plates with the tapered ends dipping into

baths of 0.005N NaCl/NaOH electrolyte solution. A potential was applied through Cu and Pt electrodes dipping into the electrolytic baths. The separations were generally performed with an applied potential of 2000 volts and a current of 4 milliamps, and took about 20 minutes. In these separations, the I^- fraction moved 12 to 15 cm., the IO_3^- fraction moved 7 to 10 cm., and the IO_4^- fraction moved 1 to 4 cm. Following the separation the strips were carefully dried, cut into 1 cm. lengths, and the individual pieces counted using a 3" x 3" NaI(Tl) scintillation well-counter with a single-channel analyser set on the 0.36 MeV γ-peak of ^{131}I.

The electrophoretic separation was demonstrated to give clean separations of I^-, IO_3^-, and IO_4^- ions using $^{131}I^-$ and synthesised $^{131}IO_3^-$ and $^{131}IO_4^-$ as tracers.

Experiments were performed using different combinations of carriers to see if reproducible results would be obtained in the separation. It was found that for a given sample of telluric acid, the same separation was achieved if the IO_4^- carrier was omitted or if H_5IO_6 was added in addition to the I^-, IO_3^-, and IO_4^- carriers

A simple rapid solvent extraction separation was employed in many of these experiments. This separation allowed only the determination of the fraction of ^{131}I activity present in reduced form (I^-, I_2, IO^-) or in oxidised form (IO_3^-, IO_4^-).

The sample was dissolved in distilled water containing a milligram amount of reagent grade $NaIO_3$. This contained 0.01 per cent I^- which served as carrier for the reduced fraction of ^{131}I. An aliquot of an aqueous solution of iodine was added and the iodine extracted into chloroform. The chloroform extraction was repeated twice. This extraction was effective in removing all ^{131}I present in the reduced forms. The efficiency and selectivity of this separation was demonstrated using $^{131}I^-$, $^{131}IO_3^-$, and $^{131}IO_4^-$ tracers.

It was found that addition of larger quantities of I^- carrier reduced the efficiency of this separation, evidently due to the formation of I_3^- in solution. In other experiments it was found that using the $NaIO_3(I^-)$ carrier, identical results were obtained for dissolution in 0.5N HNO_3 through to 0.5N NaOH. It was also found that in comparing the results of the electrophoretic and solvent extraction separations on the same samples, the same results were obtained within the experimental error for the fractions present as oxidised and reduced radioiodine.

2. Chemical Analysis for the Oxidation States of ^{132}I

In studying the decay $^{132}Te(t_{1/2}=78 \text{ hour}) \xrightarrow{\beta^-} {}^{132}I$ ($t_{1/2}=2.3$ hour), the electrophoretic separation could not be used since the parent ^{132}Te would continue to decay to

the daughter ^{132}I following dissolution and during the separation itself.

Here the solvent extraction separation was always used. This separation was modified because of the presence of the long-lived contaminants whose activities constituted an appreciable fraction of the total sample activity within days of the time of the $H_6{}^{132}TeO_6$ sample preparation.

The sample for analysis was weighed and then dissolved as before in $NaIO_3(I^-)$ carrier solution and the iodine extraction into chloroform immediately performed. A second portion of the sample of a known weight was dissolved and a gross iodine extraction was performed as described previously. A comparison of the specific activities of the two organic fractions, assayed on the .668 and .773 MeV γ-peaks of ^{132}I, gave the percentage of ^{132}I activity present in oxidised and reduced forms following the β^--decay event. The activity in both of these organic fractions was shown by γ-ray spectroscopy to be pure ^{132}I.

3. Analysis for Te(IV) and Te(VI) in Telluric Acid

A solvent extraction separation was used which allowed the determination of the fraction of tellurium activity present in the Te(IV) and Te(VI) states.

A milligram sample was dissolved in 6N HCl containing 5 mg. $ml.^{-1}$ of Te(IV) carrier. The Te(IV) was then immediately

extracted into a 25 per cent solution of T.B.P. in kerosene. This extraction was repeated twice. The ^{129}Te activity remaining in the aqueous fraction was assayed through the .460 MeV γ-peak using a well-counter and single channel analyser. However, the way in which the counting was performed depended upon the specific nuclear transformation under investigation.

In studying the $^{128}Te(n,\gamma)$ ^{129}Te nuclear reaction in telluric acid, the amounts of ^{129}Te existing as Te(IV) and Te(VI) were determined by immediately comparing the activity of the extracted aqueous phase with that of a portion of the solution which had not been extracted.

For the $^{128}Te(n,\gamma)$ ^{129m}Te nuclear reaction, following the separation the aqueous phase was set aside and the ^{129}Te activity allowed to grow back into equilibrium with the parent ^{129m}Te (^{129m}Te(34 day) $\xrightarrow{I.T.}$ ^{129}Te (69 minute)). A comparison of the activity of this solution with that of a portion of non-extracted aqueous phase allowed the fraction of ^{129m}Te activity as Te(IV) and Te(VI) to be determined. The ^{129}Te(IV) and ^{129}Te(VI) distributions formed following the isomeric transition in this same neutron irradiated sample could be determined in the above experiment if the extracted aqueous phase was also counted immediately following the separation.

Finally, in studying the chemical effects of the $^{129m}Te \rightarrow {}^{129}Te$ isomeric transition in ^{129m}Te-labelled telluric acid, the

solid sample was dissolved, the separation immediately performed, and the aqueous phase immediately counted. This same aliquot was then set aside and, following regrowth of the ^{129}Te activity back into equilibrium with the ^{129m}Te, was re-assayed.

E. General Counting Procedures

A 3" x 3" NaI(Tl) scintillation well-counter was used coupled to a Hewlett-Packard pre-amplifier and single-channel analyser. Several multi-channel analysers were used in accumulating γ-ray spectra. In all experiments routine corrections were made for background, decay, and efficiencies of separations.

F. Annealing Investigations

Both thermal and γ-ray annealing effects were studied. Thermal annealing was carried out in air in glass tubes mounted in heated copper blocks or in a thermostated water bath, these having thermal stabilities of ±0.5°C. and ±0.2°C., respectively.

γ-radiation annealing was studied using a ^{60}Co gamma cell which gave a γ-dose rate of ca. 5×10^5 Rads. $hr.^{-1}$

G. Mössbauer Spectrometer Systems Employed

A Technical Measurements Corporation (TMC) constant acceleration Mössbauer spectrometer was used in the early part of this work. A block diagram for this system is shown in Figure 6(a). The basic components included a TMC 400 channel pulse-height analyser, the TMC Model 306 Mössbauer drive unit, and the TMC Model 305 transducer. The analyser was operated in the multi-scaler mode and was synchronised with the movement of the transducer at the beginning, middle, and end of each cycle. With the analyser multi-scaling over 200 channels with a dwell-time per channel of 40 microseconds, the transducer operated at a frequency of 12 cycles per second. In this mode of operation 2 x 100 channel mirror-image spectra were obtained. This transducer is quoted as having a linearity in the velocity drive of < 1 per cent distortion over 90 per cent of the half-cycle. Frequent velocity calibrations of the system using a source of ^{57}Co in palladium measured against sodium nitroprusside and α-Fe_2O_3 standard absorbers confirmed the linearity and stability of the velocity drive.

The cryostat used with the TMC system is shown in Figure 6(b). This was a metal can 6" in diameter and 24" high, with a through tube near to the base. The can was completely encased in styrofoam insulation. The Mössbauer

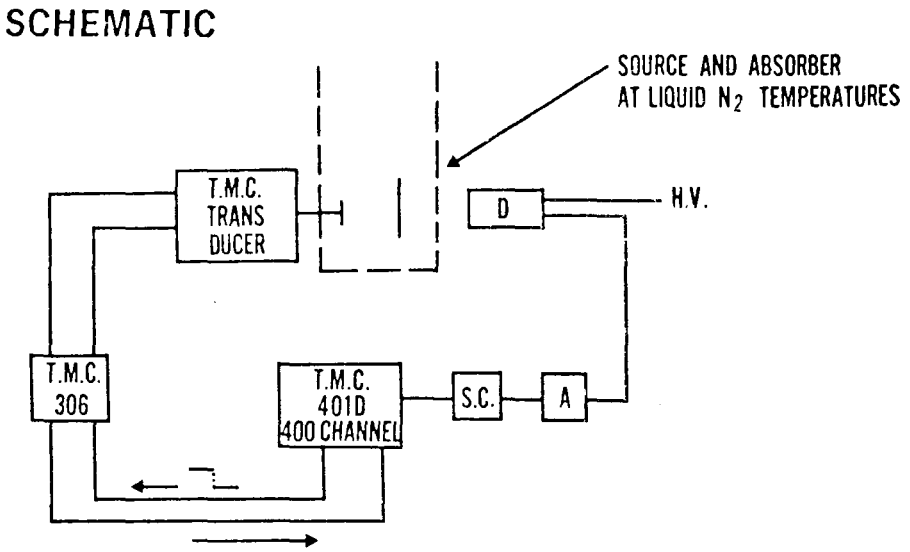

(a)

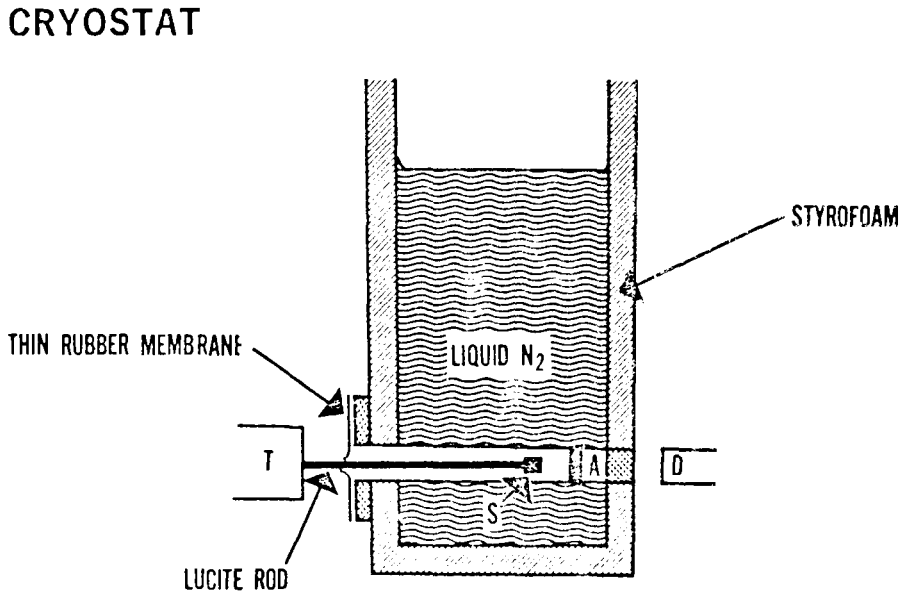

(b)

Figure 6 a. Schematic Diagram of TMC Mössbauer Spectrometer System.
b. Liquid Nitrogen Dewar Used With TMC Transducer.

source and absorber were cooled in the through tube, which was sealed at the detector end by a removable styrofoam plug, and at the source end by a rubber membrane through which the source rod was inserted. Air was blown over the rubber membrane and over the styrofoam plug to minimise the build-up of ice.

This cryostat could maintain the Mössbauer source and absorber near to liquid nitrogen temperature for a maximum of five hours, this then being one of the principle drawbacks of the system. The source and absorber temperatures were measured using an iron-constantan thermocouple, and were found to remain stable at 80 to 82°K. One advantage of this system was the speed with which Mössbauer sources could be mounted when, for example, short-lived 69 minute ^{129}Te-labelled sources were being studied.

A second system employed in this work was a Nuclear Science and Engineering Corporation (NSEC) AM-1 drive system and cryoflask which was used in conjunction with a Nuclear Data 2200 series 1024-channel analyser. A schematic diagram of this system is shown in Figure 7(a), and a diagram of the vacuum cryostat and transducer assembly is shown in Figure 7(b). This spectrometer again functioned at constant acceleration. However, here the transducer was driven by a voltage pulse generated from the output of the scaler address of the multi-channel analyser. In this way there was perfect synchronisation between the movement of the transducer and

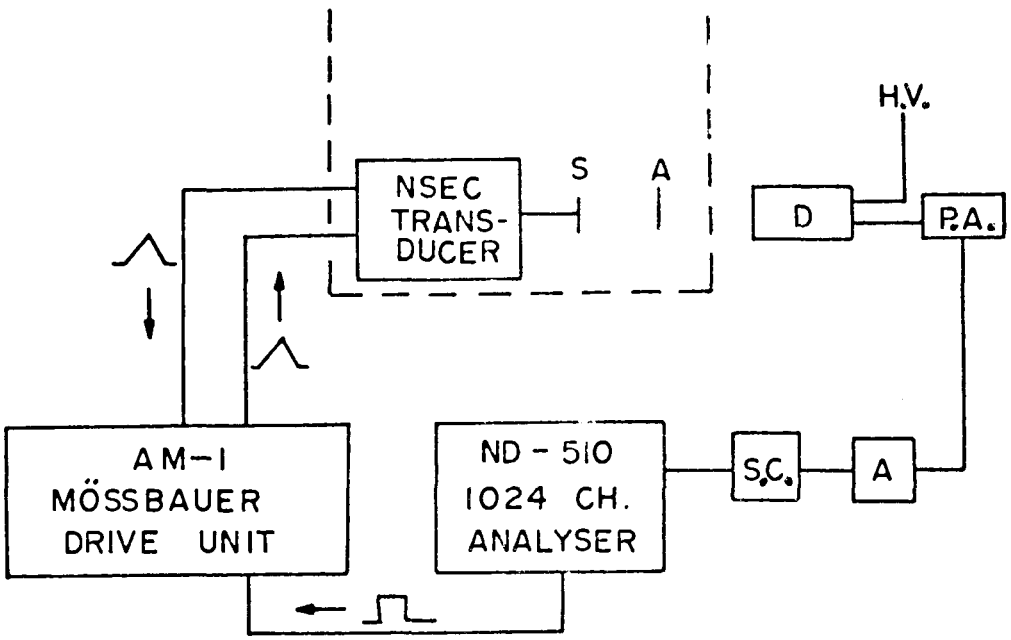

(a)

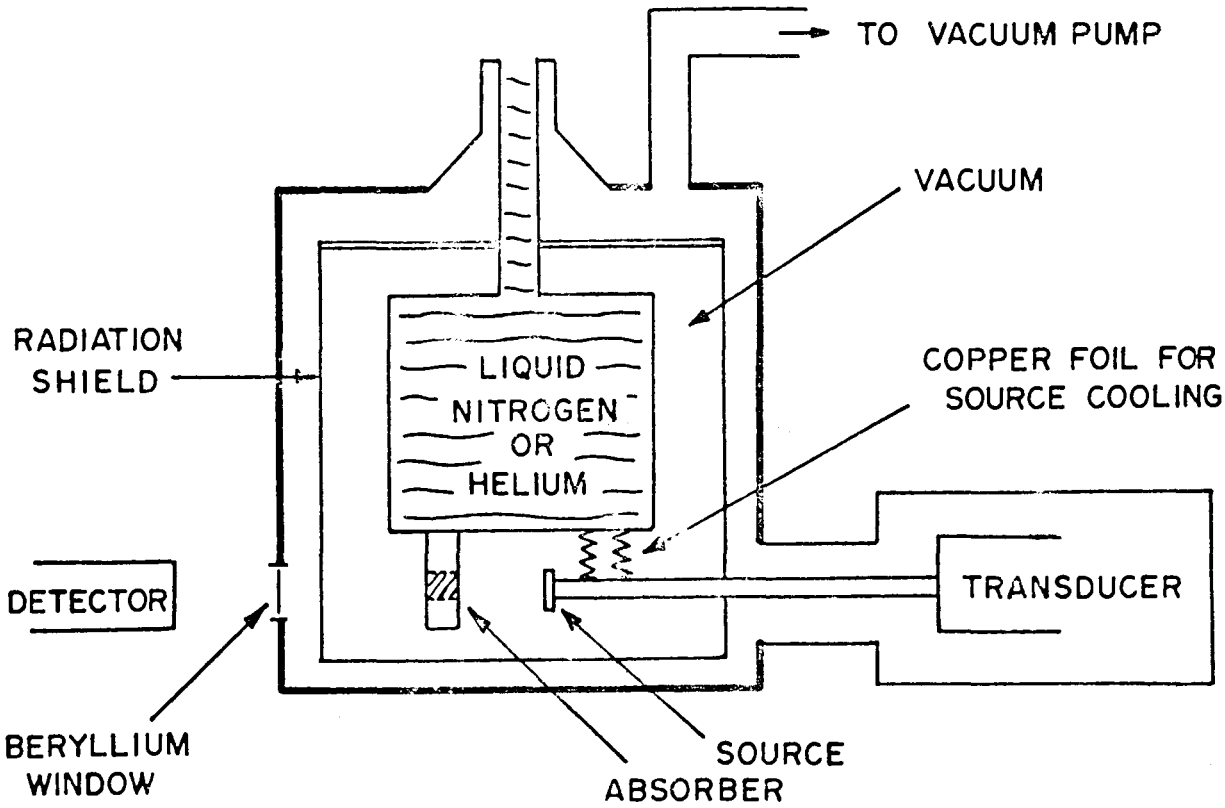

(b)

Figure 7 a. Schematic Diagram of NSEC Mössbauer Spectrometer System
b. NSEC Vacuum Cryostat.

the multi-scaler of the analyser. This resulted in excellent linearity and reproducibility in the velocity drive. Using this spectrometer, 2 x 256 channel or 2 x 128 channel sets of mirror image spectra were obtained, with the transducer operating at 25 cycles per second and a dwell time per channel of 80 microseconds or at 20 cycles per second and a dwell time of 200 microseconds, respectively.

The cryoflask used with this system was a metal vacuum cryostat which held liquid nitrogen for ca. 35 hours, maintaining the source and absorber at 80°K. for this time. Several liquid helium experiments were performed with this cryostat and the liquid helium was found to boil off in ca. 5 hours.

H. Mössbauer Experiments with ^{129}I

1. General Methods

The ^{129}I Mössbauer spectra were recorded using a Harshaw NaI(Tl) x-ray detector, integrally mounted on a photomultiplier tube, together with an Ortec model 113 preamplifier and model 440A selective filter amplifier. The pulse height analysis spectrum for ^{129m}Te sources showed only a single broad peak, the 27.7 keV Mössbauer transition and 27.4 keV tellurium x-rays not being resolved with this detector. An attempt was made to use an Ortec Ge(Li) x-ray detector, with a resolution of 300 to 400 eV at 30 keV.

While this detector partially resolved the Mössbauer transition from the x-rays, the very low counting efficiency made it impractical for use in this work.

While several experiments were performed with an indium absorber to reduce the background from the unresolved ^{129}Xe x-rays, in general experiments were not performed with such a critical absorber present, since the activity from the ^{129}I absorber was only a small fraction of the source activity.

The absorbers used throughout this work were anhydrous Na ^{129}I absorbers, sealed in a plastic cell. These absorbers were prepared by the evaporation of an aqueous solution of Na ^{129}I obtained from Oak Ridge. The dry residue, in each instance, was sealed in a plastic holder in a dry atmosphere. The two absorbers used contained ca. 8 mg. cm.$^{-2}$ and ca. 15 mg. cm.$^{-2}$ of ^{129}I, respectively. They were confirmed as single line absorbers against a Zn^{129m}Te source, and gave line widths of .94 mm. sec.$^{-1}$ and 1.25 mm. sec.$^{-1}$, respectively. These values are in excellent agreement with the values to be expected from the expression

$$\Gamma_{expt} = \Gamma_s + \Gamma_a + 0.27\ \Gamma_a\ T_a \qquad \text{(V-8)}$$

$$= 0.59 + .08\ T_a$$

$$= 0.91 \text{ mm. sec.}^{-1} \text{ (8 mg. cm.}^{-2} \text{ absorber)}$$

$$= 1.19 \text{ mm. sec.}^{-1} \text{ (15 mg. cm.}^{-2} \text{ absorber)}$$

Most of the experiments in this work were performed using the 15 mg. cm.$^{-2}$ Na ^{129}I absorber, and experimental

line widths generally varied between 1.2 to 1.4 mm. $sec.^{-1}$. A representative spectrum for $Na^{129}I$ measured against a Zn ^{129m}Te source is shown in Figure 8.

Sodium iodide is a good choice for an iodine Mössbauer absorber since it has a large recoil free fraction of f = .29[134], and a high Debye temperature of 185°K.[134]

2. Source Activities for ^{129}I Mössbauer Emission Experiments

Chemical effects of the four nuclear transformation sequences previously discussed were investigated for a variety of tellurium compounds, as shown in Table IV. For reasons which will become apparent throughout this and subsequent sections, all of the compounds listed either could not or were not investigated for each of the transformation sequences. The general techniques employed in the preparation of the labelled source coupounds will now be discussed.

The ^{129m}Te was obtained by the irradiation of 50 milligram amounts of 99.46 per cent ^{128}Te metal in quartz ampoules for two weeks at ca. 10^{-14} n. $cm.^{-2}sec.^{-1}$ in the N.R.U. Reactor at Chalk River. The tellurium metal was then used in the preparation of the compounds to be described below. These sources generally ranged in activity from 0.5 to 2.0 millicurie and were generally < 10 mg. $cm.^{-2}$ in thickness.

A novel preparative route was used in the preparation of ^{129}Te Mössbauer sources. In the past, other investigators

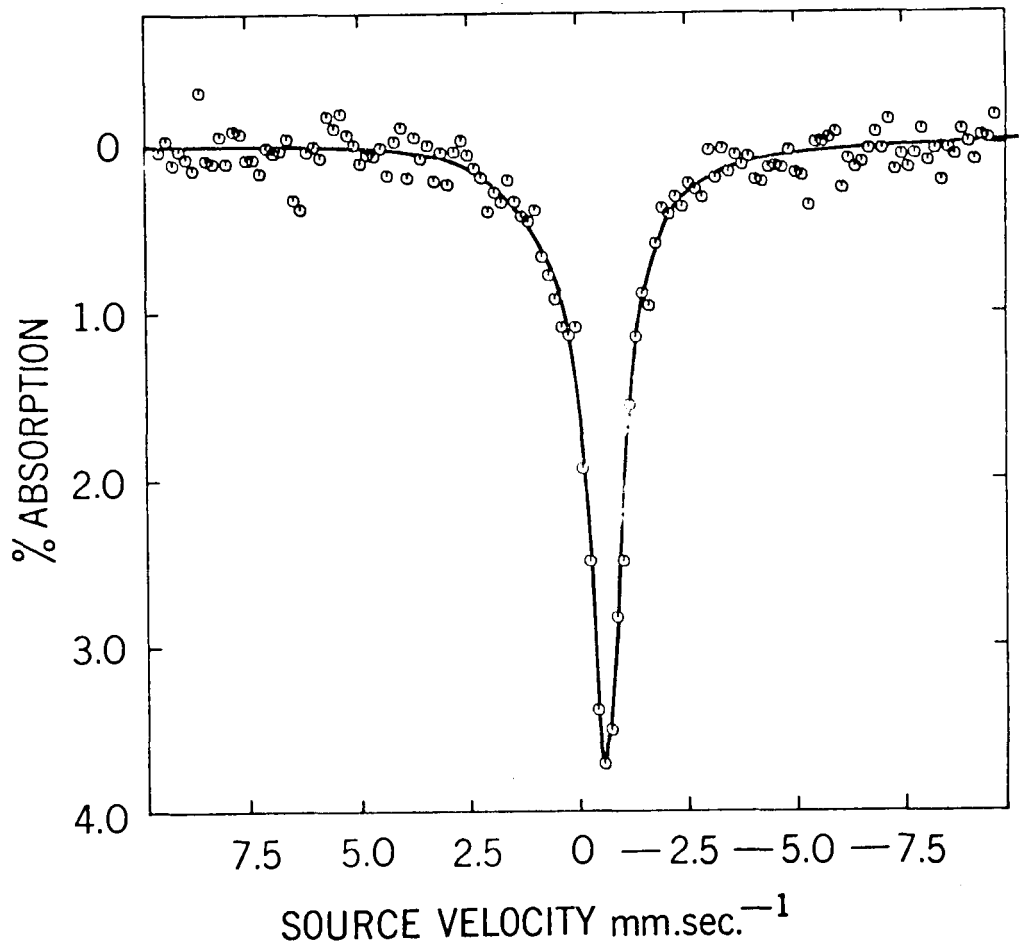

Figure 8 Mössbauer Spectrum of $Na^{129}I$ vs. a $Zn^{129m}Te$ Source Measured at 80°K.

TABLE IV

TELLURIUM COMPOUNDS AND TRANSFORMATION SEQUENCES FOR WHICH ^{129}I MÖSSBAUER EMISSION SPECTRA WERE INVESTIGATED

		^{129}Te	^{129m}Te	^{128}Te(n,γ) ^{129}Te	^{128}Te(n,γ) ^{129m}Te
1	H_6TeO_6	X	X	X	X*
2	$(H_2TeO_4)_n$	X	X		
3	Na_2TeO_4		X		
4	K_2TeO_4			X	
5	α-TeO_3	X	X	X	
6	β-TeO_3		X	X	
7	Te_2O_5		X		
8	H_2TeO_3	X	X		
9	TeO_2	X	X	X	X
10	$(NH_4)_2TeCl_6$	X	X		
11	Elemental Tellurium	X	X	X	X

* Decomposed during the irradiation

have prepared $Zn^{129}Te$ sources for ^{129}I absorbtion spectroscopy by irradiating $^{66}Zn^{128}Te$ in a reactor and immediately using this source in their experiments. The absence of a reactor near to this laboratory precluded this means of producing ^{129}Te. Instead, the isomer separation of ^{129}Te and ^{129m}Te achieved through the chemical effects of the isomeric transition in solution was employed.

^{129m}Te-labelled telluric acid was dissolved in 4N HCl. In 4N HCl solution the $^{129m}Te \rightarrow {}^{129}Te$ isomeric transition produces bond rupture in > 90 per cent of events, giving $^{129}Te(IV)$ in solution. In the presence of Te(IV) carrier, SO_2 is bubbled through the solution, this selectively reducing the $^{129}Te(IV)$ to tellurium metal, the ^{129m}Te remaining in solution as $H_6^{129m}TeO_6$. The separated ^{129}Te-labelled metal was then used in the immediate preparation of the compounds shown in Table IV. The need for rapid manipulations restricted these experiments to compounds which could be prepared and isolated as solids in less than 60 minutes. The sources prepared generally had activities in the range of 0.1 to 0.5 millicurie and were of 25 to 50 mg. $cm.^{-2}$ thickness, the thickness being determined by the amount of carrier which permitted rapid chemical preparations. Source thicknesses in this range were not observed to lead to significant line broadening.

In studying the ^{129}Te recoil atoms produced in the $^{128}Te(n,\gamma)\ ^{129}Te$ reaction, the compounds were irradiated for

60 minutes in the core of the University of Washington, Seattle, reactor at a flux of 2×10^{12} n. cm.$^{-2}$ sec.$^{-1}$, with a γ-dose rate of 10 Mrd. hr.$^{-1}$ The ambient temperature was 70°C. In some experiments the samples were irradiated in a styrofoam insulated container packed with solid CO_2.

Some of the above sources were prepared from naturally isotopic abundant tellurium, while others were enriched in ^{128}Te and ^{125}Te. All sources contained about 10 milligrams of ^{128}Te, and source thicknesses ranged from 25 to 50 mg. cm.$^{-2}$ The activity at the time of removal from the reactor was about 0.05 millicurie.

The ^{129m}Te recoil atoms produced in the reaction ^{128}Te(n,γ) ^{129m}Te were studied using ^{128}Te isotopically enriched compounds irradiated in the N.R.U. reactor in the water cooled assembly. Neutron irradiations were at a thermal neutron flux of 10^{14} n. cm.$^{-2}$sec.$^{-1}$ with a concurrent γ-dose rate of ca. 100 Mrd. hr.$^{-1}$ These compounds were, upon their return following the irradiation, used as Mössbauer source compounds.

3. Preparation and Mounting of Mössbauer Sources

In almost all instances, the Mössbauer source compounds were mixed with a small amount of silicon grease before being placed in the source holder. This was done for two reasons. Firstly, it gave good thermal contact between the source compound and the source holder, thus ensuring that the

Mössbauer source was evenly cooled to at least near liquid nitrogen temperature. Secondly, mixing with the grease made it possible to evenly distribute the source material over the surface of the source holder, this then ensuring a uniform source thickness.

I. Tellurium Compounds Prepared as Mössbauer Sources

1. H_6TeO_6

Telluric acid was prepared and characterised according to the methods described in Section A of this chapter.

2. $(H_2TeO_4)_n$

Metatelluric acid, $(H_2TeO_4)_n$, was prepared by thermal decomposition of telluric acid at 160°C.[203,204] Thermogravimetry on samples prepared in this way showed the theoretical weight loss and the samples were characterised by I.R. spectroscopy.[202]

The similarity in the I.R. spectra of $(H_2TeO_4)_n$ and H_6TeO_6 is interpreted as evidence that in metatelluric acid the tellurium must be hexaco-ordinate and that Te-O-Te edge bridging between adjacent units is present. The value for n is variously reported as 3, 10, and 11, and appears to depend on the method of measurement used.[202]

3. $\underline{Na_2TeO_4}$, $\underline{K_2TeO_4}$

Sodium tellurate was prepared according to the method of Halpern and Dancewicz[113] in which TeO_2 was dissolved in 29 per cent NaOH and then oxidised with 30 per cent H_2O_2. The Na_2TeO_4 precipitate was filtered and washed with hot 29 per cent NaOH.

The potassium tellurate used was obtained from Alfa Inorganics Incorporated, and was used without further purification. The I.R. spectrum for this material showed it to be free of contaminating K_2TeO_3 and TeO_2.

The structure of the tellurates is somewhat in question. The recent work of Erickson and Maddock[207] suggests, on the basis of the I.R. and ^{125}Te data, that tellurates have a structure based on a linear polymeric anion composed of TeO_6 octahedra each sharing two edges, and with the unshared oxygen atoms in cis-positions on a third edge.

4. $\underline{\alpha\text{-}TeO_3}$

This polymeric compound is a bright yellow amorphous powder prepared by thermal decomposition of H_6TeO_6 at 310°C.[202-204] The I.R. spectrum again shows the tellurium to be hexaco-ordinate,[207] and the previously reported ^{125}Te Mössbauer absorption parameters are consistent with this interpretation.[207] The ^{125}Te Mössbauer spectrum also clearly shows the presence of contaminating TeO_2, and in the

present work different samples of α-TeO_3 were found to contain 10 to 40 per cent of TeO_2.

5. β-TeO_3

This is a grey crystalline material prepared by heating telluric acid with 18M H_2SO_4 in a sealed tube at 310°C.[210] for 24 hours. The resulting residue was boiled in turn with 29 per cent NaOH and 12N HCl, and the product finally washed with water and dried. The I.R. spectra and x-ray powder photographs on samples of β-TeO_3 were identical to those of Laub,[205] and $Na_2H_4TeO_6$, which is reported as a frequently observed contaminant,[207] was not found to be present.

It has been proposed on the basis of the I.R. and ^{125}Te Mössbauer absorption data that this compound probably has a ReO_3-type structure, the tellurium again being octahedrally surrounded by oxygens.[207]

6. Te_2O_5

On heating telluric acid at 405°C. in an open tube it is reported that Te_2O_5 is obtained.[203] However, this compound is known to yield Te(IV) and Te(VI) ions on dissolution in KOH.[202] The compound may well be a stoichiometric mixture of TeO_3 and TeO_2.

7. $\underline{H_2TeO_3}$

Tellurous acid, H_2TeO_3, was prepared by a method similar to that described by Feher.[211] A solution of TeO_2 in nitric acid was neutralised with NaOH and at neutrality the white solid H_2TeO_3 precipitated out. This product was then washed with cold water and, while wet, was mounted and the ^{129}I Mössbauer emission spectrum immediately measured. This was necessary because H_2TeO_3 readily loses water to give TeO_2.[212]

Samples of H_2TeO_3 were characterised by showing that they yielded only TeO_2 on dehydration at 120°C.

8. $\underline{TeO_2}$

Thermal decomposition of telluric acid at 550°C. finally yields tetragonal TeO_2[203,204] which is readily characterised by I.R. spectroscopy and x-ray powder diffraction methods.[202,207]

Tellurium dioxide is found in two crystal modifications. The naturally occurring mineral tellurite is orthorhombic TeO_2, while all synthetic preparations are reported to yield the tetragonal form.[212] The structures of these two forms are shown in Figure 9. In both instances the tellurium is 4 co-ordinate. However, in the tetragonal form each oxygen is bonded to different telluriums (corner bridging), while in the orthorhombic modification, two of the four bridging oxygens are shared by adjacent telluriums (edge bridging).

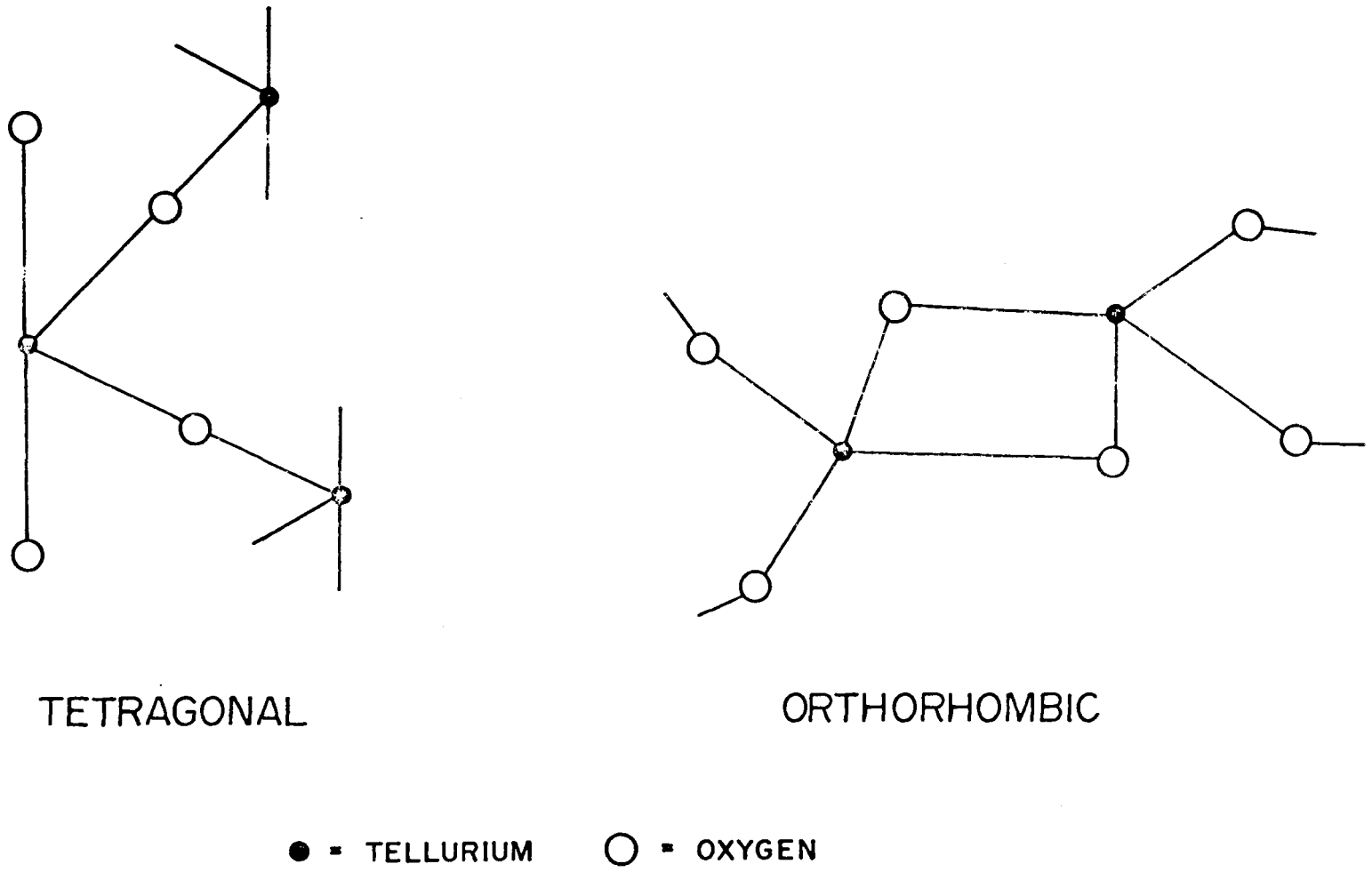

Figure 9 Structure of Tetragonal and Orthorhombic TeO_2.

9. $\underline{(NH_4)_2\ TeCl_6}$

This compound was studied because it can be rapidly prepared and isolated.[213] Tellurium metal was dissolved in HNO_3/H_2O and the solution evaporated to dryness. While very hot, the TeO_2 residue was dissolved in 12N HCl and a few drops of a saturated aqueous solution of NH_4Cl added. On cooling, fine yellow crystals of $(NH_4)_2TeCl_6$ precipitated which were filtered, washed with 12N HCl, and dried.

The Raman[214] and ^{125}Te absorption spectra[215,216] of this product were identical to those previously reported.

10. Elemental Tellurium

The ^{129}I Mössbauer emission spectra of several tellurium samples prepared in several different ways were studied. Thus, elemental tellurium as obtained from Oak Ridge was investigated following the N.R.U. reactor irradiation. This material was a fine powder. Tellurium precipitated from acid solution by reduction of Te(IV) with SO_2 was studied,[107,108] while other tellurium samples were prepared by melting the powdered element at 950°C. in an evacuated quartz tube.

The crystalline metallic form obtained from the melt is known to have a hexagonal lattice, containing spiral chains of tellurium atoms with Te-Te bond distances of 2.86Å, and Te-Te-Te bond angles of 102-103°.[217] The finely divided powder forms of tellurium in the other two types of sample were probably finely divided crystalline tellurium rather than an amorphous allotrope.

11. ZnTe

Zinc telluride was prepared by mixing stoichiometric amounts of powdered tellurium and zinc and sealing in an evacuated silica tube.[127] This was heated to 750°C. for several hours, this producing the red cubic solid ZnTe.

J. Mössbauer Experiments with ^{125}Te

In characterising the tellurium compounds used in this work, the ^{125}Te Mössbauer absorption spectra were measured and compared with those reported in the literature.

The features of the Mössbauer effect with ^{125}Te have been reported in several papers.[124,125,187-189,215,216] The principle difficulty in such experiments derives from the fact that the 35.5 keV Mössbauer transition has a K-shell internal conversion coefficient of 11. This leads to a very high tellurium x-ray background (TeK_{α} = 27.4 keV, Te K_{β} = 31.2 keV) which cannot be resolved from the Mössbauer transition. This problem may be alleviated by using a $Xe(CO_2)$ proportional detector and counting the 6 keV escape peak resulting from the photoelectric effect of the 35.5 keV γ-ray with xenon and the subsequent escape of the xenon x-ray from the detector.

In the present work a 20 millicurie ^{125}I on copper source from New England Nuclear was used. The characteristics of the $^{125}I \rightarrow {}^{125}$Te electron capture decay were shown earlier

in Figure 4(a). A 5 mil copper absorber was placed immediately in front of the source and this reduced considerably the background under the 6 keV escape peak in the detector. The 8 keV copper x-rays produced were effectively absorbed in the absorber holder, the vacuum dewar window, and the detector window. A 2 atmosphere $Xe(CO_2)$ proportional detector was used in conjunction with a Canberra charge-sensitive pre-amplifier.

The tellurium compounds studied contained varying amounts of ^{125}Te, though the majority of these compounds contained only the natural isotopic abundance of ^{125}Te (6.99 per cent). In studying the $^{128}Te(n,\gamma)$ ^{129}Te reaction, compounds were synthesised with enriched materials and contained ca. 70 per cent ^{128}Te and ca. 30 per cent ^{125}Te. However, the absorber thickness in these experiments was often restricted by the amount of material available from the previous ^{129}I emission experiment. As a result, the ^{125}Te spectra often had low per cent absorptions, and to offset this long counting times were employed. The total counts per channel normally ranged from 1 to 4 x 10^6 over a total of 512 channels.

The ^{125}Te isomer shifts and quadrupole splittings obtained for the compounds investigated in this work are compared in Table V with several values previously reported in the literature. Figure 10 shows four representative spectra for some of these compounds.

TABLE V

COMPARISON OF THE ^{125}Te MÖSSBAUER PARAMETERS MEASURED IN THIS WORK WITH PREVIOUSLY REPORTED VALUES

	δ (mm. sec.$^{-1}$)	Δ (mm. sec.$^{-1}$)	REF.
$\underline{H_6}\underline{TeO_6}$	-1.23±.09		*
	-1.14±.06		216
	-1.15±.04		125
	-1.20±.05		207
$(H_2TeO_4)_n$	-1.20±.05		*
α-TeO_3	-1.01±.07		*
	-1.07±.05		125
	-1.09±.02		207
β-TeO_3	-1.18±.07		*
	-1.20±.02		207
	-1.3± .2		187
TeO_2-TET.	+ .74±.11	6.76±.09	*
	+ .72±.02	6.63±.06	207
	+ .75±.12	6.25±.03	216
	+ .72±.07	6.54±.08	125
	+ .78±.08	7.3 ±.1	124
H_2TeO_3	.63±.34	6.71±.29	*
	1.3± .3	7.7±1.2	215
$(NH_4)_2TeCl_6$	1.70±.05		*
	1.8± .3		215
	1.79±.05		216
Elemental Tellurium	.50±.05	7.72±.11	*
	.78±.10	7.10±.11	125
	.51±.04	7.4 ±.2	124

* This work

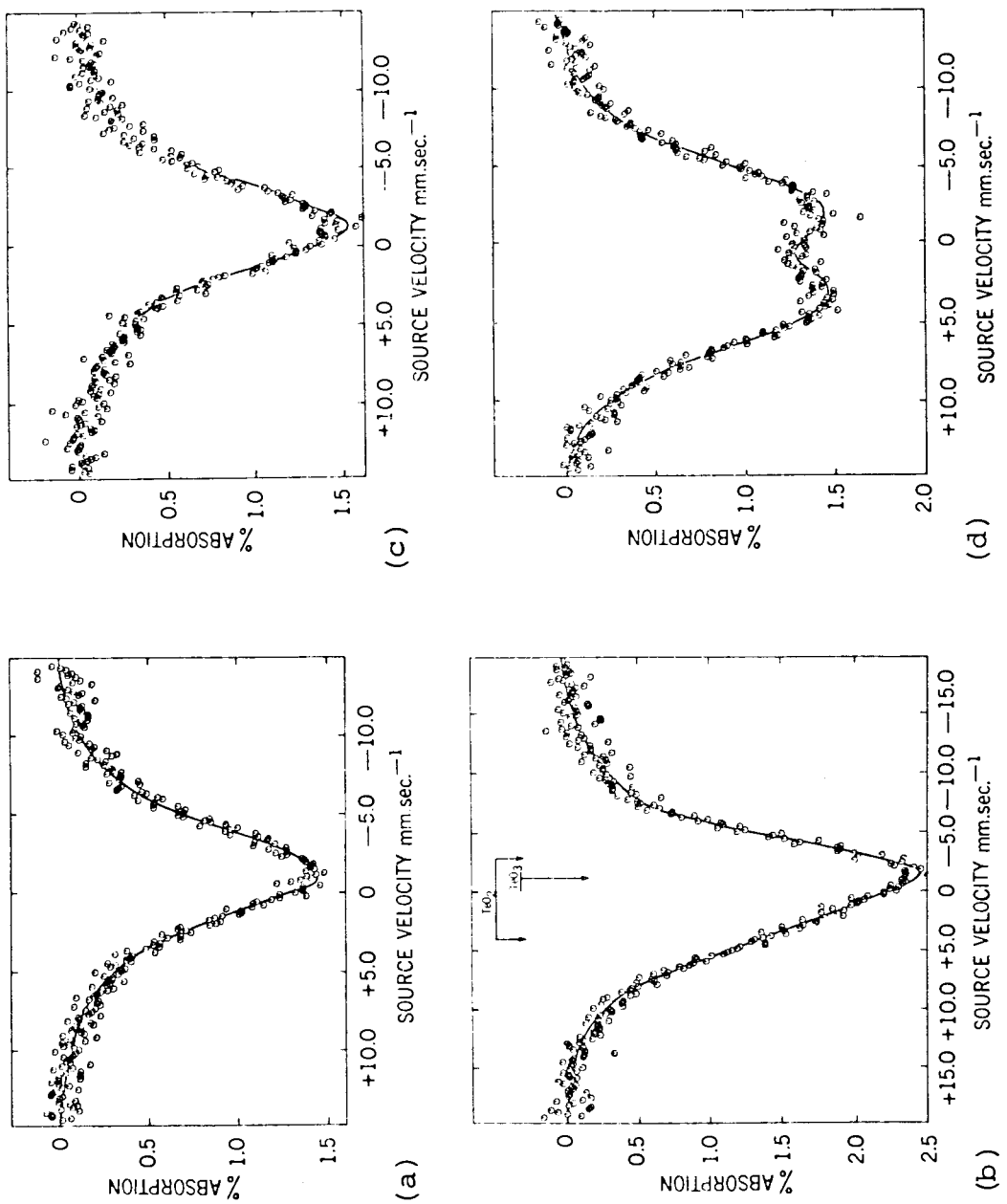

Figure 10 ^{125}Te Mössbauer Absorption Spectra of an ^{125}I on Cu Source vs. (a) $H_6{}^{125}TeO_6$, (b) α-$^{125}TeO_3$, (c) β-$^{125}TeO_3$, and (d) Tetragonal $^{125}TeO_2$.

K. Computer Analysis of Mössbauer Spectra

The Mössbauer spectra were fitted to Lorentzian absorption lines by means of a computer analysis.[218] The program used required initial estimates of the line positions, full-widths, and intensities, and allowed for the constraining of any number of these parameters during the fitting procedure. In an ideal case, all such constraints should be removed during the latter part of the computation. However, for the more complex ^{129}I spectra, some of which contained two superimposed 8-line quadrupole split spectra, it was found necessary to constrain many of the absorption line parameters throughout the fitting process. The program gave a value of chi-squared, χ^2, for each fit, which allowed a ready assessment of the statistical acceptability of the fit. Only when the χ^2 value indicated a degree of confidence within the 10 per cent and 90 per cent limits, as determined by the number of degrees of freedom in the fit, was the computer fit of a spectrum judged to be acceptable.

All of the spectra obtained in this work were mirror-image spectra and the two halves were always computed separately.

The diagrams of spectra shown throughout this thesis are the folded spectra. The folding of the two mirror-image spectra eliminates the sine-wave component of the non-resonant background which results from the physical motion of the

source towards and away from the detector. The spectra shown are the experimentally observed spectra, and thus the source velocities are those measured in the emission experiment.

IX. RESULTS AND DISCUSSION OF CHEMICAL INVESTIGATIONS OF IODINE AND TELLURIUM RECOIL SPECIES IN TELLURIC ACID

A. Experimental Results for Studies of Iodine Recoil Atoms

1. Initial Distributions of Recoil Products

The chemical forms of the iodine recoil atoms identified following the different nuclear transformations investigated are shown in Table VI. The electrophoretic separation was used for all but the ^{132}Te samples. In each instance two values are given. The "room temperature" values were determined by studying each of the transformations listed at ambient temperature. These values will reflect the chemical effects of the transformations, followed by any annealing reactions of the recoil products in the crystal which occur at room temperature.

The distributions referred to as "no annealing" values in Table VI were determined for crystal samples in which thermal annealing reactions were minimised. For example, in the case of samples labelled with ^{131}Te, ^{131m}Te, or ^{132}Te, the study was made by cooling the samples to liquid nitrogen temperature during the decay of the parent isotope. In these experiments the crystals were dissolved at ambient temperature in the solvent for the chemical analysis, and thus some thermal annealing will undoubtedly have occurred

TABLE VI

INITIAL DISTRIBUTIONS OF IODINE RECOIL PRODUCTS IN TELLURIC ACID

	TRANSFORMATION SEQUENCE		PER CENT IODINE AS		
			Reduced Form	IO_3^-	IO_4^-
1	$H_6{}^{130}TeO_6(n,\gamma){}^{131}Te \xrightarrow{\beta^-} {}^{131}I$	No Annealing	34 ± 1	63 ± 1	3 ± 2
		Room Temperature	43 ± 1	54 ± 1	3 ± 2
2	$H_6{}^{131}TeO_6 \xrightarrow{\beta^-} {}^{131}I$	No Annealing	11 ± 1*	49 ± 2*	40 ± 2*
		Room Temperature	33 ± 1*	27 ± 2*	40 ± 2*
3	$H_6{}^{131m}TeO_6 \xrightarrow{\beta^-} {}^{131}I$	No Annealing	11 ± 1	69 ± 2	20 ± 2
		Room Temperature	30 ± 2	50 ± 2	20 ± 2
4	$H_6{}^{132}TeO_6 \xrightarrow{\beta^-} {}^{132}I$	No Annealing	27 ± 1	73 ± 1	
		Room Temperature	27 ± 1	73 ± 1	

* Corrected for $H_6{}^{131m}TeO_6$ contamination

as the samples were warmed to ambient temperature during the dissolution. For the neutron irradiated sample the irradiation was carried out at solid CO_2 temperature and was for only one minute, thus minimising annealing during the irradiation itself.

It is apparent from Table VI that, with the exception of $H_6{}^{132}TeO_6$, thermal annealing reactions were occurring in the samples even at room temperature. Moreover, whatever the thermal annealing process may have been, it did not produce a change in the fraction of daughter radioactivity which analysed in the IO_4^- form.

The electrophoretic analysis used in obtaining the results of Table VI has several inherent limitations. Thus, the presence of I^-, I_2 or IO^- as products following the transformation could not be distinguished since they would all analyse as I^- in NaOH solution in the presence of I^- carrier. Moreover, if, following the decay of the parent tellurium isotope, the iodine atom remained bonded to the ligands of the precursor molecule, then the H_5IO_6 molecule should be observed as a recoil product. However, in aqueous solution H_5IO_6 exists in a pH-dependent equilibrium with several other ions as shown below[219]

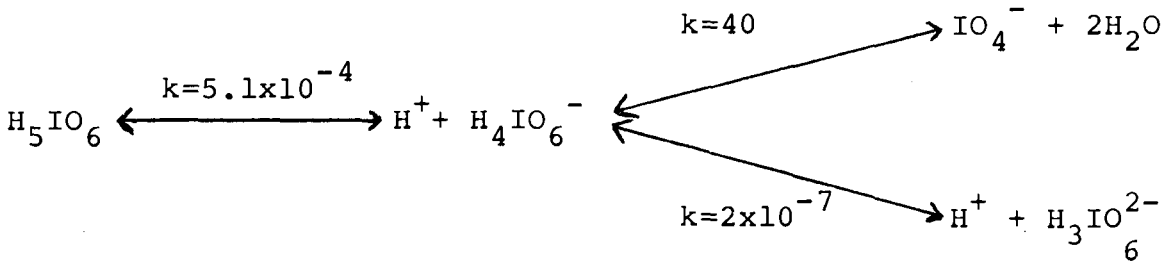

Under the conditions of the electrophoretic analysis, $H_4IO_6^-$, $H_3IO_6^{2-}$, and IO_4^- would all be present in solution. Since the IO_4^- ion was known to move only ca. 1 cm. in the electrophoretic separation, all of the above ions would presumably be observed in the fraction referred to as IO_4^-.

In the present work no evidence was found in the electrophoretic separation for the existence of the previously reported IO_2^- ion as a recoil product.[90,95] For the previous investigations where this ion has been observed, other explanations may be invoked to explain the experimental results. Thus, in the work of Bertet, Chanut, and Muxart,[90] the experimental results may have been due in part to exchange or oxidation-reduction reactions of the iodine recoil fragments and iodine carriers occurring in acidic or neutral media. In the electrophoretic work of Hashimoto *et al.*,[95] only single iodine carriers of high concentrations were used. This analytical method raises some question as to the significance of the results they obtained.

In the light of the above discussion, a brief examination of the results of Table VI shows that extensive

molecular fragmentation appears to accompany each of the nuclear transformations. If we assume that the IO_4^- fraction is representative of the recoil atoms present in the crystal as H_5IO_6 molecules, then it is apparent that the different transformation sequences lead to different amounts of molecular decomposition. It is unfortunate that the short half-life of ^{132}I together with the presence of contaminating activities precluded the determination of the IO_4^- fraction in this sample.

The assumption that the IO_4^- fraction may truly reflect the percentage of iodine atoms that did not undergo bond rupture in the decay event may obviously be an over-simplification. However, the iodine product distributions in the different samples were certainly different, and these differences must reflect the different chemical effects associated with each of the nuclear transformations involved. Thus, the comparison of the relative chemical effects of the different transformations was the point of interest, rather than the identification of the precise origin of each of the iodine chemical products observed in solution.

Since annealing reactions were observed to occur in the solid samples even at room temperature, it was of some importance to study the annealing reactions in detail.

2. Thermal Annealing of ^{131}I Recoil Atoms

Following the neutron irradiation of telluric acid, the $^{131,131m}Te \xrightarrow{\beta^-} {}^{131}I$ decay was allowed to occur at room temperature. Samples of the solid were then heated at several temperatures for varying times, and portions of the heated solid were then analysed, in most cases using the solvent extraction technique. The results of these experiments are shown in Figure 11(a). The iodine product distribution was found to change in an extremely complex way as a function of the temperature and time of heating. The complexity of the processes involved is further illustrated in Figure 11(b) which represents the results of a similar experiment to the above, only now the sample of telluric acid was irradiated under different conditions in the reactor. It is apparent that the γ-irradiation of the sample in the reactor, and to a lesser extent the temperature of the sample during the irradiation, played a very significant role in influencing the subsequent thermal annealing reactions of the recoil products.

Samples of telluric acid labelled with ^{131}Te and ^{131m}Te were allowed to undergo β^--decay to ^{131}I at room temperature, and the samples were then thermally annealed. The results of these experiments, again in most cases obtained using the solvent extraction method of analysis, are shown in Figure 12. It is apparent that the annealing curves for the samples at comparable temperatures show

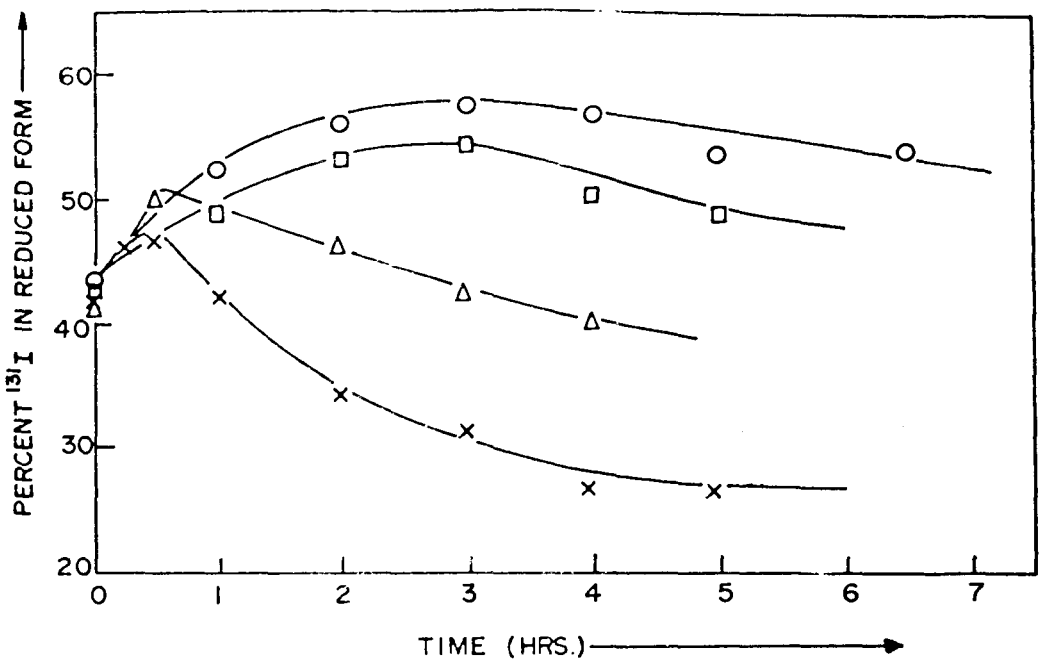

(a)

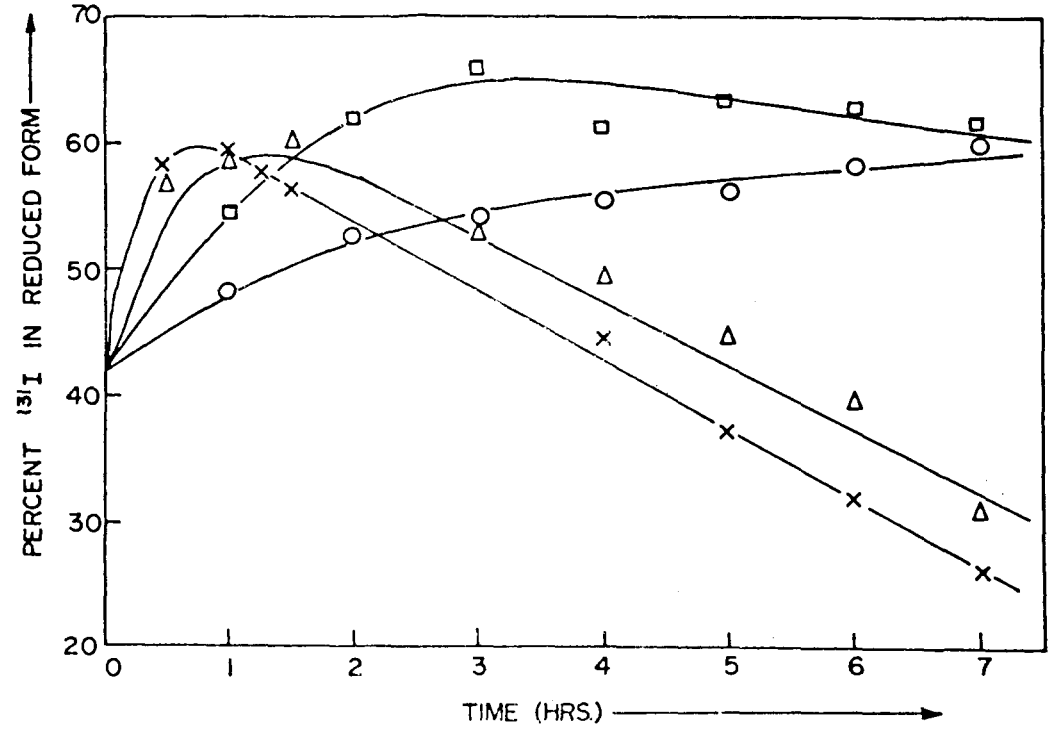

(b)

Figure 11 Thermal Annealing of ^{131}I Produced By $(n,\gamma) + \beta^-$ in H_6TeO_6

(a) The sample was irradiated for 25 minutes and Annealed at o 79°C., □ 87°C., Δ 95°C., X 102°C.

(b) The Sample Was Irradiated for One Minute and Annealed as Shown

Irradiation Temperature	Annealing Temperature
Ambient, Solid CO_2	o 90°C., □ 99°C.
Ambient	Δ 109°C.
Solid CO_2	X 109°C.

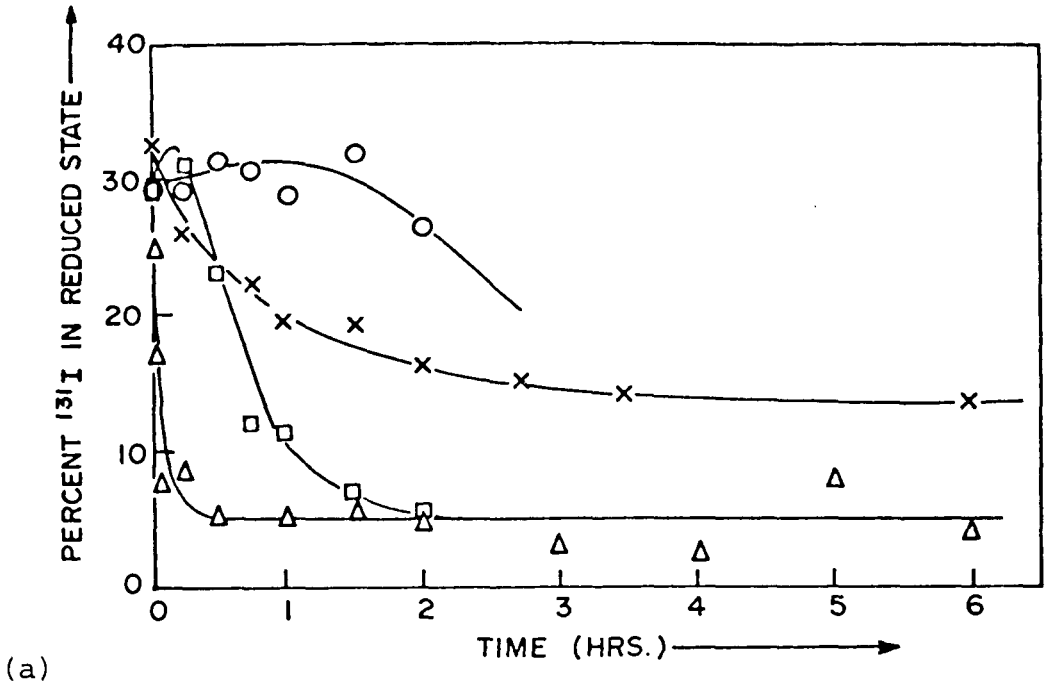

(a)

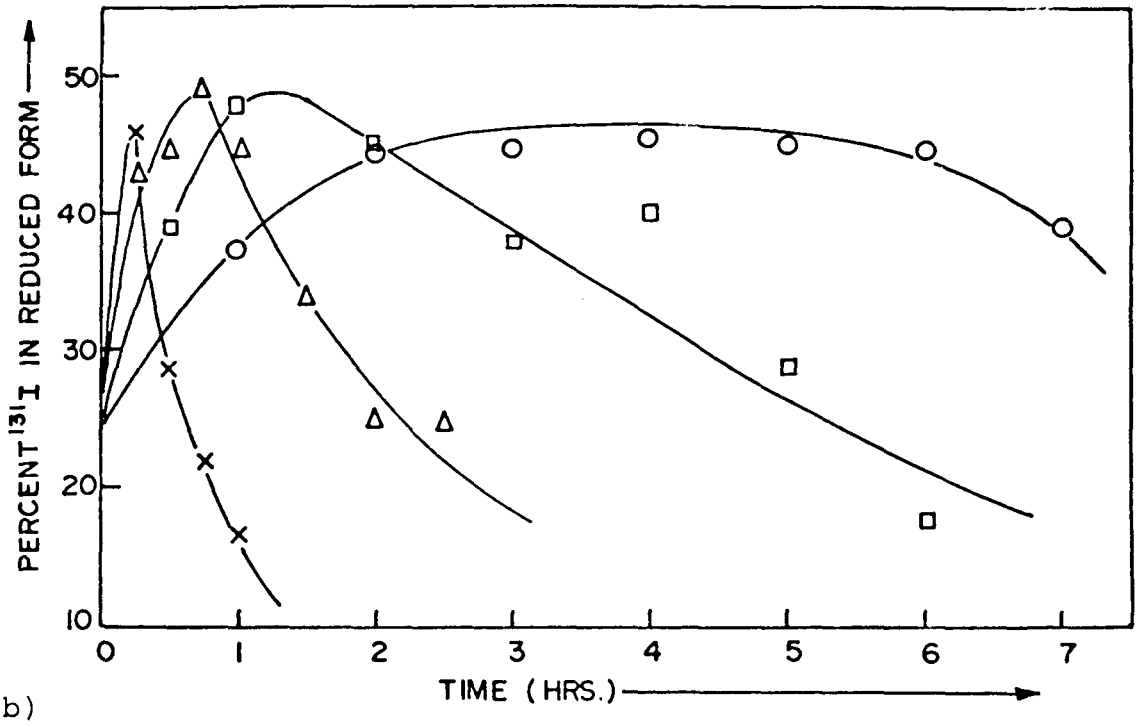

(b)

Figure 12 Thermal Annealing of ^{131}I in (a) $H_6{}^{131}TeO_6$ and (b) $H_6{}^{131m}TeO_6$.
(a) The $H_6{}^{131}TeO_6$ Was Annealed at o 47°C., □ 67°C., Δ 80°C. Within 48 Hours of its Preparation; X Sample Annealed at 67°C. 12 Days Following its Preparation
(b) The $H_6{}^{131m}TeO_6$ Was Annealed at o 67°C., □ 71°C., Δ 78°C., X 89°C.

very significant differences. Moreover, the ^{131}Te sample contained ^{131}I which in ca. 20 to 36 per cent of events had been born in the decay of ^{131m}Te. If the annealing data for the $H_6{}^{131}TeO_6$ sample are corrected for this component, then the difference between the $H_6{}^{131}TeO_6$ and $H_6{}^{131m}TeO_6$ samples becomes even greater.

Some thermally annealed samples which were analysed using the electrophoretic method showed that the IO_4^- fraction in these samples did not change in the annealing reaction.

The results of thermal annealing experiments for ^{132}Te-labelled telluric acid will be presented in a later section for reasons which will become apparent in the following section.

Returning to the results of Figure 10, the dependence of the thermal annealing of the recoil products on the conditions of the reactor irradiation suggests that lattice defects generated in the crystal during the irradiation may be playing a role in these annealing reactions. In order to examine this proposal further, the following experiments were performed.

3. The Role of Crystal Defects in the Thermal Annealing Reaction

If crystal defects, such as electrons or positive holes trapped at defect trap-sites throughout the crystal lattice, are involved in the thermal annealing reaction,

then any means of altering the defect trap population before the recoil atom is produced in the solid will presumably have a marked influence on the subsequent annealing reactions of the recoil atoms. One such experiment of the above type is to heat the solid before the neutron irradiation or radioactive decay, and to observe what effect this has on the following annealing reactions.

A sample of telluric acid was heated for one hour at 100°C. before the reactor irradiation. This sample was then irradiated and the $^{131m,131}Te$ β^- decay allowed to occur at room temperature. The thermal annealing of the recoil products was then studied in this sample as before and the results are shown in Figure 13. A comparison of the data of Figure 13 with that of Figure 11 clearly shows that heating the crystals before the irradiation had a very pronounced effect as anticipated. It should be emphasised that heating telluric acid up to 100°C. was shown by I.R. spectroscopy, x-ray powder diffraction patterns, and thermogravimetry, not to change the crystal structure or chemical composition of the sample in any way.

In similar experiments with $H_6{}^{131}TeO_6$ and $H_6{}^{131m}TeO_6$, immediately following the chemical preparation of these labelled samples, the crystals were heated at 100°C. for a short period of time before any appreciable decay of the tellurium parents had occurred. For the $H_6{}^{131}TeO_6$ sample an error was introduced in this experiment by the decay

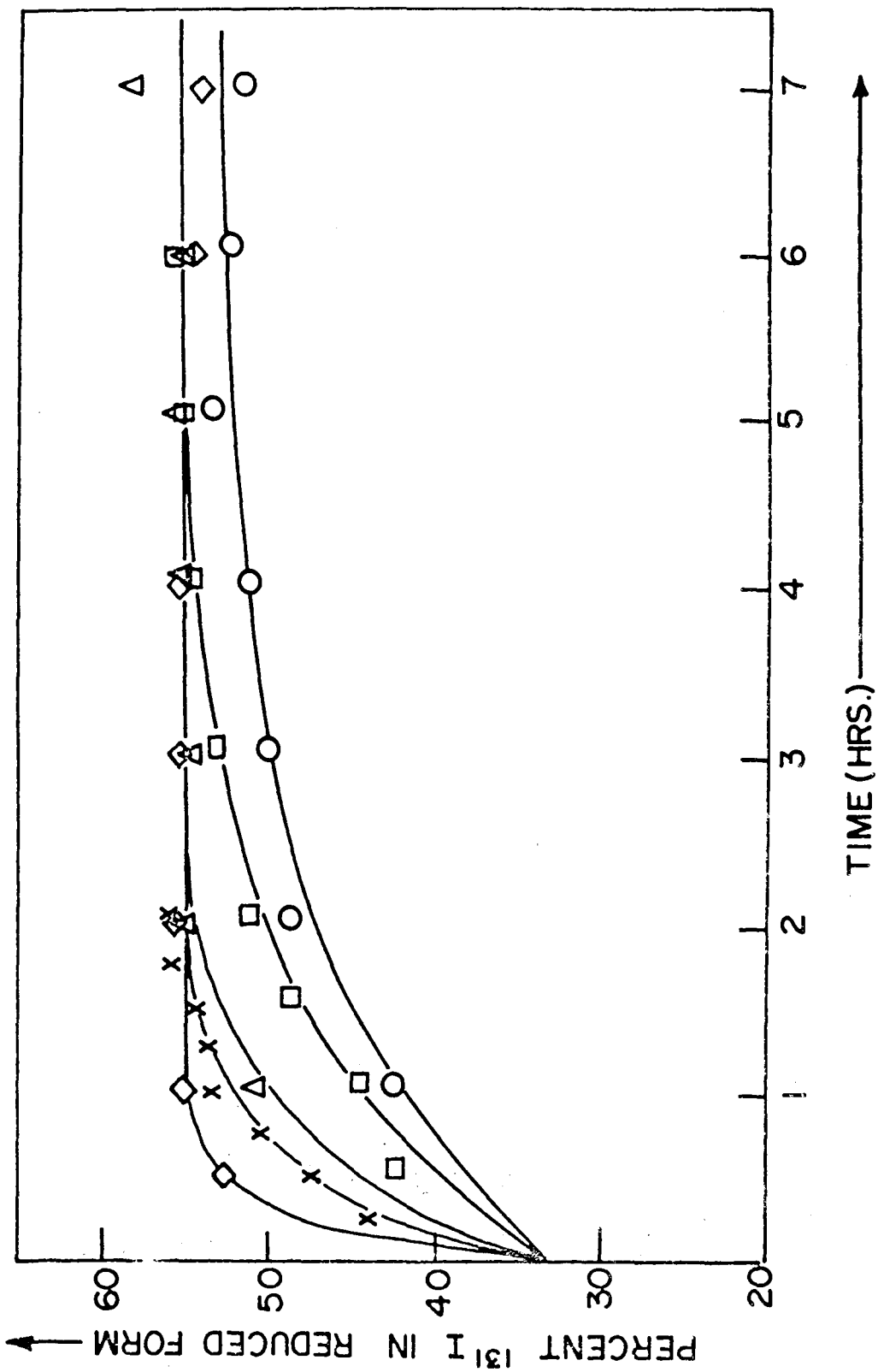

Figure 13 Thermal Annealing of ^{131}I Produced By $(n,\gamma) + \beta^-$ In H_6TeO_6 Where the Sample Was Heated at 100°C. For One Hour Before the Reactor Irradiation. Following the Irradiation the Sample Was Heated at o 90°C., □ 94°C., △ 99°C., X 104°C., ◇ 109°C.

of ca. 20 per cent of the ^{131}Te before and during the heat treatment. These samples were then stored at room temperature while the decay of ^{131}Te and ^{131m}Te to ^{131}I took place, and the thermal annealing reactions of the recoil atoms investigated. The results are summarised in Table VII. It was found that little recoil-product thermal annealing was now observed in these samples, in comparison with the annealing reactions which were reported in Figure 12. Thus again, heating the crystals before production of the recoil atom in the solid was found to have a marked effect on the subsequent thermal annealing reactions.

In addition to the above type of experiment, many other experiments may be performed to study the effects of defect or trap populations in the crystal on annealing reactions. In particular, γ-irradiation of the crystal will result in radiolysis of the crystal, with the production of trapped defects in the solid. During the present investigation it was found that chemically identical samples of $H_6{}^{131}TeO_6$ and of $H_6{}^{131m}TeO_6$, prepared labelled with very different specific activities of ^{131}Te and ^{131m}Te, yielded exactly the same initial distributions for the iodine recoil atoms, but thermally annealed in slightly different ways. Thus the different samples yielded annealing curves qualitatively similar to those of Figure 12, but the rate of reaction and per cent change in the reduced (I^-) fraction for heating at any one temperature was different. Evidently the self-

TABLE VII

RESULTS OF THERMAL ANNEALING IN $H_6{}^{131}TeO_6$ AND $H_6{}^{131m}TeO_6$ HEATED AT 100°C. PRIOR TO β^--DECAY OF THE PARENT TELLURIUM

SAMPLE	TREATMENT OF THE SAMPLE FOLLOWING β^- DECAY	% ^{131}I IN REDUCED FORM
$H_6{}^{131}TeO_6$ pre-heated at 100°C. for 4 min. before appreciable β^- decay	no annealing	11.5 ± 1.0
	81°C. 30 min.	12.0 ± 1.0
	81°C. 60 min.	14.0 ± 1.0
	81°C. 90 min.	13.3 ± 1.0
	81°C. 120 min.	15.1 ± 1.0
	81°C. 21 hr.	15.7 ± 1.0
$H_6{}^{131m}TeO_6$ heated at 100°C. for 60 min. before β^- decay	no annealing	10.7 ± 1.0
	80°C. 60 min.	13.5 ± 1.0
	80°C. 90 min.	11.3 ± 1.0
	80°C. 120 min.	14.2 ± 1.0

irradiation of the solid with β^--particles and γ-rays during the decay of the parent isotope played an important part in producing trapped defects. In the pre-heated samples such specific activity effects were absent.

In a few experiments the effects of externally γ-irradiating the crystals using a ^{60}Co γ-source was studied. This was again found in the case of ^{131m}Te-labelled telluric acid to lead to small quantitative changes in the annealing curves, though showing no effect on the initial iodine product distribution.

4. Thermal Annealing of ^{132}I Recoil Products

The radioactive transient equilibrium which exists between the parent ^{132}Te and daughter ^{132}I activities allows a very detailed investigation of the thermal annealing reactions in the solid. The $H_6{}^{132}TeO_6$ sample was allowed to reach radioactive equilibrium at room temperature. Portions of the solid were then heated and analysed by solvent extraction. These results are shown in Figure 14(a). As the time of the heating becomes comparable with the half-life of the daughter ^{132}I (2.3 hour), then the recoil atom population changes in the crystal. Of the iodine recoil atoms present in the crystal at the end of a 19 hour heating period, almost all would have been produced by decay during the annealing experiment itself. For such long times of heating, the recoil-

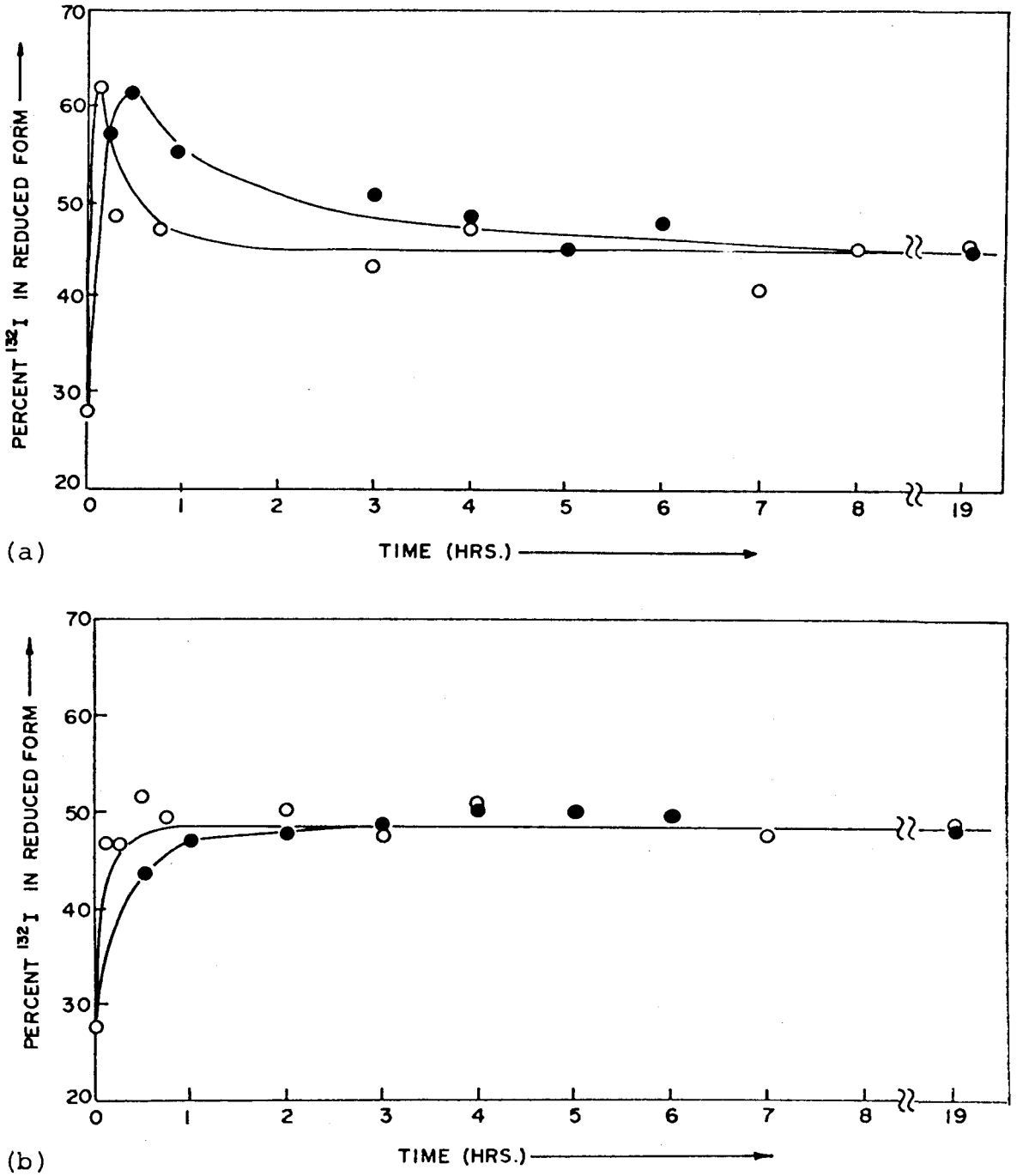

Figure 14 Thermal Annealing of ^{132}I in $H_6{}^{132}TeO_6$. Following the β^--Decay, the Samples were Heated at ● 80°C., o 100°C.
a. Thermal annealing in $H_6{}^{132}TeO_6$.
b. The $H_6{}^{132}TeO_6$ sample was heated at 100°C. for one hour, was cooled and allowed to stand at room temperature for twenty-four hours, and the thermal annealing then studied.

iodine distribution plateaued as seen in Figure 14(a) and did not change further with time.

A portion of this same sample of $H_6{}^{132}TeO_6$ was heated at 100°C. for one hour, was cooled to room temperature, and was then allowed to stand for 24 hours. In this time all of the iodine recoil atoms present in the initial experiment would have decayed away to be replaced by a new population born in the decay at room temperature. This sample was thermally annealed and analysed as before. The results of these experiments are shown in Figure 14(b).

There are two important points to note. The difference between the annealing curves of Figure 14(a) and Figure 14(b) must represent the effects on the telluric acid lattice of the thermal annealing in the first experiment. However, following this first heat treatment, thermal annealing reactions were still observed to occur in the solid as seen in Figure 14(b). This latter point is in contrast to the results observed for $H_6{}^{131}TeO_6$ and $H_6{}^{131m}TeO_6$, where it was found that heating the sample before the radioactive decay occurred in the solid greatly diminished the thermal annealing reactions subsequently observed.

B. Experimental Results for Studies of Tellurium Recoil Atoms

The chemistry of tellurium ions in solution is much simpler than that of iodine, in that there are far fewer stable oxidation states and chemical forms for tellurium. The solvent

extraction analysis used in this work allowed the determination of the per cent tellurium in the (IV) and (VI) oxidation states following the nuclear transformations. These results are shown in Table VIII.

The results shown for the experiment $^{128}Te(n,\gamma)^{129m}Te$ are probably not very meaningful. The sample was irradiated in the high-flux N.R.U. reactor in order to produce sufficient ^{129m}Te activity to perform the experiment. Although the sample

TABLE VIII

INITIAL DISTRIBUTIONS OF TELLURIUM RECOIL PRODUCTS IN TELLURIC ACID

	NUCLEAR TRANSFORMATION SEQUENCE	Te(VI)	Te(IV)
1	$^{128}Te(n,\gamma)^{129m}Te$	95 ± 2	5 ± 2
2	$^{128}Te(n,\gamma)^{129m}Te$ I.T. ^{129}Te	63.5 ± 1	36.5 ± 1
3	^{129m}Te I.T. ^{129}Te	64 ± 1	36 ± 1
4	$^{128}Te(n,\gamma)^{129}Te$	56.3 ± 1	46.7 ± 1

was cooled during the irradiation, some thermal annealing and γ-irradiation of the sample would have occurred. These latter processes evidently reconverted the anticipated $^{129m}Te(IV)$ decomposition products back into the parent $^{129m}Te(VI)$ form. This point is illustrated in the $^{128}Te(n,\gamma)^{129}Te$ experiment.

Here the sample was irradiated in the Seattle reactor at a thermal neutron flux of 2×10^{12} n. $cm.^{-2} sec.^{-1}$ for 60 minutes, this irradiation producing a large amount of the 69 minute ^{129}Te activity. It was found in the neutron capture reaction that in at least 47 per cent of events fragmentation of the parent H_6TeO_6 molecule was observed with the formation of a $^{129}Te(IV)$ species in the crystal. Even in this experiment some thermal annealing of the sample would have occurred during the reactor irradiation. On heating the sample for 15 minutes at 100°C. following the irradiation, the $^{129}Te(IV)$ fraction was found to decrease to 21.4 per cent, the $^{129}Te(VI)$ fraction increasing by the corresponding amount.

In this radiochemical study the chemical product of the thermal annealing reaction was indistinguishable from the parent Te(VI) chemical form.

The main point of interest was the investigation of the ^{129m}Te (34 day) → ^{129}Te (69 minute) isomeric transition decay in ^{129m}Te-labelled telluric acid. This isomeric transition is highly internally converted and the chemical effects associated with the Auger charging process should be observed in this system. For the decay occurring at room temperature in the labelled crystals, the isomeric transition was found to produce bond rupture in ca. 36 per cent of decay events, with the formation of a $^{129}Te(IV)$ recoil product.

If the labelled crystals were allowed to reach radiochemical equilibrium with the daughter ^{129}Te atoms at room temperature and were then heated, thermal annealing reactions were observed to occur in which

$$^{129}Te(IV) \rightarrow {}^{129}Te(VI)$$

as shown in Figure 15(a). This radiochemical system is similar to that of $^{132}Te \rightarrow {}^{132}I$, the parent and daughter isotope existing in radioactive equilibrium together. Thus it was possible to take an aliquot of the thermally annealed sample and store it at room temperature for several hours, during which time the ^{129}Te recoil-atom population in the sample was replaced by an unannealed population. The sample was then heated again and a second thermal annealing experiment performed. These results are shown in Figure 15(b). The results of Figures 15(a) and 15(b) are found to be identical. Thus the $^{129}Te(IV)$ recoil atoms thermally annealed to yield Te(VI) in a way that was totally independent of the previous thermal history of the solid. This process bears some resemblance to that for ^{132}I recoil atoms in $H_6{}^{132}TeO_6$, although the latter did show some dependence.

A further experiment on the isomeric transition process was carried out following the $^{128}Te(n,\gamma)^{129m}Te$ nuclear reaction. In this sample, as pointed out earlier, the ^{129m}Te was present as ca. 95 per cent in the Te(VI) form, evidently due to thermal annealing which had occurred during

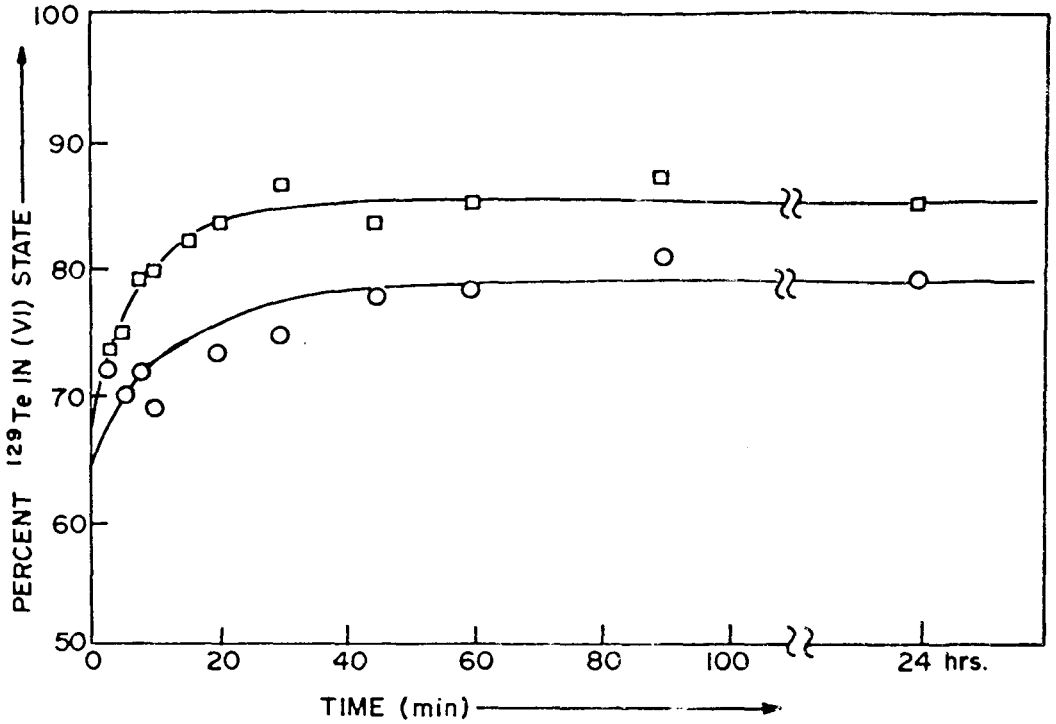

(a)

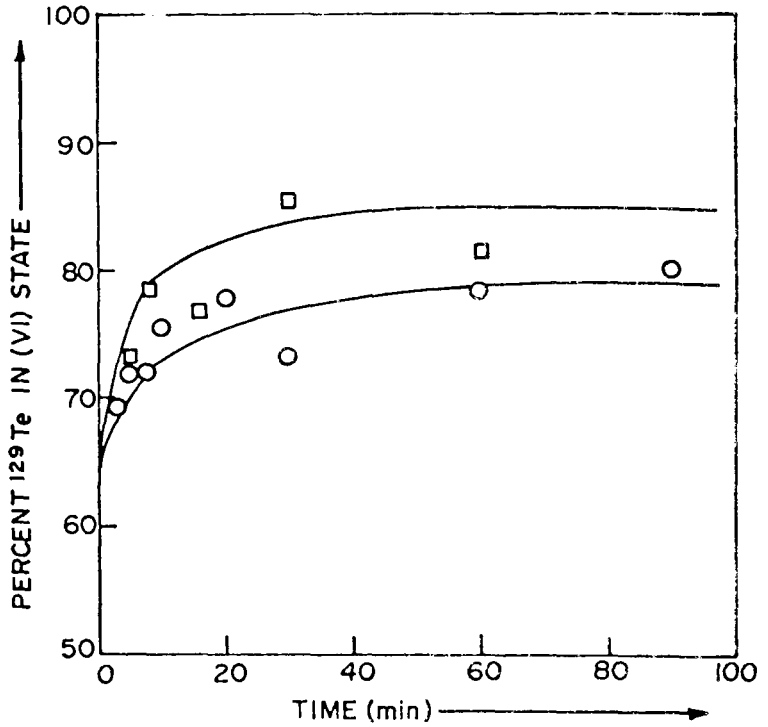

(b)

Figure 15 Thermal Annealing of ^{129}Te in $H_6{}^{129m}TeO_6$.
a. The Sample Was Annealed at o 86°C., □ 98°C.
b. The Samples Were o Heated for 24 Hours at 86°C. and □ Heated for 24 Hours at 98°C., Stood at Room Temperature for 24 Hours, and then Annealed at 86°C. and 98°C., Respectively.

the irradiation. It was then possible to study the chemical effects of the $^{129m}Te \rightarrow {}^{129}Te$ isomeric transition occurring in the thermally annealed (n,γ) lattice site. The result, which is included in Table VIII, may be described in the following way:

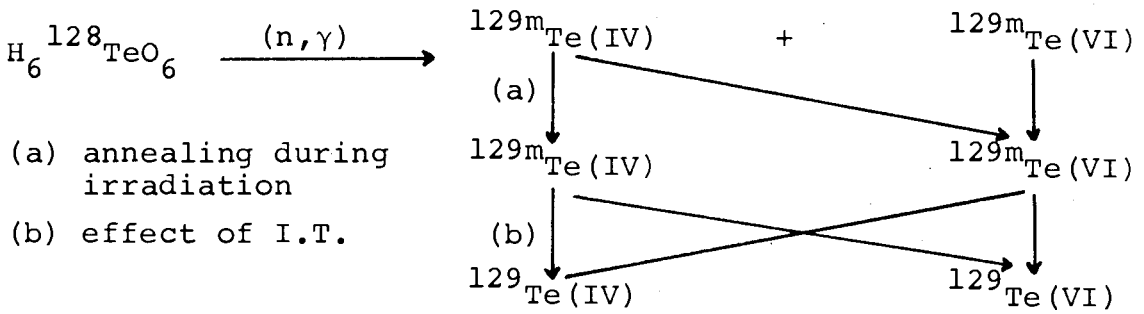

The distribution of ^{129}Te atoms was found to be very similar indeed to that observed in chemically labelled $H_6{}^{129m}TeO_6$. Moreover, the thermal annealing reactions of the ^{129}Te isomeric transition recoil atoms in this sample were also found to be essentially the same as those in the labelled molecule, as shown in Figure 16(a). The similarity in the thermal annealing in these two samples is clearly brought out in Figure 16(b), where the two samples were heated at varying temperatures for a constant period of time. The time of heating used was varied between 1 1/2 and 24 hours without affecting the results in any way, as the annealing curves of Figures 15 and 16(a) were shown to be very flat over this time range. The small difference that appears in the values for heating the samples above 90°C. may derive from the small percentage of $^{129m}Te(IV)$ initially present

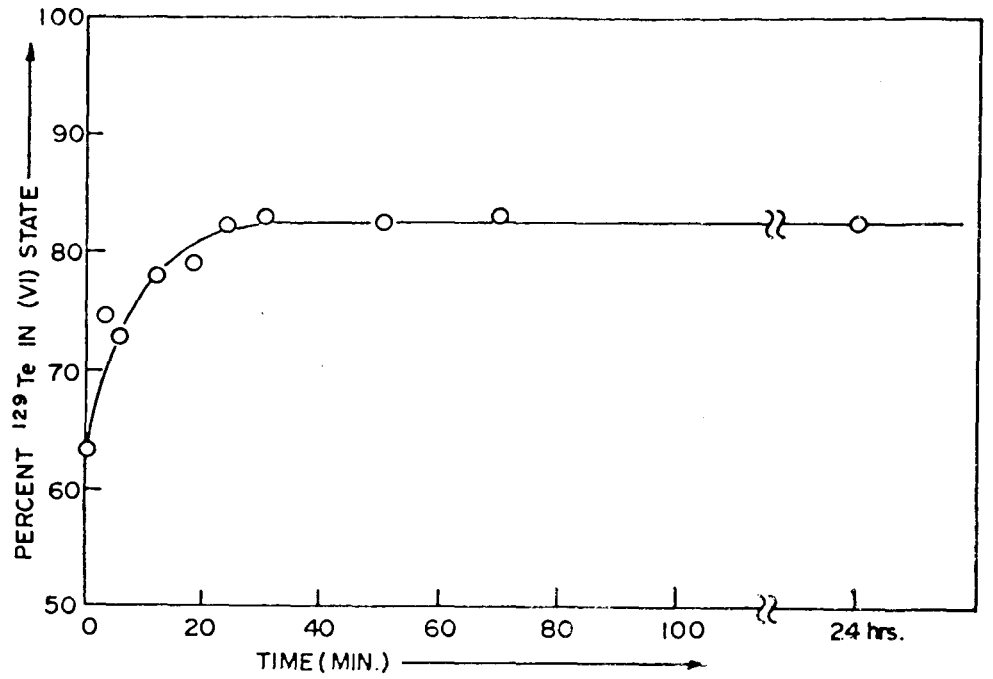

(a)

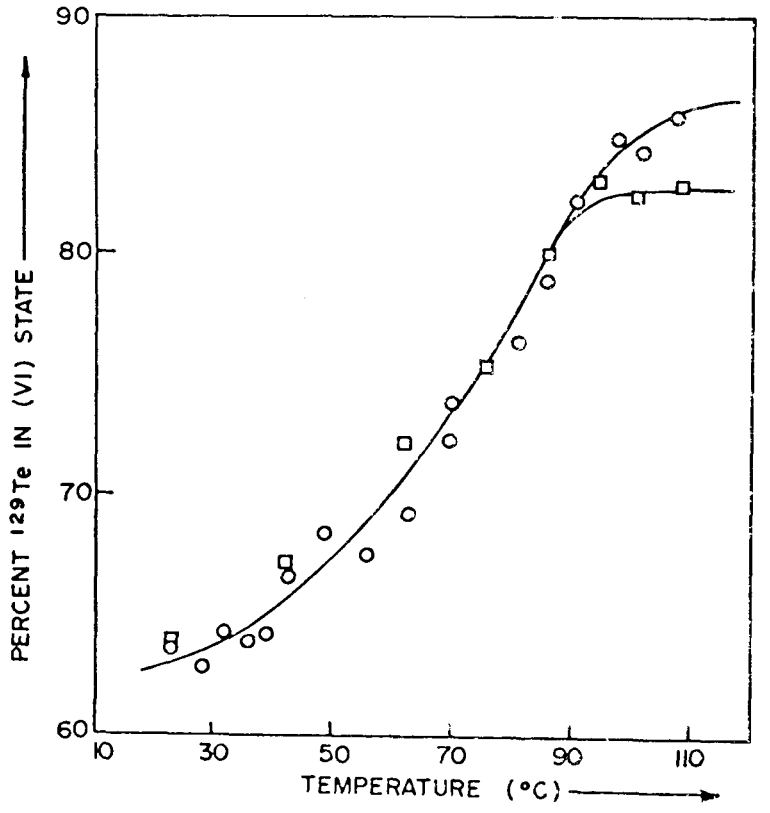

(b)

Figure 16 a. Thermal Annealing at 94°C. of ^{129}Te Produced by (n,γ)+ I.T. in $H_6{}^{128}TeO_6$

b. A Comparison of Thermal Annealing of ^{129}Te Produced by □ (n,γ) + I.T. in $H_6{}^{128}TeO_6$ and 0 I.T. in $H_6{}^{129m}TeO_6$. The Samples were Heated for 1 1/2 to 24 Hours at the Annealing Temperatures and then Analysed.

in the reactor irradiated sample. Thus it would appear that the ^{129m}Te atom in the labelled molecule and in the thermally annealed product found following the $^{128}Te(n,\gamma)$ ^{129m}Te reaction was identical.

C. Discussion of the Radiochemical Results

In discussing these experimental results it must be emphasised that the prime objective of the experiments was to compare and contrast the molecular decomposition accompanying the various nuclear transformations and, if possible, to relate the observed differences to known differences in the decay schemes of the isotopes. The radiochemical results provide three types of information which may be examined, and these are:

(a) the initial distribution of recoil products
(b) the thermal annealing reactions of the recoil products
(c) the dependence of the thermal annealing reactions on the previous thermal history of the sample.

The results for the samples labelled with ^{131}Te, ^{131m}Te, ^{132}Te, and ^{129m}Te will be discussed first.

1. ^{131}Te-, ^{131m}Te-, ^{132}Te-, and ^{129m}Te-Labelled Samples

Following the $^{131}Te \rightarrow {}^{131}I$ β^--decay, 40 per cent of the iodine atoms were found as IO_4^-, 49 per cent as IO_3^-, and 11 per cent as I^-. In the β^--decay of ^{131m}Te, the corresponding distributions were 20 per cent, 69 per cent, and 11 per cent. These distributions may be interpreted as evidence for very extensive molecular decomposition occurring in each decay. If the iodine survived the decay in the parent chemical form, then the resulting H_5IO_6 molecule would presumably analyse in the IO_4^- fraction. The high yields of IO_3^- observed may indicate bond-rupture in the decay event, or may arise from the chemical instability of H_5IO_6 in the telluric acid lattice, or chemical reactions of the primary recoil product(s) in solution. The products observed are qualitatively similar to those observed following nuclear reactions in periodates and iodates, or following transfer annealing in perchlorates and periodates doped with ^{131}I.[63] However, the periodate yield is higher in telluric acid then that generally found in the other cases.

The differences in the distributions of ^{131}I for ^{131}Te and ^{131m}Te must reflect differences in the decay schemes of the two isotopes. The decays of these isotopes differ principally in the relative timing of internal conversion events with respect to the β^--decay. Thus, in the decay of ^{131}Te, internal conversion of the .150 MeV transition in

^{131}I occurs in some 18 per cent of events following the β^--decay, while in the decay of ^{131m}Te the internal conversion of the .1817 MeV isomeric level occurs in 18 per cent of events preceding the β^--decay. While the excitation and ionisation of the daughter iodine molecule on the one hand, or the parent telluric acid molecule on the other, might be expected to lead to different patterns of molecular fragmentation, it is difficult to rationalize a 20 per cent difference in product distribution on this basis alone.

If we examine the recoil kinetic energy acquired in the two decays, it is found that the β^--transitions in the decay of ^{131}Te impart the highest recoil kinetic energy. Moreover, since the β^--transitions in ^{131}Te are high energy transitions in comparison with those observed for ^{131m}Te, "shake-off" due to non-adiabatic processes might be expected to be more important for ^{131}Te than ^{131m}Te. Thus the ^{131}Te decay is the more energetic process and yet yields a product distribution which may be interpreted as evidence of less molecular disruption. While the product distributions must in some way reflect differences in the decay of the two isotopes, it is not immediately apparent what the correlation between the two may be.

An examination of the thermal annealing data for the ^{131m}Te-labelled samples (Figure 12) shows that the thermal annealing reactions of the recoil atoms in the two samples exhibited quite marked differences. Since the two experiments

were identical except for the isotope with which the molecules were labelled, the different annealing reactions must reflect differences in the immediate lattice environments of the ^{131}I atoms produced in the two decay processes. However, if the labelled crystals were heated before the parent radioisotope underwent decay, then it was found that the iodine recoil atoms did not undergo significant thermal annealing in either case (see Table VII).

One consistent explanation for the above findings is that in the radioactive process the radiations emitted produce radiolysis of the surrounding lattice, this generating electrons and positive holes which are trapped at trap-sites in the crystal. On heating, thermal ionisation of the trapped defect may occur and the mobile electron or positive hole may diffuse to the recoil site initiating what is then observed as an annealing reaction. If the crystal is heated prior to the decay event, then the concentration of traps in the crystal must be changed in such a way that the subsequent heating no longer gives rise to an annealing reaction. Thus the concentration of traps may have been reduced in the heating process or, alternatively, the number of traps may have been greatly increased, thus leading to a decreased mobility of the trapped electrons and positive holes. Explanations of this kind have been invoked by a number of authors for a variety of annealing reactions in solids. As was discussed earlier, Andersen was able to directly correlate

the thermal annealing reactions of recoil atoms with the thermoluminescence glow curves and electrical conductivity for the solids concerned, this lending considerable support to the idea that electronic defects are involved in these processes.[65-67]

The absence of thermal annealing in the $H_6{}^{131}TeO_6$ and $H_6{}^{131m}TeO_6$ samples for the experiments of Table VII shows that, in each case in the absence of the participation of the trapped electronic defects in the crystal, little or no annealing of the recoil site is observed on heating.

Turning to the results for $H_6{}^{132}TeO_6$, we now see effects which can be clearly ascribed to the excitation and ionisation which accompanies the $^{132}Te \xrightarrow{\beta^-} {}^{132}I$ decay. Following the β^--decay, internal conversion of the .053 MeV γ-transition in ^{132}I will lead to Auger charging of the daughter iodine atom in >83 per cent of events. Thus, the chemical effects accompanying this decay may be expected to be more marked than in the decay of ^{131}Te or ^{131m}Te, which proceed in ca. 80 per cent of events by simple β^--decay. In Table VI it is seen that a much larger fraction of the daughter iodine activity analyses as the reduced form than was the case for ^{131}Te or ^{131m}Te. This appears to show more extensive molecular decomposition in the decay of ^{132}Te. As previously discussed, it was not possible to measure the IO_4^- fraction here

The thermal annealing data of Figure 14 shows that, while heating the $H_6{}^{132}TeO_6$ crystals before the production

of the recoil atom in the lattice did remove a small component in the annealing reaction, it did not lead to a total inhibition of the subsequent annealing reactions. The decay of ^{132}Te leads to the production of an ^{132}I recoil atom which can always undergo thermal annealing in a certain fraction of events, independent of the previous thermal history of the solid lattice.

In the case of $H_6{}^{129m}TeO_6$, the effects of the Auger charging accompanying the isomeric transition lead to molecular decomposition in at least 36 per cent of decay events, with the identifiable decomposition product being a tellurium in the +4 oxidation state. The thermal annealing reaction leads to the conversion of the recoil product back to the Te(VI) form, and this annealing reaction is completely independent of the previous thermal history of the sample (see Figure 15). This latter property is very similar to that for ^{132}I recoil atoms.

We may describe this above type of annealing reaction as being an intrinsic process, i.e., one involving molecular fragments or trapped electronic defects generated in the radioactive decay event itself. In both the ^{132}Te and ^{129m}Te samples the Auger charging accompanying the decay appears to be responsible for the production of this type of recoil site. In contrast, in $H_6{}^{131}TeO_6$ and $H_6{}^{131m}TeO_6$, the observed thermal annealing reactions of ^{131}I recoil atoms appear to be primarily extrinsic process, involving only defects present throughout the bulk of the lattice. In those

cases, the radioactive decay does not appear to generate a particularily defective recoil site. The small amount of annealing observed for the experiments shown in Table VII may be evidence of a small intrinsic component arising from the ca. 18 per cent of Auger charging which occurs in those decay processes.

It is apparent from the above discussion that the study of the thermal annealing reactions provides some useful information about the chemical environment surrounding the recoil atom in the solid. Even more useful information would be available if the precise chemical reactions occurring in the annealing process could be identified. However, since the chemical identity of the recoil atoms in the solid can only be surmised from the subsequently observed distribution in solution, a detailed description of the annealing reactions is precluded. Moreover, the experiments described here do not allow a positive identification of the crystal defects which appear to be involved.

Some general comments can be made about the annealing reactions which are observed. The fact that thermal annealing leads to a chemical redistribution of the radioiodine products clearly shows that the chemical form of the recoil atom in the crystal is changed on heating. It therefore appears quite probable that the iodine atoms are present initially in the crystal in other chemical forms in addition to that of the H_5IO_6 molecule. Thus the spectrum of iodine products

observed in the chemical analysis probably does not arise solely from reactions occurring in solution, and some I^- and IO_3^- are probably present in the crystal following the radioactive decay. It is also interesting that in the annealing reactions in $H_6{}^{131}TeO_6$ and $H_6{}^{131m}TeO_6$, the IO_4^- ion yield does not change. If the IO_4^- product is representative of H_5IO_6 molecules in the solid, the annealing reaction does not appear to reform the "parent" molecule.

In the case of the ^{129}Te atoms formed in $H_6{}^{129m}TeO_6$, on heating the solid the annealing reaction led to the oxidation of part of the Te(IV) fraction to the Te(VI) form, which was indistinguishable from telluric acid itself.

2. Neutron Irradiated Samples

The experiments on $^{130}Te(n,\gamma)^{131,131m}Te \xrightarrow{\beta^-} {}^{131}I$ showed the presence of very large fractions of IO_3^- and I^- following the irradiation. Again the results are very difficult to interpret in any quantitative way because of the almost certain presence of some annealing during the irradiation, coupled with the fact that two tellurium isotopes are produced in the (n,γ) reaction. However, the presence of very little IO_4^- ion as shown in the radiochemical analysis must indicate the presence of molecular decomposition in the primary (n,γ) recoil event in these irradiations. The thermal annealing reactions clearly show the important role played by γ-irradiation during the neutron bombardment and also the temperature during the irradiation (see Figure 11). Both

of these factors must be related to the production of trapped electronic defects in the solid during the irradiation. Consistent with this interpretation, the effect of heating the crystals before the neutron irradiation was to greatly inhibit the subsequent annealing processes (Figure 13). The annealing that was still observed to occur in that sample may be explained either by intrinsic annealing occurring within the defective (n,γ) recoil site or by virtue of trapped defects created by the concomitant γ-radiation.

The molecular fragmentation which accompanies the (n,γ) reaction was clearly shown in the $^{128}Te(n,\gamma)^{129}Te$ study (Table VIII). However, perhaps the most important point to be brought out here concerns the nature of the thermal annealing process which occurs in the crystal following the (n,γ) reaction. For the sample of telluric acid containing the $^{129m}Te(n,\gamma)$ recoil atoms produced in the N.R.U. reactor irradiation, these atoms were observed to have annealed in the irradiation back to the (VI) form, as previously discussed. In this sample the $^{129m}Te \rightarrow {}^{129}Te$ isomeric transition was then used as a probe to provide information about the immediate chemical environment surrounding the annealed ^{129m}Te atoms. As has been previously described, it was found that the $^{129m}Te \xrightarrow{I.T.} {}^{129}Te$ decay occurring in a thermally annealed (n,γ) recoil site in the crystal, was almost identical to that observed in $H_6{}^{129m}TeO_6$ chemically labelled samples, where there would be

no local lattice decomposition present from a preceding (n,γ) recoil event (see Figure 16(b)). This experiment indicates that the product of thermally annealing ^{129m}Te (n,γ) recoil atoms is probably a telluric acid molecule in a normal lattice environment.

. . . .

In discussing the above radiochemical results, an attempt was made to avoid speculation, while drawing from the results conclusions consistent with all the experimental information. The picture is obviously a confusing and complicated one, even in the relatively simple case where the radioactive decay of a molecule labelled with a single isotope was studied. Nevertheless, the radiochemical results do provide some useful information concerning the nature of the chemical environment of the recoil atom in the solid, and it will be of interest to compare these results with those of the Mössbauer investigation.

X. ^{129}I MÖSSBAUER EMISSION STUDIES

A. Introduction

In studying the chemical effects of the nuclear transformations in H_6TeO_6 by Mössbauer spectroscopy, it was necessary to study the spectra of several related compounds to aid in the interpretation of the results obtained. Thus the compounds H_6TeO_6, $(H_2TeO_4)_n$, α-TeO_3, H_2TeO_3, and tetragonal TeO_2 were all studied labelled with ^{129}Te and ^{129m}Te isotopes. The (n,γ) reaction was also studied in H_6TeO_6, α-TeO_3, and TeO_2.

The α-TeO_3 prepared by thermal decomposition of telluric acid contained TeO_2 as impurity. For this reason β-TeO_3, which is prepared by the dehydration of H_6TeO_6 in the presence of H_2SO_4 and does not contain any TeO_2, was also investigated. The method of preparation unfortunately precluded the synthesis of ^{129}Te-labelled β-TeO_3.

Sodium and potassium tellurate were investigated, although here again the ^{129}Te-labelled compound was not studied.

The compound $(NH_4)_2TeCl_6$ is not directly related to the other compounds investigated, but was studied because it could be readily prepared labelled with both ^{129}Te and ^{129m}Te. It was also of some interest because it contains an octahedrally co-ordinated Te(IV), and allowed a comparison with the

octahedrally co-ordinated Te(VI) in telluric acid.

Since elemental tellurium was routinely irradiated to prepare the ^{129m}Te activity, it was convenient to study the possible chemical effects in this material as well.

Throughout the following sections the Mössbauer spectra shown are the experimentally observed spectra. Because all of these experiments are emission experiments, the measured isomer shifts, relative to the $Na^{129}I$ absorber, are not consistent with those reported for standard absorption experiments. To clarify the following discussion and allow a ready comparison of the data with the values in the literature, all isomer shifts have been corrected so that they correspond to isomer shifts for absorption experiments relative to a zinc telluride source. To achieve this correction, the following expression was used.

$$\text{REPORTED } \delta = -(\text{EXPERIMENTALLY OBSERVED } \delta + 0.46) \text{ mm. sec.}^{-1}$$

The 0.46 mm. $sec.^{-1}$ term is the isomer shift for a $Na^{129}I$ absorber relative to a zinc telluride source.

In addition to the discussion of the studies of chemical effects of the nuclear transformations, several parameters which could be obtained from the Mössbauer spectra and which are of more general interest are discussed in an Appendix.

B. ^{129}Te-Labelled Sources

The ^{129}I Mössbauer emission spectra for ^{129}Te-labelled sources are shown in Figures 17 to 20, and the spectrum parameters obtained by computer fit are shown in Table IX.

1. ^{129}Te-Labelled Tellurium (VI) Compounds

The ^{129}I Mössbauer emission spectra obtained for ^{129}I produced following β^--decay in ^{129}Te-labelled H_6TeO_6, $(H_2TeO_4)_n$, and α-TeO_3 are shown in Figures 17 and 18. These spectra are interpreted as a direct evidence that chemical effects accompanying the β^--decay of the parent ^{129}Te are not seen in any of these compounds. In each instance the ^{129}I remains bonded to the ligands of the parent ^{129}Te molecule.

The spectrum measured for monoclinic telluric acid at liquid nitrogen temperature (Figure 17(a)) was interpreted as exhibiting a small quadrupole splitting as a consequence of the distorted octahedron of surrounding -OH ligands found in the monoclinic telluric acid structure. The positions and relative intensities of the eight lines in the quadrupole split spectrum are shown in this figure. This spectrum is in excellent agreement with that reported by Pasternak.[192] The isomer shift for monoclinic telluric acid of -3.59 mm.sec.$^{-1}$ measured in this work is in close agreement with that reported for $Na_3H_2{}^{129}IO_6$ relative to a standard Zn^{129}Te source (-3.35 mm.sec.$^{-1}$), indicating that the molecule remained intact

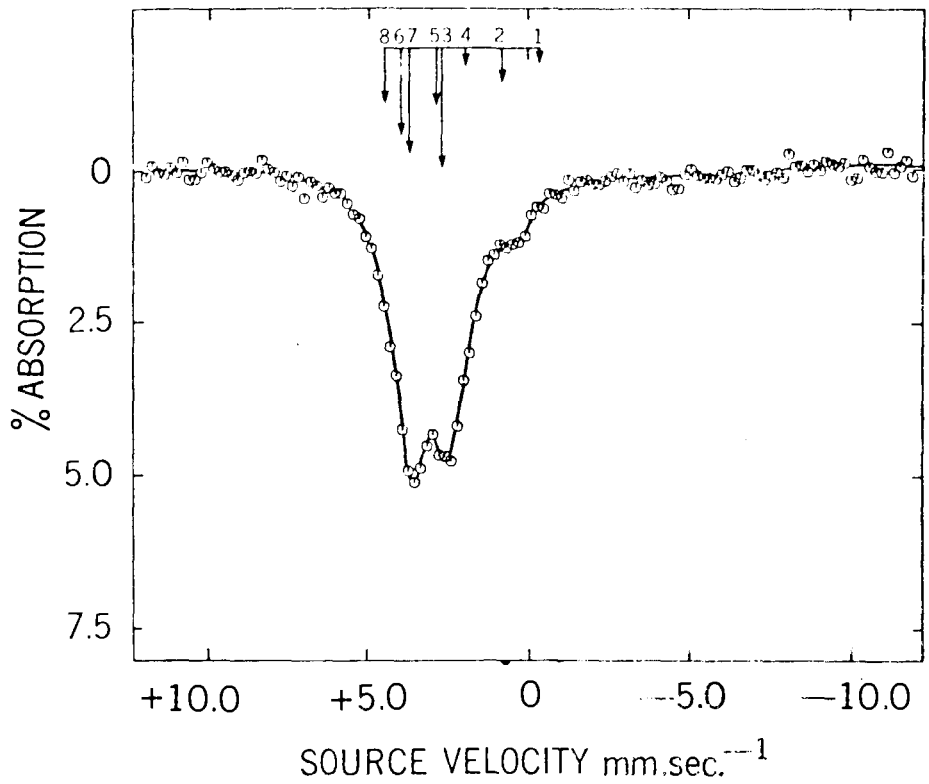

(a)

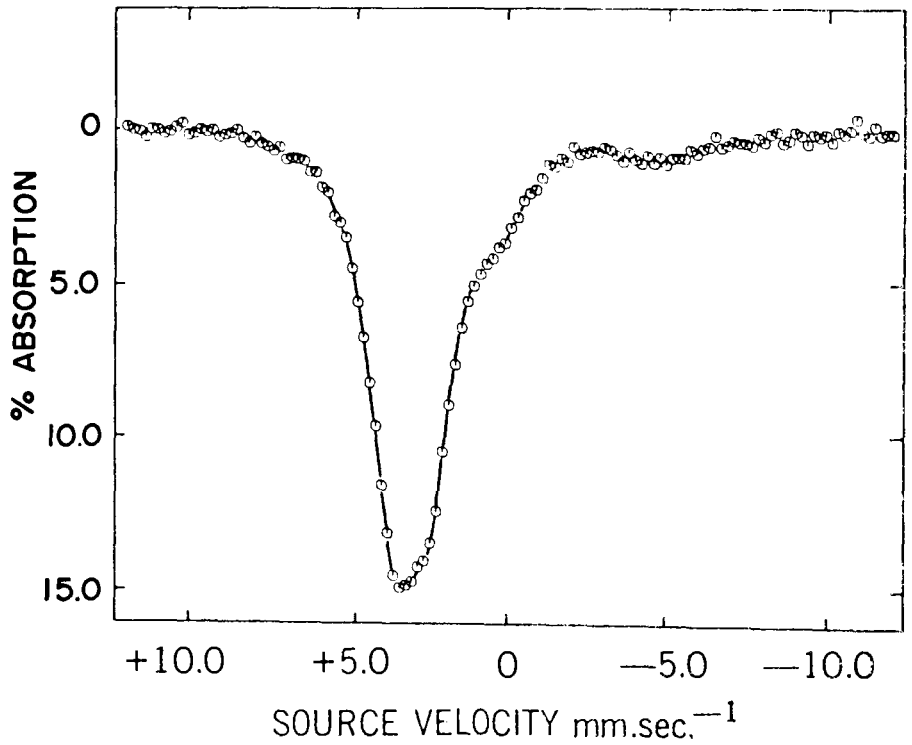

(b)

Figure 17 ^{129}I Mössbauer Emission Spectra For Na^{129}I Absorber vs. $H_6{}^{129}TeO_6$ Source Measured at
(a) Liquid Nitrogen Temperature and
(b) Liquid Helium Temperature.

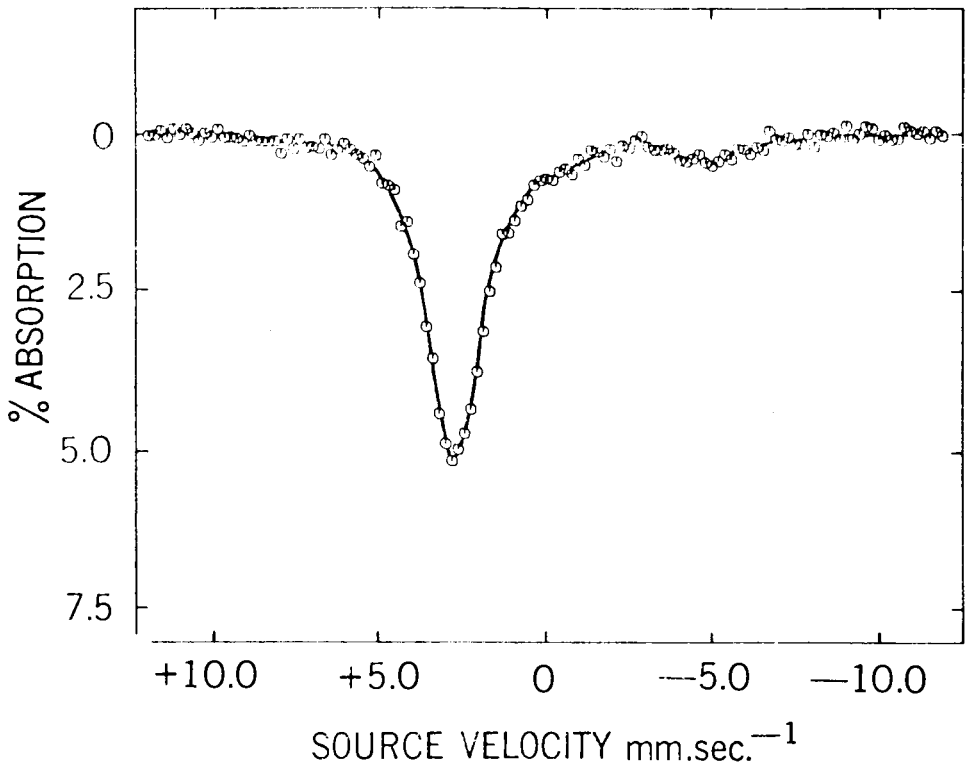

(a)

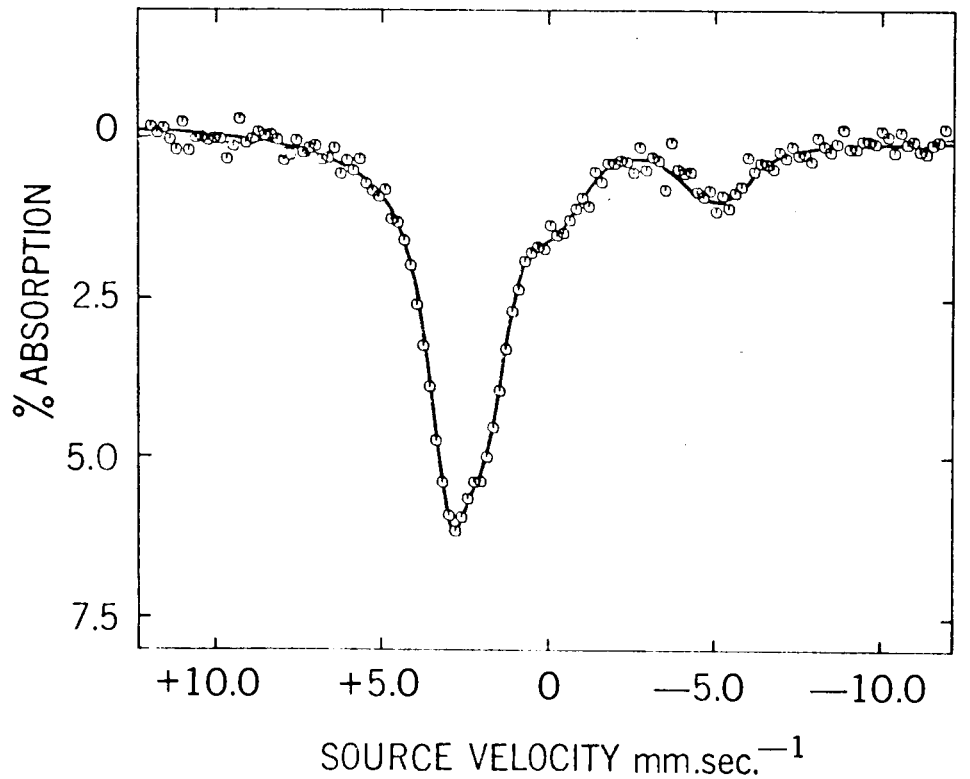

(b)

Figure 18 ^{129}I Mössbauer Emission Spectra Measured at 80°K. For $Na^{129}I$ Absorber vs. (a) $(H_2{}^{129}TeO_4)_n$ Source and (b) α-$^{129}TeO_3$ Source.

TABLE IX

PARAMETERS OF ^{129}I MÖSSBAUER EMISSION SPECTRA OF ^{129}Te-LABELLED SOURCE COMPOUNDS

COMPOUND	δ^* mm.sec.$^{-1}$	$e^2qQ^\dagger$ Mc.sec.$^{-1}$	η	Γ_{expt} mm.sec.$^{-1}$
H_6TeO_6 (MONOCLINIC)	-3.59±0.11	+192±5		1.26±.04
$(H_2TeO_4)_n$	-3.44±0.03			1.99±.04
α-TeO_3	-3.05±0.04			2.34±.07
H_2TeO_3	+1.74±0.17	+839±21	0.40±0.06	1.44±.09
TeO_2 (TETRAGONAL)	+2.74±0.14	+812±21	0.52±0.07	1.24±.08
$(NH_4)_2TeCl_6$	+6.03±0.30			1.19±.22
ELEMENTAL TELLURIUM	+0.52±0.13	-349±11	0.69±0.2	1.20±.20

*Quoted as isomer shifts for absorption spectra relative to a $Zn^{129}Te$ source.

†The sign of the quadrupole coupling constants reported here are also consistent with those obtained in standard absorption experiments.

following the β^--decay. In the liquid helium spectrum for this same compound (Figure 17(b)) the per cent effect was greatly increased, although the quadrupole splitting was even less well resolved than at 80°K. However, the two spectra computed to yield the same parameters within the error of the fit. The loss of resolution observed here was found in all spectra measured at liquid helium temperature, and was attributable to line broadening resulting from vibrations in the source and absorber caused by the rapid boil-off of the liquid helium in the vacuum dewar.

The interpretation of the spectra in terms of a small quadrupole splitting is supported by the fact that any attempt to fit the spectra with a combination of single lines yielded isomer shifts for those lines which did not correspond to any known iodine ion. Consistent with this interpretation, the spectrum of cubic $H_6{}^{129}TeO_6$ would be expected to be a single line. Since the cubic modification can only be obtained by slow crystalisation from solution, and even then only in the presence of large amounts of the monoclinic form, the cubic form could not be studied.

For the polymer, $(H_2TeO_4)_n$ (Figure 18(a)), it is apparent that the ^{129}I quadrupole splitting was much smaller than that in monoclinic telluric acid, and the spectrum, computed as a broad single line, had an isomer shift again very close to that for $Na_3H_2{}^{129}IO_6$. (The presence of some contaminating ^{129m}Te in this sample led to the presence of

other lines in this spectrum.) This data is consistent with the I.R. data which in the polymer shows only a broad band with essentially no fine structure, while in monoclinic telluric acid three distinct bands are observed which correspond to the three Te-OH distortion modes in the distorted octahedral structure.[207] Thus, in the polymer the geometry around the tellurium must be close to octahedral and this is reflected in the single, though broadened, ^{129}I emission line.

In α-$^{129}TeO_3$ (Figure 18(b)), the presence of TeO_2 impurity was clearly discernable. The assignment of the Mössbauer emission lines in this spectrum was made on the basis of a single absorption line and eight lines corresponding to the quadrupole split spectrum of ^{129}I produced by β^--decay in $^{129}TeO_2$. The ^{129}I emission spectra and ^{125}Te absorption spectra of the same samples of α-$^{129}TeO_3$ gave very close agreement for the percentage of $^{129}TeO_2$ impurity present in these samples. The single emission line attributable to ^{129}I produced following β^--decay in α-$^{129}TeO_3$ had about the same isomer shift as observed in $H_6{}^{129}TeO_6$ and $(H_2{}^{129}TeO_4)_n$, indicating that here again the parent tellurium is octahedrally surrounded by O-ligands. The broadening observed in this single line may again be attributed to a very small, irresolvable quadrupole splitting in α-TeO_3, resulting from some apparent distortion from perfect octahedral symmetry about the tellurium atom.

2. ^{129}Te-Labelled Tellurium (IV) Compounds

The ^{129}I Mössbauer emission spectra were studied for the tellurium (IV) compounds H_2TeO_3, tetragonal TeO_2, and $(NH_4)_2TeCl_6$. Again, chemical effects of the $^{129}Te \rightarrow {}^{129}I$ β^--decay were not observed in these source compounds.

For $H_2{}^{129}TeO_3$ (Figure 19(a)), the ^{129}I emission spectrum had an isomer shift similar to that reported for the iodate ion in $K^{129}IO_3$. The quadrupole splitting, however, was close to the value observed for HIO_3 from N.Q.R. measurements.[220] Moreover, the spectrum also exhibited an asymmetry parameter, η, similar to that for the HIO_3 molecule, while the iodate ion which has axial symmetry is known to have an asymmetry parameter of zero.[134] These values are compared below.

	δ	e^2qQ_{gnd}	η
$H_2{}^{129}TeO_3$	1.74±.17 mm.sec.$^{-1}$	839±21 Mc.sec.$^{-1}$	.40±.06
$K^{129}IO_3$ [134]	1.56±.2	698.9	0
$H^{129}IO_3$ [220]	-	799.9	.434

Thus is may be concluded that following β^--decay, the parent molecular configuration is retained for ^{129}I in H_2TeO_3.

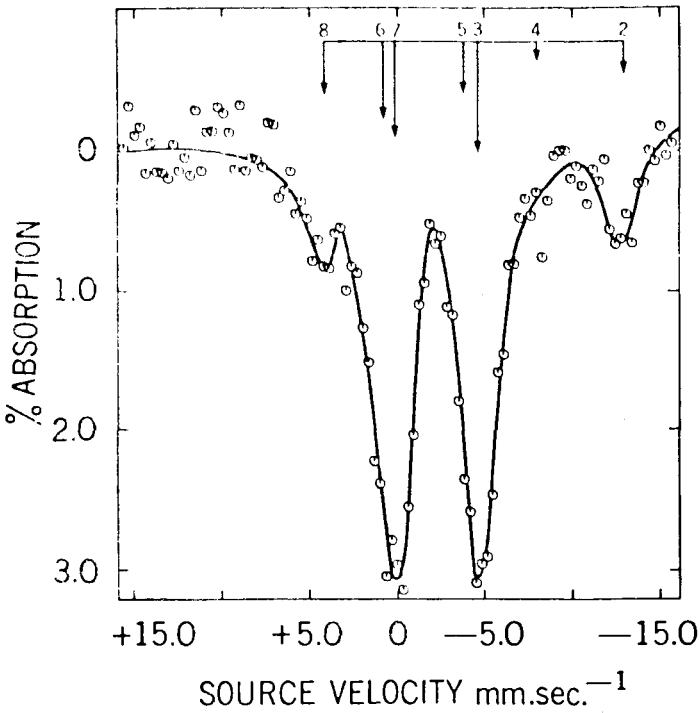

(a)

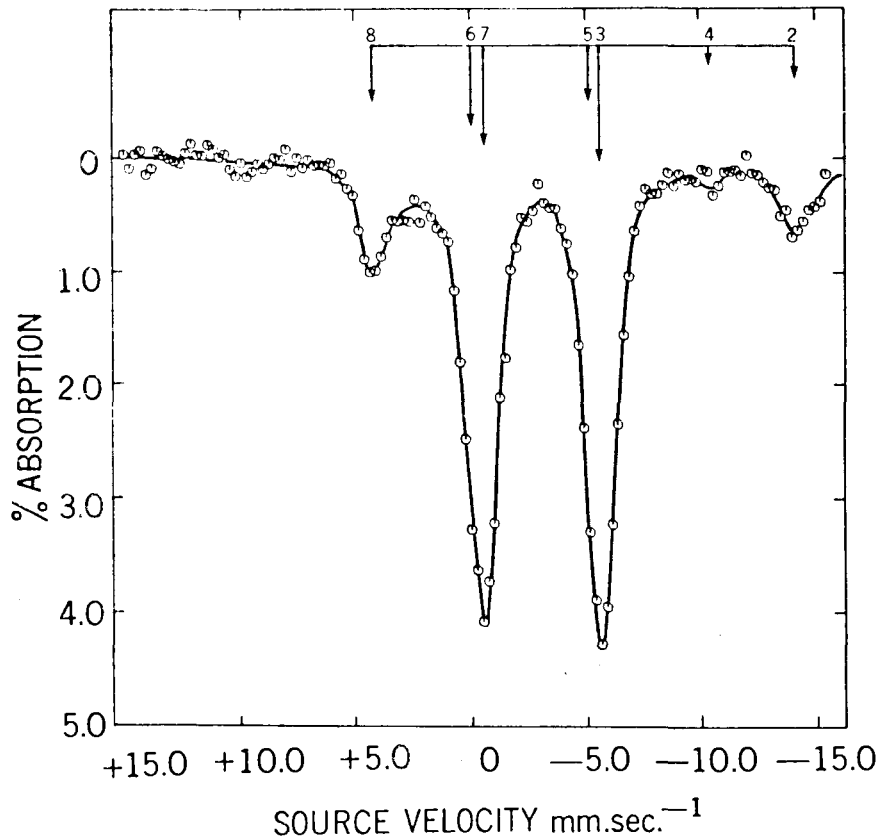

(b)

Figure 19 ^{129}I Mössbauer Emission Spectra Measured at 80°K. For Na^{129}I Absorber vs. (a) $H_2{}^{129}TeO_3$ Source and (b) Tetragonal $^{129}TeO_2$ Source

For tetragonal TeO_2 (Figure 19 (b)), the spectrum was again quadrupole split. Only one iodine lattice site was observed following the β^--decay, and again the iodine presumably finds itself in the same lattice environment as the parent tellurium. It is of interest to note that the isomer shift for tetragonal TeO_2 measured here is different from that reported for the orthorhombic modification,[193] but that the two have about the same quadrupole coupling constant and asymmetry parameter, as shown below.

$^{129}TeO_2$-structure	δ	e^2qQ_{gnd}	η
orthorhombic[193]	+1.52±.06 mm.sec.$^{-1}$	786±7 Mc.sec.$^{-1}$	.55±.05
tetragonal	+2.74±.14	812±21	.52±.07

The two crystal structures for TeO_2 were discussed previously (see page 108 and Figure 9). The similarity in the disposition of bonds about the tellurium is reflected in the similar quadrupole splittings and asymmetry parameters measured for these two compounds. The difference in isomer shifts must then presumably derive from differences in the s-character of the I-O bonds for ^{129}I in these two lattices. The more positive isomer shift in the emission spectrum of the tetragonal form is evidence of a higher s-electron density at the ^{129}I nucleus than for ^{129}I in the orthorhombic TeO_2 structure. This point will be returned to in the discussion in the Appendix.

The emission spectrum for ^{129}I in $(NH_4)_2{}^{129}TeCl_6$ Figure 20(a)) showed a single sharp line with a very large positive isomer shift of δ = 6.03 mm.sec.$^{-1}$. The single emission line observed indicates that the ^{129}I atom produced in the β^--decay is surrounded octahedrally by chlorine liqands. The parent $TeCl_6^{2-}$ ion is also octahedral, as was evidenced by the single line observed in the ^{125}Te absorption spectrum for this compound. The single line ^{129}I spectrum is consistent with the formation of ICl_6^- in the β^--decay.

3. Elemental Tellurium

The ^{129}I spectrum reported here for elemental tellurium precipitated from aqueous solution (Figure 20(b)) is identical to that previously reported for neutron irradiated elemental tellurium.[193] The spectrum provides two pieces of evidence that following the β^--decay of ^{129}Te, the ^{129}I atom finds itself in a quite different lattice environment from that of the parent tellurium.

Pasternak and Bukshpan[193] noted that if the ^{129}I is formed in the same chemical environment as the tellurium then for a series of tellurium parent compounds the ratio $\frac{e^2qatQ\ (^{125}Te)}{e^2qatQ\ (^{129}I)}\ (1 + \frac{\eta^2}{3})^{1/2}$ should be a constant, which they found to be 0.4. However, for elemental tellurium the value of 1.17 was observed in their work, and a similar value of 1.27±.05 was obtained in the present investigation. Thus

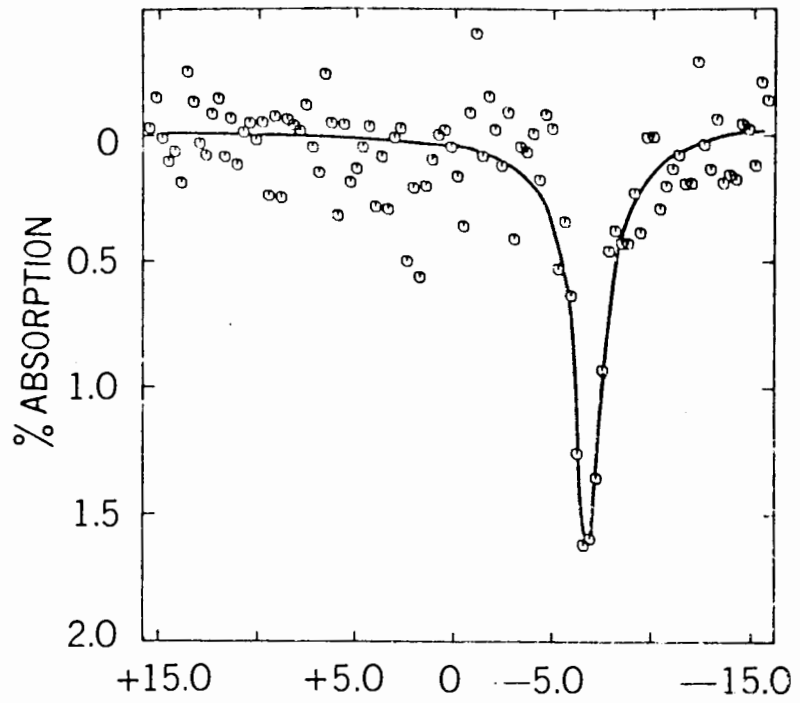

(a)

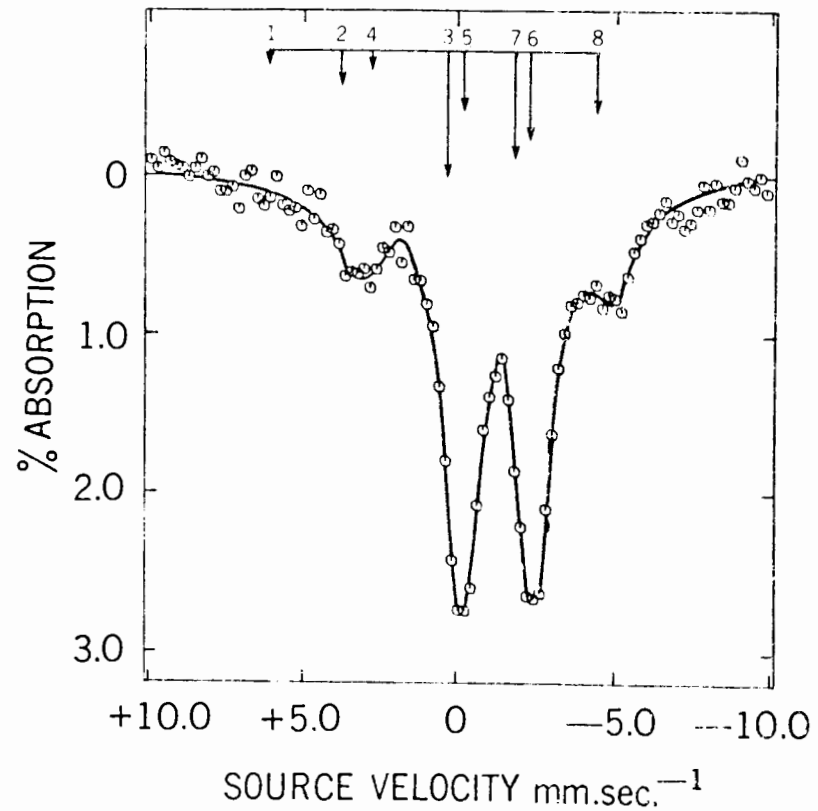

(b)

Figure 20 ^{129}I Mössbauer Emission Spectra Measured at 80°K. for $Na^{129}I$ Absorber vs. (a) $(NH_4)_2{}^{129}TeCl_6$ Source and (b) Elemental Tellurium Source .

the daughter ^{129}I atoms in the elemental tellurium lattice must experience a very different electrostatic field gradient from that of the tellurium atoms.

The second piece of evidence relates to the value of the isomer shift. If the daughter iodine remains bonded to the same atoms as the parent tellurium, then the ratio of the isomer shifts $\frac{\delta(^{125}Te)}{\delta(^{129}I)}$ should be a constant for a series of tellurium parent compounds. The values obtained in the present work are shown in Figure 21, and it can be seen that the values for elemental tellurium lie a long way off the least squares fit to the other data points.

It is apparent from the above discussion that following the decay of ^{129}Te, the ^{129}I atom does not remain bonded to both of the adjacent tellurium atoms in the helical chain structure of the tellurium lattice. This phenomenon probably does not arise from the chemical effects of recoil or electronic excitation arising from the β^--decay, but may simply be due to the different bonding characteristics of iodine and tellurium in the tellurium lattice.

Pasternak has reported a divergence from theoretical line intensities for the ^{129}I emission spectrum in tellurium, which is attributable to an anisotropy in the recoil-free fraction. In the present work, the errors in the line intensities did not allow the measurement of these very small effects.

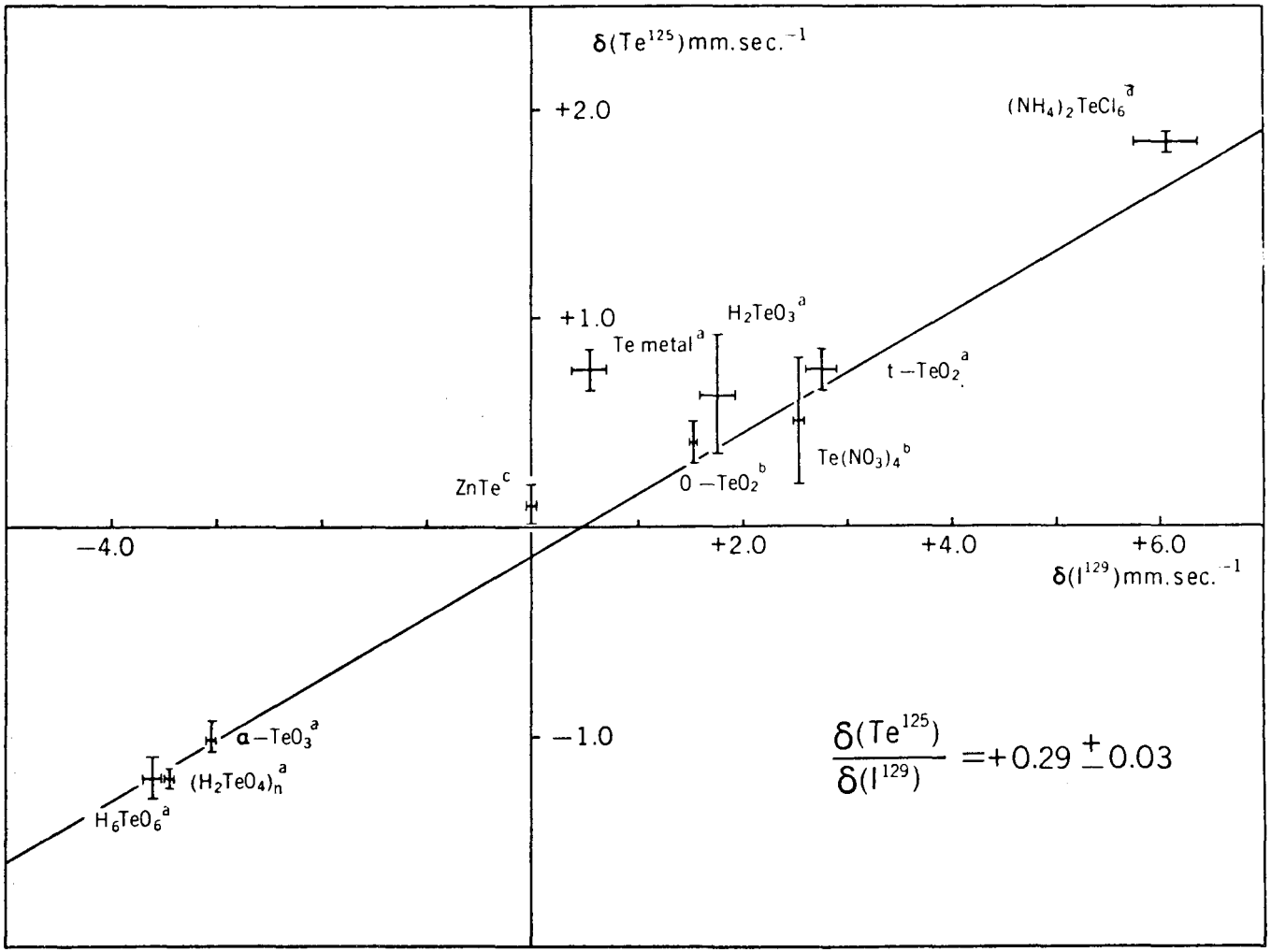

Figure 21 $\delta(^{129}I)$ vs. $\delta(^{125}Te)$ a. This Work; b. [192]; c. [124].

. . . . .

In concluding this section it can be stated that with the exception of elemental tellurium, in the compounds studied labelled with ^{129}Te, the ^{129}I β^--decay products appear to be iso-structural and iso-electronic with the parent tellurium molecules. In each instance, no effects of recoil or electronic excitation arising from the β^--decay are observed, and the molecule remains intact following the β^--decay event. The isomer shift data of Figure 21 serves to clearly illustrate this point.

C. ^{129m}Te-Labelled Sources and Neutron Irradiated Sources

1. Telluric Acid

Of the tellurium oxy-compounds investigated, telluric acid showed the most clear effects of molecular disruption accompanying both the $^{129m}Te \rightarrow {}^{129}Te$ isomeric transition decay and the $^{128}Te(n,\gamma)^{129}Te$ nuclear reaction. In Figures 22 and 23 are shown sample spectra for several telluric acid sources.

In these experiments $H_6{}^{129m}TeO_6$ sources were allowed to reach radioactive equilibrium with the daughter ^{129}Te at either liquid nitrogen (Figure 22(a)) or liquid helium (Figure 22 (b)) temperature, and the Mössbauer spectrum was then recorded at that temperature. Again we see that the

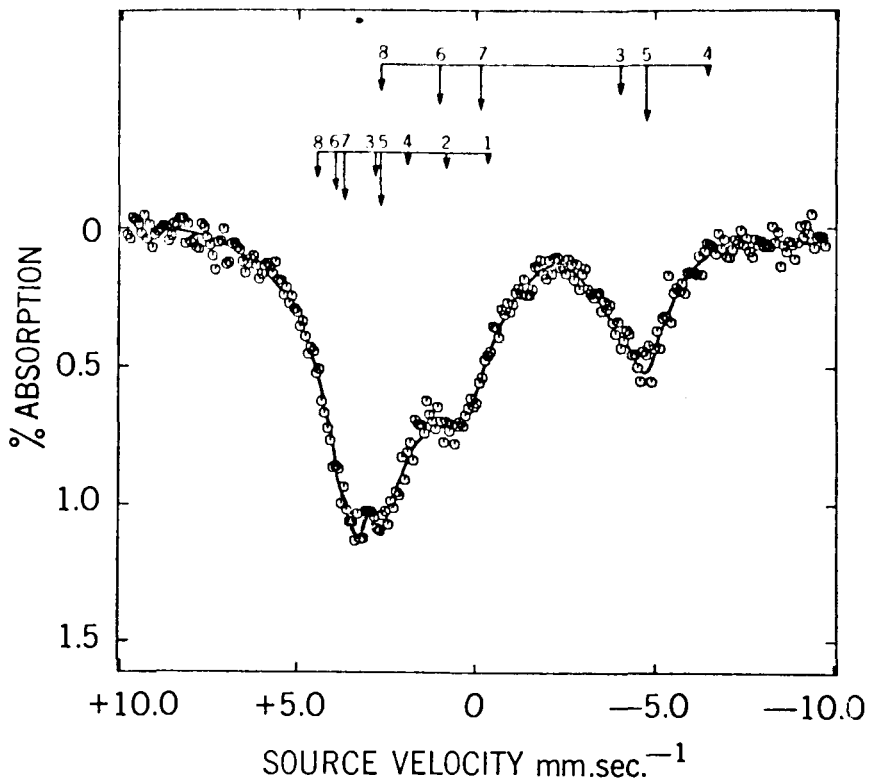

(a)

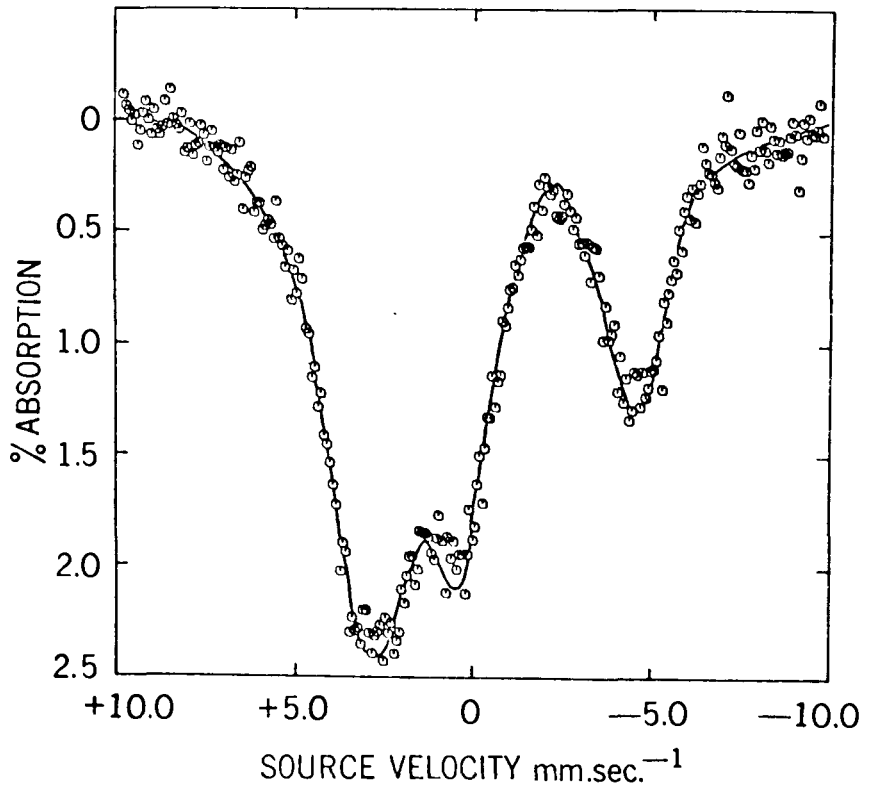

(b)

Figure 22 ^{129}I Mössbauer Emission Spectra for Na^{129}I Absorber vs. $H_6{}^{129m}TeO_6$ Source Measured at
(a) Liquid Nitrogen Temperature and
(b) Liquid Helium Temperature.

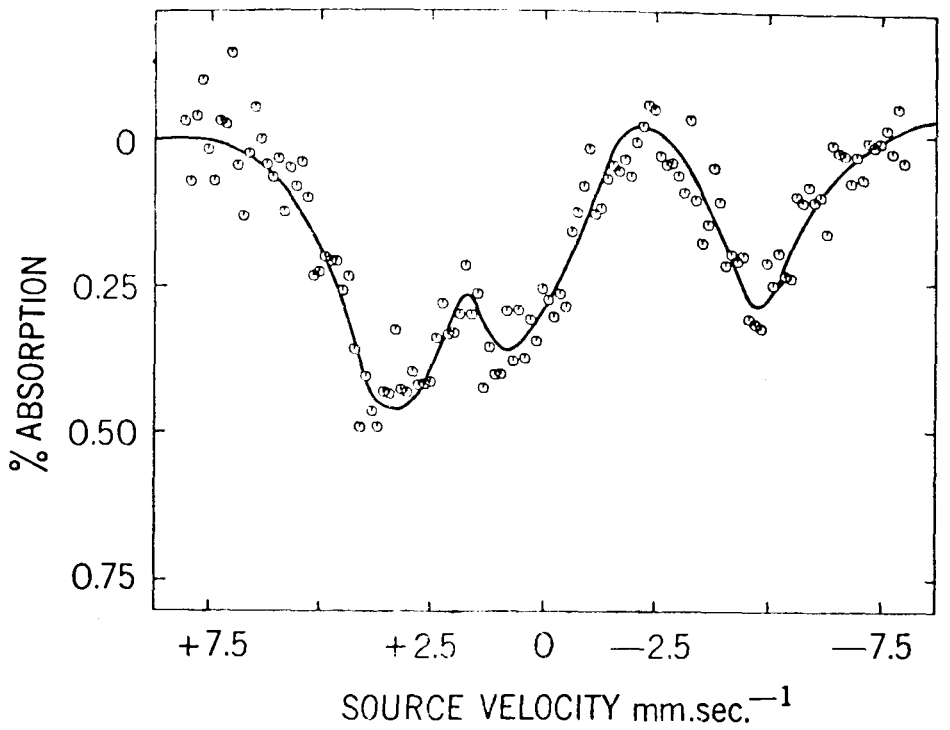

(a)

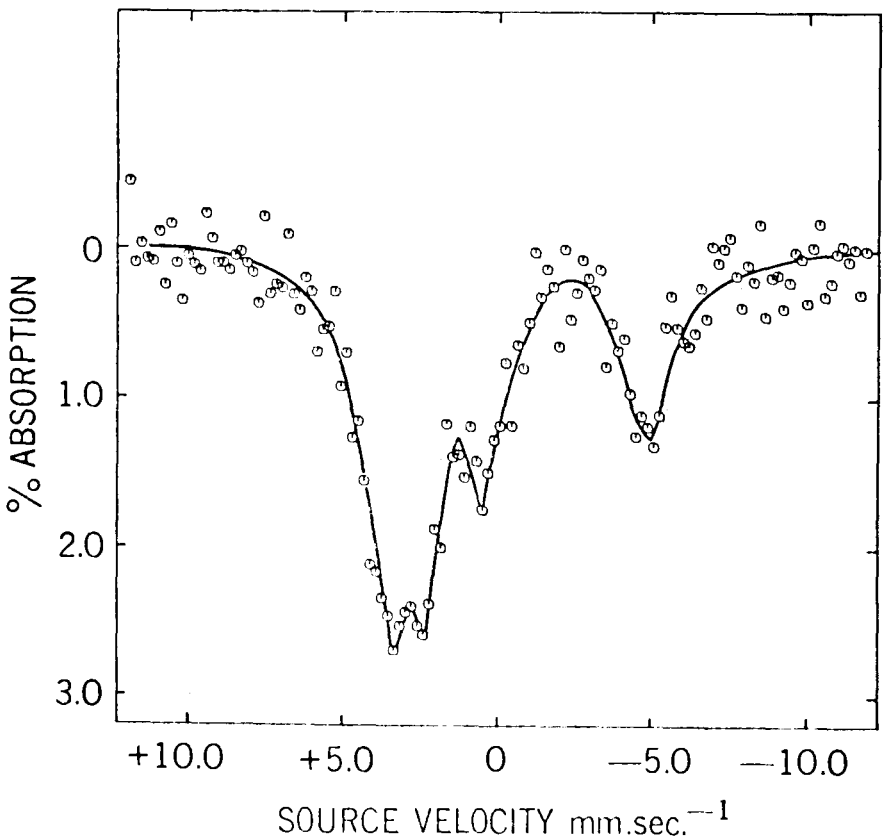

(b)

Figure 23 ^{129}I Mössbauer Emission Spectra Measured at 80°K. For Na^{129}I Absorber vs. (a) $H_6{}^{129m}TeO_6$ Source in Water Frozen at 80°K. and (b) $H_6{}^{128}TeO_6$ $(n,\gamma)^{129}$Te Source.

emission lineswere broadened in the liquid helium spectrum, though for both the liquid nitrogen and liquid helium experiments the line widthswere the same as were measured in emission spectra of the corresponding ^{129}Te-labelled source experiments.

In one experiment an aqueous solution of $H_6{}^{129m}TeO_6$ was frozen at 80°K., the sample stored at this temperature while the $^{129m}Te \rightarrow {}^{129}Te$ radioactive equilibrium was reached, and the spectrum for the ice matrix then recorded at that temperature. This spectrum is shown in Figure 23(a).

For the study of the $^{128}Te(n,\gamma)^{129}Te$ nuclear reaction in telluric acid, irradiations were performed at ambient temperature (ca. 70°C.) in the Seattle reactor, and the Mössbauer emission spectrum was then recorded at liquid nitrogen temperature immediately following the irradiation. This spectrum is shown in Figure 23 (b).

Each of the above experiments was repeated on many samples of H_6TeO_6, all of which were shown by I.R. and ^{125}Te absorption spectroscopy to be free of contaminating TeO_2 and $TeO_3{}^{2-}$ species.

An attempt was also made in this work to study the $^{128}Te(n,\gamma)\ ^{129m}Te\ I.T.{}^{129}Te$ transformation sequence in telluric acid. However, although the samples were cooled to $\leq$ 40°C. during the reactor irradiation in the N.R.U. reactor, they were found to have completely decomposed to TeO_2, presumably as a result of the high concomitant γ-dose received during the

irradiation (ca. 100 Mrd.hr.$^{-1}$).

A comparison of the data of Figures 22 and 23 with that of Figure 17 clearly shows that following isomeric transition decay or thermal neutron capture in telluric acid, the ^{129}Te atoms are stabilised in the solid not only in the parent H_6TeO_6 form, but also as an apparently Te(IV) fragment. The spectra of Figures 22 and 23 could be accurately computer fitted, assuming the presence of a Te(VI) component identical to monoclinic telluric acid and a tellurite ion with the same δ and e^2qQ as for H_2TeO_3, but with η=0. The results of these analyses are shown in Table X. It is implicit in these analyses that there are no effects of the β^--decay in these compounds and that the ^{129}I spectra accurately reflect the chemical forms of the ^{129}Te atoms following the transformation.

Independently prepared telluric acid sources yielded reproducible spectra, although the analysis of the relative areas in the absorption spectrum deriving from ^{129}Te(VI) and ^{129}Te(IV) fractions yielded differences of ±3 per cent. In all telluric acid sources the lower valence fraction could be fitted assuming the same values for δ and e^2qQ, i.e., for H_2TeO_3. If H_2TeO_3 itself were formed as a product of the decomposition, then the lower valence fraction would be expected to have an asymmetry parameter, η, which reflects the non-axial symmetry in this molecule deriving from an inequality in the lengths of the Te-OH and Te-O bonds.

TABLE X

DISTRIBUTION OF ^{129}Te (VI) AND ^{129}Te (IV) FOLLOWING ISOMERIC TRANSITION AND NEUTRON CAPTURE IN Te (VI) SOURCE COMPOUNDS

SOURCE	Distribution‡ of Products in %	
	Te^{129} (VI)	Te^{129} (IV)
$H_6{}^{129m}TeO_6$ liquid N_2	53±3	47±3
$H_6{}^{129m}TeO_6$ liquid He	56±3	44±3
$H_6{}^{129m}TeO_6$ (ice)	50±3	50±3
$H_6{}^{128}TeO_6$ $(n,\gamma)^{343°K}$	59±3	41±3
$(H_2{}^{129m}TeO_4)_n$ liquid N_2	63±3	37±3
$(H_2{}^{129m}TeO_4)_n$ liquid He	62±3	38±3
$Na_2{}^{129m}TeO_4$ liquid N_2	100	
$K_2{}^{128}TeO_4$ $(n,\gamma)^{343°K}$	65±3	35±3

‡ Computed from the relative areas under the absorbtion peaks, assuming that the recoil free fraction for the two parent Te species are the same.

However, since η is only reflected in the positions of lines 4 and 8 in a quadrupole split spectrum, it is very difficult in the present case to totally exclude the possibility that H_2TeO_3 is formed. Line 4 in the quadrupole split spectrum has a very low intensity, and line 8 is completely overlapped in these spectra by the emission spectrum of $H_6{}^{129}TeO_6$ in the source. However, it was found that if it was assumed that $\eta=0$, then a statistically more acceptable fit was obtained for all of the spectra of Figures 22 and 23. On this basis it is concluded that the decomposition product formed in the nuclear transformation probably had axial symmetry. Thus the fragment may well be the TeO_3^{2-} ion. However, since the values for δ and e^2qQ were much closer to those for ^{129}I born in $H_2{}^{129}TeO_3$, it is conceivable that the decomposition product may be the $Te(OH)_3^+$ complex, which would again have axial symmetry.

It is interesting that in the molecular decomposition accompanying the nuclear transformation the bonding to the tellurium changes very markedly in character. In the parent H_6TeO_6 molecule the tellurium employs sp^3d^2 hybrids in forming bonds with the -OH groups leading to a low s-electron density at the nucleus, as reflected in the isomer shift. Following molecular fragmentation, the tellurium now employs almost pure p-orbital bonding, again as reflected in the isomer shift, which now indicates a high s-electron density at the parent tellurium nucleus. Thus the molecular

disruption which occurs does not lead simply to a change in the co-ordination number of the tellurium, but leads to a very fundamental change in the nature of the bonding.

2. $(H_2TeO_4)_n$ and Tellurate Salts

In the polymer, $(H_2TeO_4)_n$, molecular fragmentation was observed following the isomeric transition as in telluric acid. The experiments were carried out in a similar way. Sources of $(H_2{}^{129m}TeO_4)_n$ were allowed to reach radioactive equilibrium with the daughter ^{129}Te at liquid nitrogen (Figure 24(a)) and liquid helium temperatures (Figure 24(b)), and the spectra then recorded at those temperatures. The ^{129}Te(IV) fragment observed in these samples was analysed to be the same ^{129}Te (IV) species as that produced in H_6TeO_6, although the yield of the Te(IV) fragment was now significantly decreased in comparison with that for telluric acid. The samples used in these experiments were also found to be totally free of TeO_2 or any other tellurium impurity.

The spectrum for sodium tellurate prepared labelled with ^{129m}Te and measured at liquid nitrogen temperature is shown in Figure 25 (a). Here, perhaps somewhat surprisingly, chemical effects of the internally converted isomeric transition decay were not found. The single emission line observed was quite broad with Γ_{expt} = 2.64 mm.sec.$^{-1}$, and has an isomer shift of δ = -3.30±.05 mm. sec.$^{-1}$, which again corresponds very closely to that for $Na_3H_2IO_6$. This value

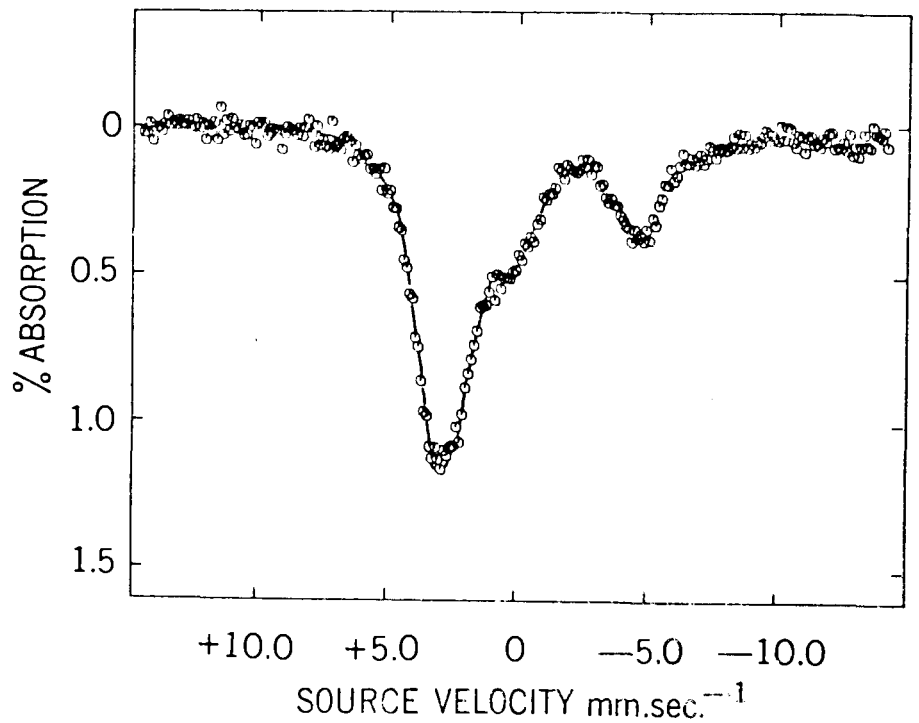

(a)

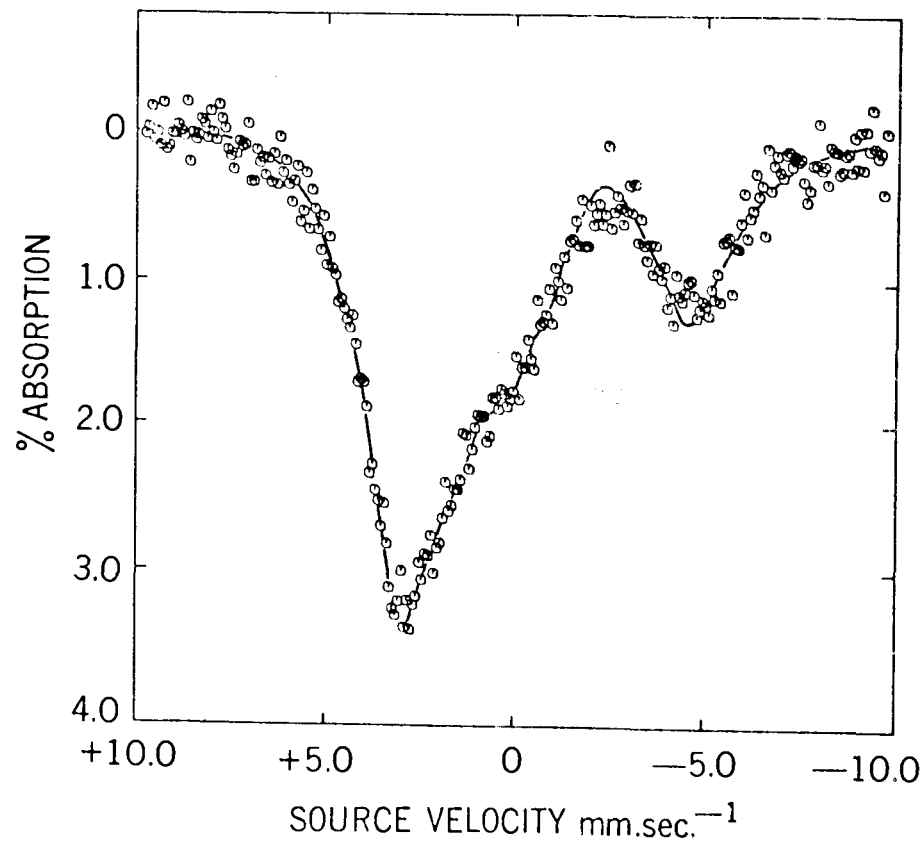

(b)

Figure 24 ^{129}I Mössbauer Emission Spectra for $Na^{129}I$ Absorber vs. $(H_2{}^{129m}TeO_4)_n$ Source Measured at
(a) Liquid Nitrogen Temperature and
(b) Liquid Helium Temperature.

of the isomer shift lends considerable support to Erickson and Maddock's proposal, based on I.R. spectral data, that the tellurium atom in these tellurate compounds has octahedral rather than tetrahedral symmetry.[207] The very broad emission line observed in this Mössbauer spectrum indicates the presence of some distortion from regular octahedral geometry in the polymeric anion. In the absence of observable chemical effects accompanying the isomeric transition, it was not considered necessary to study the ^{129}Te-labelled compound.

Some molecular fragmentation was found to occur in K_2TeO_4 following the $^{128}Te(n,\gamma)^{129}Te$ nuclear reaction, as seen in Figure 25(b). This spectrum was analyzed as showing the presence of a Te(IV) fragment very similar to that observed in H_6TeO_6 and $(H_2TeO_4)_n$. However, the statistics and per cent absorption observed in this spectrumwere quite poor, making any detailed analysis of the chemical nature of the Te(IV) fragment most difficult.

A broad single emission line (Γ_{expt} = 2.6 mm.sec.$^{-1}$) having an isomer shift of δ = -2.92±.11 mm.sec.$^{-1}$ was observed in the remaining fraction of events in this K_2TeO_4 (n,γ) spectrum. The large negative isomer shift observed again shows the central tellurium atom to be surrounded by an octahedron of oxygen ligands.

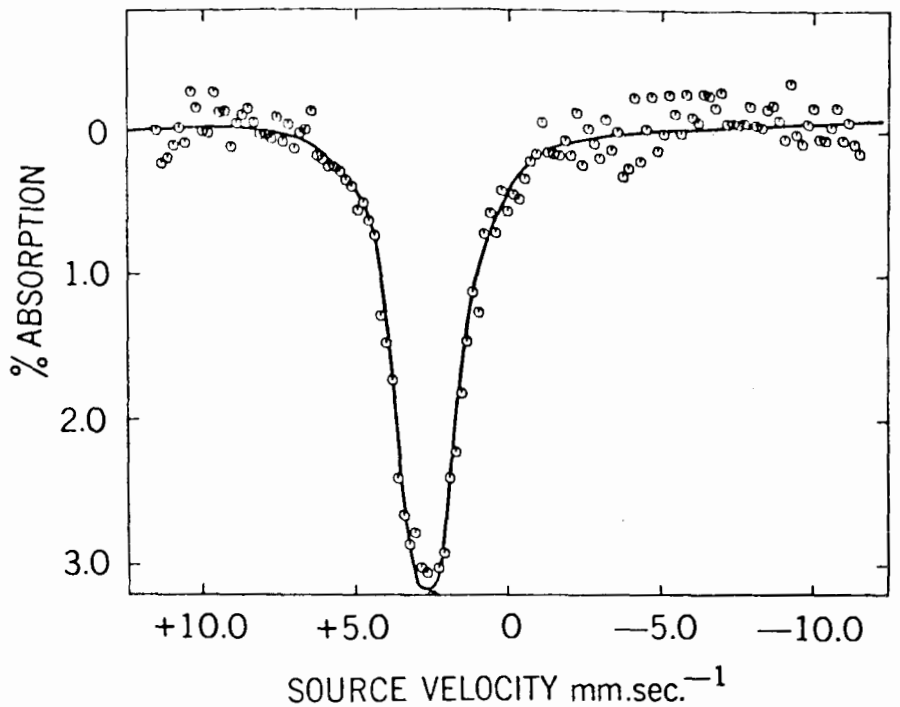

(a)

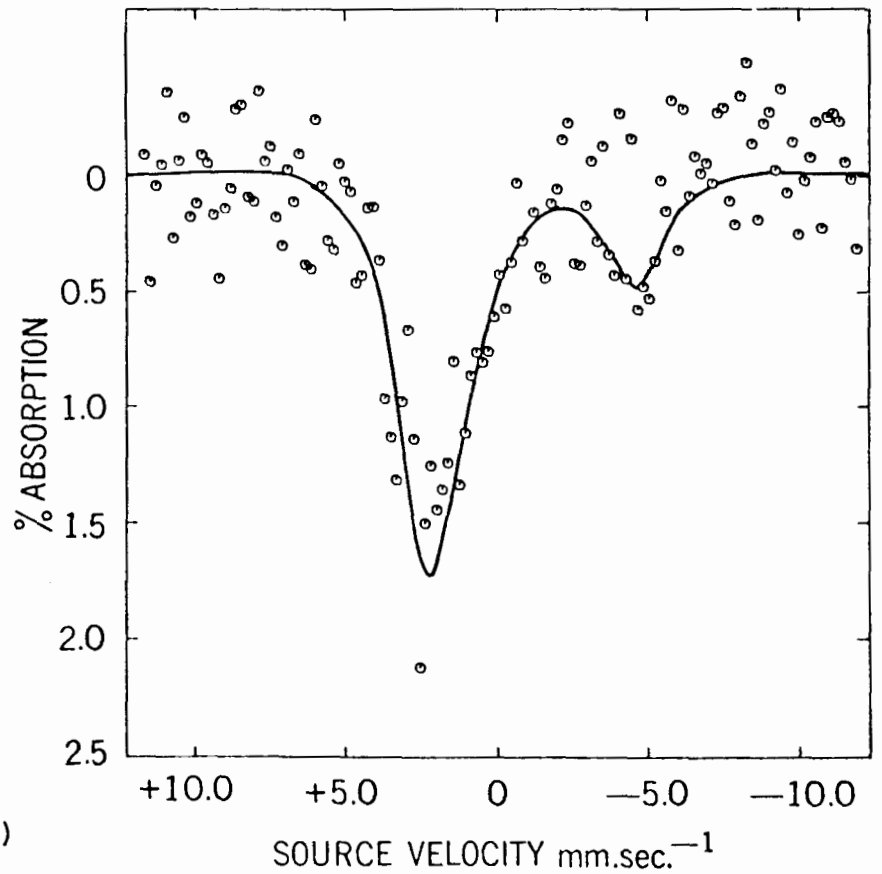

(b)

Figure 25 ^{129}I Mössbauer Emission Spectra Measured at 80°K. For $Na^{129}I$ Absorber vs. (a) $Na_2{}^{129m}TeO_4$ Source and (b) $K_2{}^{128}TeO_4$ $(n,\gamma)^{129}Te$ Source.

3. Tellurium Trioxide and Tellurium Pentoxide

For α-$^{129m}TeO_3$, the known presence of TeO_2 impurity from the preparation considerably complicated the interpretation of the spectra obtained. The irresolved quadrupole split spectrum for TeO_2 overlapped that of any decomposition products formed in the nuclear transformation. The α-$^{129m}TeO_3$ spectrum shown in Figure 26(a) was measured for a sample prepared doubly labelled with ^{129}Te and ^{129m}Te. The spectrum shown by the dashed line in the figure represents the spectrum for the ^{129}Te-labelled sample where the spectrum was measured for a short time immediately following the source preparation. The source was then allowed to stand while a new population of ^{129}Te species was produced through the isomeric transition decay in the sample. The emission spectrum was then re-measured and the result is shown in Figure 26(a). The ^{129}Te and ^{129m}Te spectra, normalised in per cent absorption so that they may be directly compared, provide some evidence that a small amount of molecular disruption occurred in α-$^{129m}TeO_3$ and that a Te(IV) fragment was produced. The spectrum for reactor irradiated α-TeO_3 was also studied, but because of the uncertainty raised by the sometimes large amounts of contaminant TeO_2 present, the results of these experiments are not reported here.

The spectrum observed for $^{129m}Te_2O_5$ (Figure 26(b) was identical to that reported by Pasternak[192] for ^{129}Te-labelled Te_2O_5. The spectrum is interpreted as showing

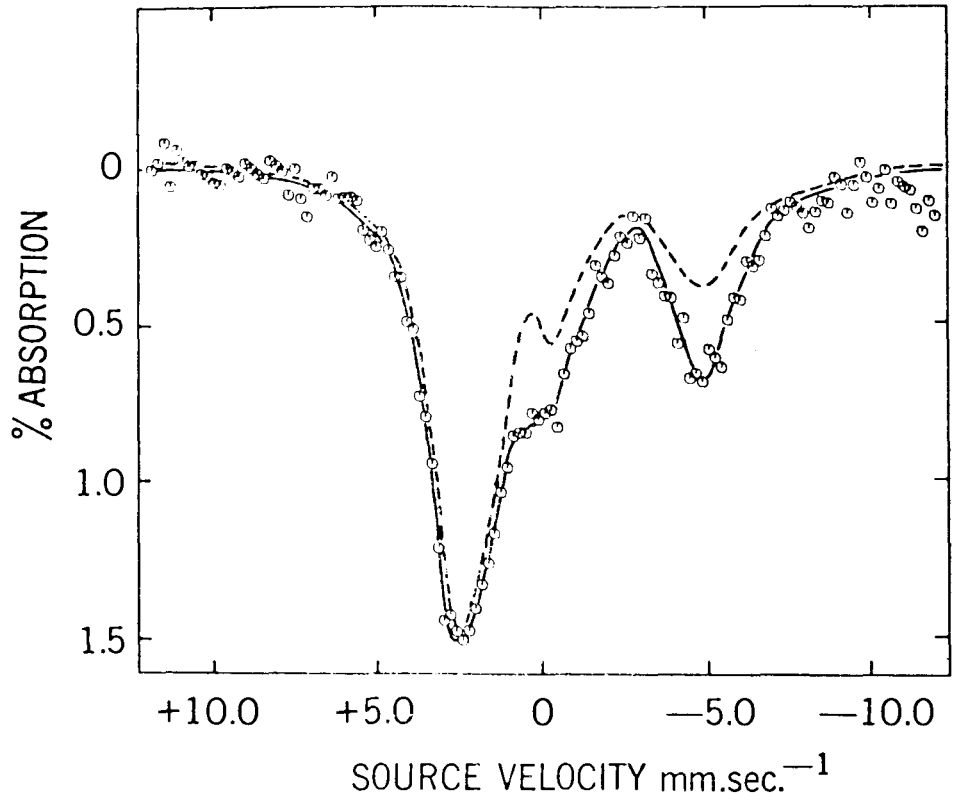

(a)

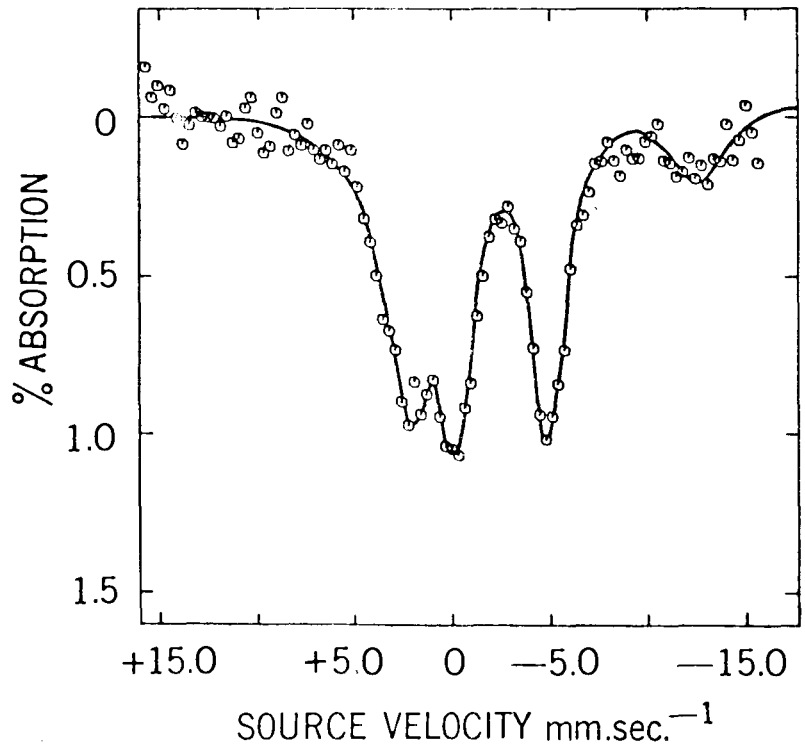

(b)

Figure 26 ^{129}I Mössbauer Emission Spectra Measured at 20°K. For Na^{129}I Absorber vs. (a) α-$^{129m}TeO_3$ Source and (b) $^{129m}Te_2O_5$ Source.

Te_2O_5 to be a stoichiometric mixture of TeO_3 and TeO_2, as was indicated by the chemical properties of this material.[202] No attempt was made to study this compound any further.

Because of the difficulty in preparing pure α-TeO_3 samples, β-TeO_3 was prepared and the chemical effects of isomeric transition and thermal neutron capture investigated in this compound. The preparation of β-TeO_3 takes up to 24 hours,and thus the ^{129}Te-labelled compound could not be studied. The samples of β-TeO_3 investigated in this work were shown by I.R. spectroscopy, x-ray powder photography, and by ^{125}Te absorption spectroscopy (see Figure 10(c)) to be pure β-TeO_3. The ^{129}I emission spectra observed for this compound, however, were most confusing to interpret.

The emission spectrum for the ^{129m}Te-labelled sample, illustrated in Figure 27(a), shows the presence of two ^{129}I species, both giving single, narrow emission lines, but with very different isomer shifts and thus having quite different s-electron densities at their respective nuclei. The spectrum parameters for these emission lines are as shown below.

	PER CENT ABUNDANCE	δ (mm.sec.$^{-1}$)	Γ_{expt} (mm.sec.$^{-1}$)
Species I	68	-3.05 ±.03	1.32 ±.05
Species II	32	+7.50 ±.05	1.61 ±.14

The isomer shift and narrow line width for Species I shows the presence of a ^{129}Te(VI) compound which has nearly

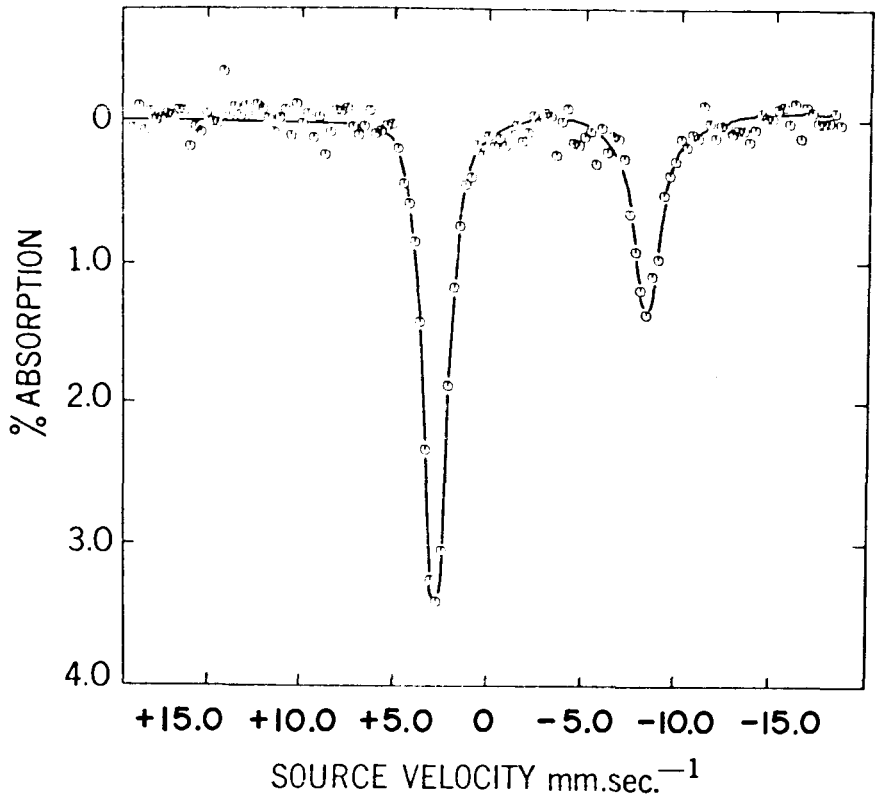

(a)

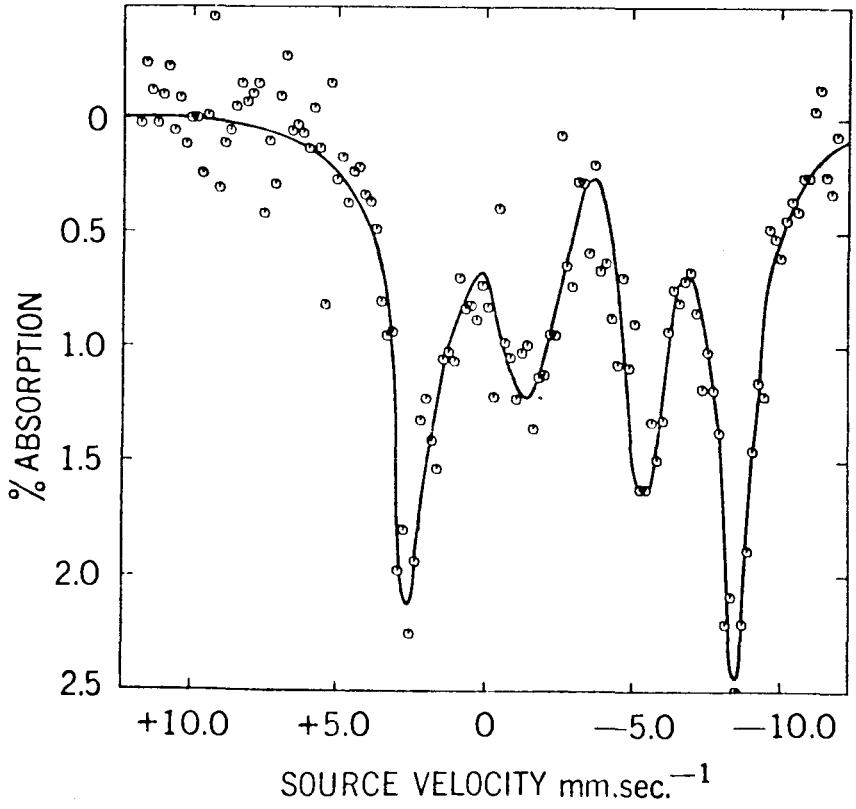

(b)

Figure 27 ^{129}I Mössbauer Emission Spectra Measured at 80°K. For Na^{129}I Absorber vs. (a) β-$^{129m}TeO_3$ Source and (b) β-$^{128}TeO_3(n,\gamma)^{129}$Te Source.

perfect octahedral symmetry. This supports the proposal of Erickson and Maddock that β-TeO_3 has a ReO_3-type structure, with the tellurium octahedrally surrounded by six oxygen ligands.[207] Species II in this spectrum, however, could not be identified as any known iodine or tellurium compound, and the ^{129}I isomer shift for this compound has an incredibly high value. The corresponding tellurium parent was not observed in the ^{125}Te absorption spectrum, and it is tempting to conclude that Species II was the product of the isomeric transition. However, this finding is totally different from that ascribed to the chemical effects of the nuclear transformation in the other Te(VI) compounds, and this introduces some doubt that this interpretation is the correct one.

Whether the tellurium parent of Species II originated in the isomeric transition or was present as an impurity in the β-TeO_3 solid, the ^{129}I isomer shift identifies it as a most peculiar molecule, having by far the largest isomer shift of any iodine compound reported.

The ^{129}I spectrum of neutron irradiated β-TeO_3 was even more complex (Figure 27(b)). Here, in addition to the two lines observed in the ^{129m}Te-spectrum, a third, quadrupole split component was found to be present, and this presumably derived from an (n,γ) recoil product. The isomer shift and quadrupole splitting of this molecule was very different from that of TeO_2 or the decomposition product in H_6TeO_6.

Thus, the β-TeO_3 spectra presented here could not be interpreted in detail. The possible presence of impurities in the samples, together with the very unusual nature of the iodine products observed, place some doubt on the meaning of the results. The experiments have been described here because the spectra showed the presence of a novel iodine compound, although it is not clear that the tellurium parent was born in the preceding nuclear transformations.

4. Tellurium (IV) Compounds and Elemental Tellurium

The ^{129}I emission spectra for ^{129m}Te-labelled H_2TeO_3, tetragonal TeO_2, $(NH_4)_2TeCl_6$, and elemental tellurium are shown in Figures 28(a-d). A comparison of Figures 28(a-d) with Figures 19 and 20 shows that in each case the ^{129}Te and ^{129m}Te spectra were identical, except for the obvious decrease in the per cent absorptions due to the much higher background radiation in the latter samples. It is concluded that chemical effects of internal conversion accompanying the isomeric transition decay were not observed in any of these source compounds.

In addition to the above investigations, tetragonal TeO_2 was studied following the reaction sequences $^{128}Te(n,\gamma)$ ^{129}Te and $^{128}Te(n,\gamma)^{129m}Te \xrightarrow{I.T.} {}^{129}Te$, and in each instance the spectra were again identical to the ^{129}Te spectra. Neutron irradiation studies were not carried out on H_2TeO_3 because of the chemical instability of this compound.

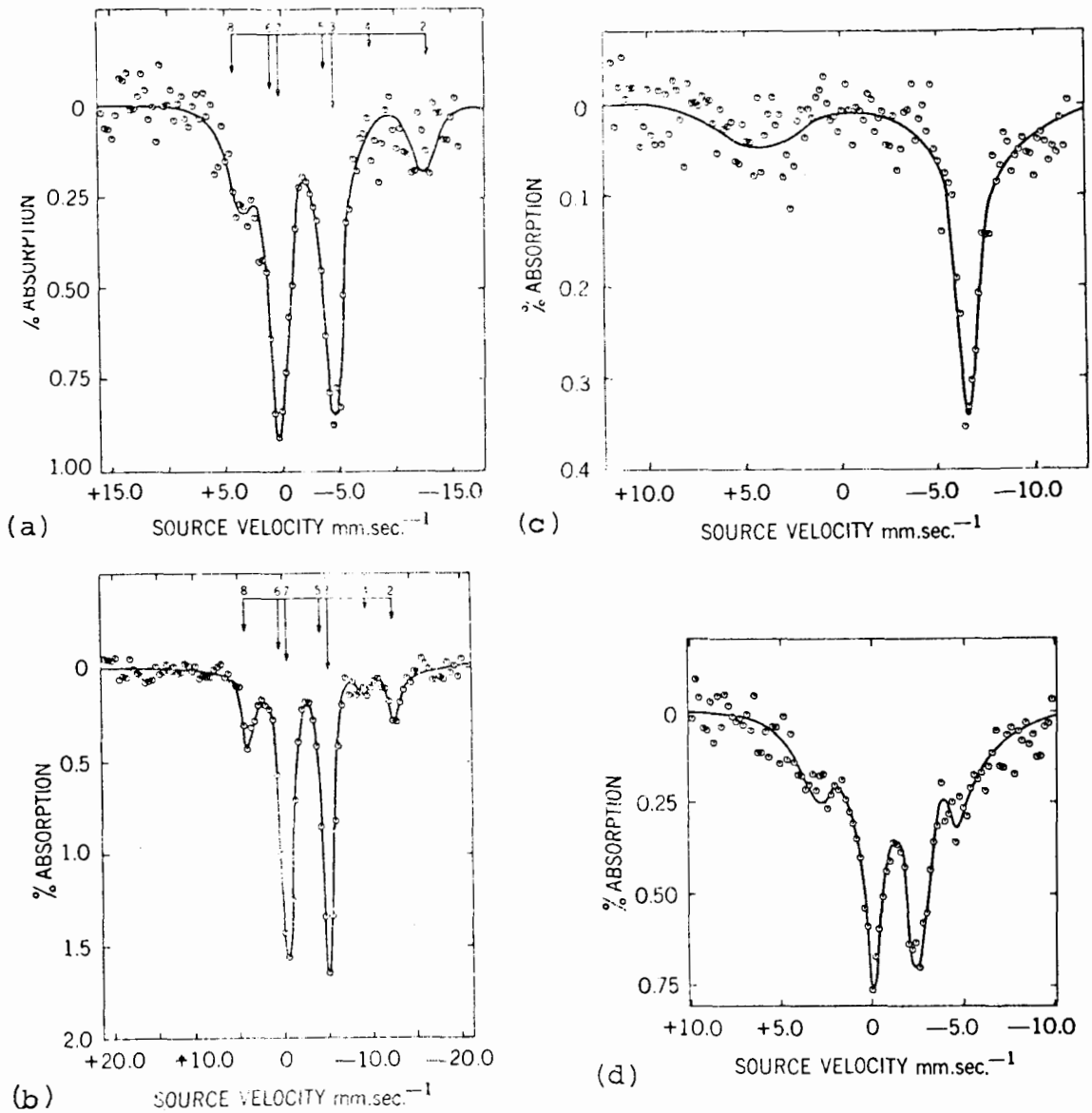

Figure 28 ^{129}I Mossbauer Emission Spectra Measured at 80°K. For a $Na^{129}I$ Absorber vs. (a) $H_2{}^{129m}TeO_3$ Source (b) Tetragonal $^{129m}TeO_2$ Source (c) $(NH_4)_2{}^{129m}TeCl_6$ Source, and (d) Elemental Tellurium Source.

Samples of elemental tellurium, as obtained from Oak Ridge, were also investigated following neutron irradiation to give ^{129}Te and ^{129m}Te labelled sources. These sources also gave identical spectra to the ^{129}Te sources prepared by precipitation from solution. Furthermore, melting the ^{129m}Te sources and allowing the molten metal to crystallise gave samples which again yielded the same ^{129}I spectrum. It is concluded, therefore, that in elemental tellurium, in the several different forms in which samples were prepared, chemical effects of either the isomeric transition or (n,γ) reaction were not observed. Moreover, the ^{129}I nuclei were formed in identical lattice environments in each of these tellurium samples, and thus no phase effects were observed in any of the differently prepared samples.

5. Discussion of Results

In the pure Te(VI) compounds, monoclinic H_6TeO_6 and $(H_2TeO_4)_n$, molecular fragmentation was observed to accompany the nuclear transformation in a significant fraction of events with the production of a single decomposition product in each instance. This decomposition product was characterised by its δ and e^2qQ values as a Te(IV) ion, and the apparent absence of an asymmetry parameter, η, suggests that the fragment may have been the TeO_3^{2-} ion or $Te(OH)_3^+$ complex ion.

The isomeric transition decay in $Na_2{}^{129m}TeO_4$ did not produce any measurable decomposition, although the (n,γ) reaction in K_2TeO_4 did result in bond rupture in some events, again with the formation of a Te(IV) ion. The picture for α-TeO_3, Te_2O_5, and β-TeO_3 was a complicated one and for the purposes of the present discussion it will suffice to say that there was some tentative evidence for molecular decomposition accompanying the isomeric transition in a small fraction of events in α-TeO_3.

The experimental results clearly showed that in H_2TeO_3, TeO_2, $(NH_4)_2TeCl_6$, and elemental tellurium, chemical effects of the decay of ^{129m}Te were not observed, and that the (n,γ) reaction in TeO_2 and elemental tellurium did not give rise to any associated chemical effects. The Auger charging accompanying the decay of ^{129m}Te did not lead to the stabilisation of higher oxidation states in the Te(IV) compounds.

Returning to the case of H_6TeO_6, the chemical effects of the nuclear transformation in this compound were exceedingly simple. A large number of chemical products was not observed. Only one decomposition product was formed, and this may well have been the stable $TeO_3{}^{2-}$ ion. Moreover, this same decomposition product was formed both following the Auger charging in the isomeric transition, and following kinetic recoil in the (n,γ) reaction. The per cent decomposition accompanying the (n,γ) reaction appeared to be slightly greater than that following the isomeric transition process.

It is apparent that Auger charging did not lead to the stabilisation of a spectrum of high charge states on the tellurium. Moreover, there was no evidence of a molecular explosion. Chemical bond rupture led to the formation of only one stable recoil product, which in fact, contained tellurium in a lower oxidation state than in the parent molecule.

In the (n,γ) reaction, the tellurium atoms acquire a spectrum of recoil kinetic energies. The different kinetic energies, together with the different initial trajectories of the recoil atom with respect to the bond axes might have been expected to produce a variety of differently bonded tellurium atoms. However, again this was not observed, and the recoil atoms were stabilised in either the parent molecular form or as the single Te(IV) decomposition product.

The above features of the nuclear transformations appear to correspond more closely to Walton's model [55] for the dissipation of electronic excitation or recoil energy, rather than to the disorder model of Müller [49,50] or to the hot-zone model of Harbottle and Sutin. [46] The chemical products observed following the transformations in both instances appear to be governed more by the basic chemical bonding and structure properties of tellurium rather than by the deposition of excessive amounts of energy in the recoil site.

There is some evidence that the ability of the lattice to dissipate the excitation energy generated in the isomeric

transition decay was an important factor. Thus, molecular fragmentation in $H_6{}^{129m}TeO_6$, in which the molecules are held together only by hydrogen bonding, was greater than in $(H_2{}^{129m}TeO_4)_n$. Furthermore, decomposition in $(H_2{}^{129m}TeO_4)_n$, in which relatively small polymeric units are present, was greater than in $Na_2{}^{129m}TeO_4$ in which the tellurium is present in the polymeric octahedrally co-ordinated lattice. Thus, the more polymeric the host lattice, the less molecular decomposition that was observed.

The present study allowed a comparison of the decomposition accompanying the nuclear transformations in telluric acid with normal thermal decomposition. In the latter case, telluric acid first polymerises, then loses H_2O with the formation of polymeric TeO_3, and finally eliminates O to give TeO_2, as shown below.

$$Te(OH)_6 \rightarrow (H_2TeO_4)_n + 2H_2O \rightarrow TeO_3 + H_2O \rightarrow TeO_2 + 1/2\ O_2$$

In the nuclear transformation in H_6TeO_6 there was no evidence for the formation of the polymer $(H_2{}^{129}TeO_4)_n$ or $^{129}TeO_3$, which would give a single line in the Mössbauer spectrum overlapping the quadrupole split spectrum of monoclinic H_6TeO_6. Also, the observed decomposition product had an isomer shift and asymmetry parameter significantly different from those of TeO_2. The molecular decomposition following the nuclear transformation differs significantly from that of thermal decomposition.

The above results show some similar trends to the results of several experiments reported in the literature. Thus, Jung and Triftshauser,[125] studying the chemical forms of ^{125}Te produced following the electron capture decay of ^{125}I, observed in $Na_2{}^{125}IO_4$ the formation of TeO_4^{2-} and TeO_3^{2-} (or TeO_3). In the present work there was no evidence whatever for the stabilisation of higher oxidation states in H_2TeO_3 or TeO_2.

The previous work on the $^{125m}Te \rightarrow {}^{125}Te$ isomeric transition in H_6TeO_6 and $Na_2H_4TeO_6$ indicated the presence of a broad asymmetric emission line interpreted as evidence of molecular fragmentation.[187] However, a detailed account of that work has yet to appear. The present work allowed a much more detailed study of the processes occurring than was possible with the broad irresolved ^{125}Te spectra.[124-126,187]

D. Thermal Annealing Studies

1. Experimental Results

The study of thermal annealing effects in telluric acid provided further concrete evidence of the occurrence of molecular decomposition accompanying both the isomeric transition and the (n,γ) reaction. In describing these experiments it must be emphasised that in the $^{129m}Te \rightarrow {}^{129}Te$ isomeric transition, the daughter ^{129}Te atoms exist in radioactive equilibrium with the parent ^{129m}Te atoms and that

equilibrium is reaches in about 8 hours. This radioactive equilibrium permits the study of the effect of temperature on the chemical products formed in the isomeric transition.

Thus on allowing a sample of $H_6{}^{129m}TeO_6$ to reach radioactive equilibrium at 373°K., then cooling the sample to liquid nitrogen temperature and immediately recording the Mössbauer spectrum for a short counting period (≃40 min.), the chemical effects of the isomeric transition at 373°K. were observed. A spectrum observed in this way is shown in Figure 29, where it is compared with the emission spectrum for the same $H_6{}^{129m}TeO_6$ sample in which radioactive equilibrium was reached at 80°K.

In another experiment (Figure 30), a different sample of $H_6{}^{129m}TeO_6$ was allowed to reach equilibrium at room temperature. The sample was then heated for 2 hours at 343°K. (and 373°K.) and the Mössbauer spectrum then immediately recorded for a 40 minute counting period at 80°K. The spectra were also taken of this sample following equilibration at room temperature both before and after the annealing experiments.

The distributions of $^{129}Te(IV)$ and $^{129}Te(VI)$ measured in these experiments are given in Table XI. Of the ^{129}Te atoms decaying to populate the Mössbauer level in ^{129}I during the above 40 minute counting periods, ca. 80 per cent were representative of the atoms which had undergone the annealing process.

Obviously, in such experiments the counting period had to be kept very short, and as a consequence the spectra

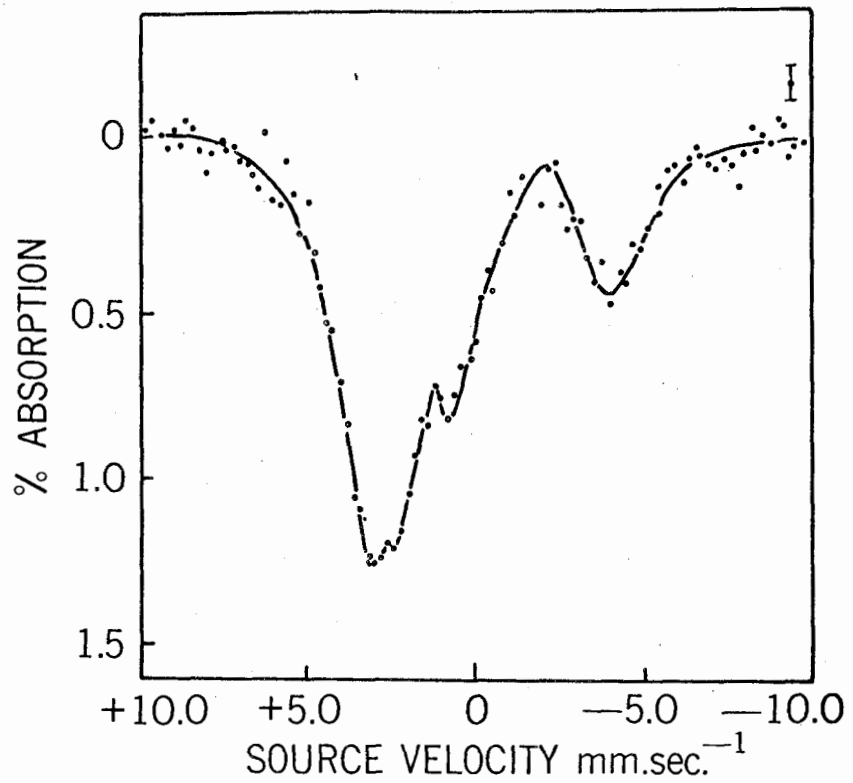

(a)

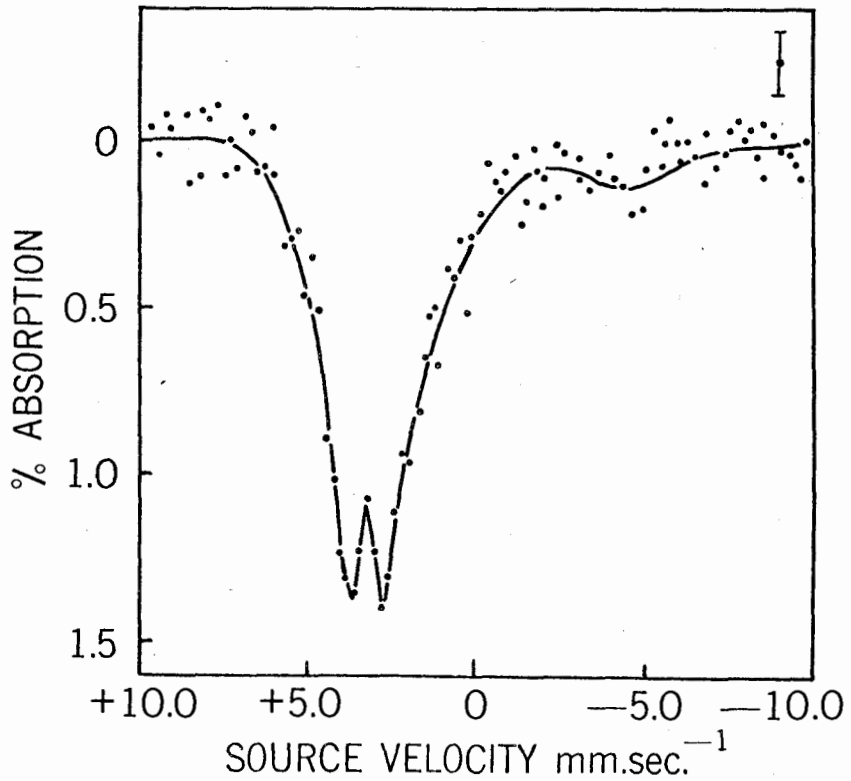

(b)

Figure 29 ^{129}I Mössbauer Emission Spectra Measured at 80°K. For a $Na^{129}I$ Absorber vs. $H_6{}^{129m}TeO_6$ Source Where the ^{129}Te Atoms Were Produced at (a) 80°K. and (b) 373°K.

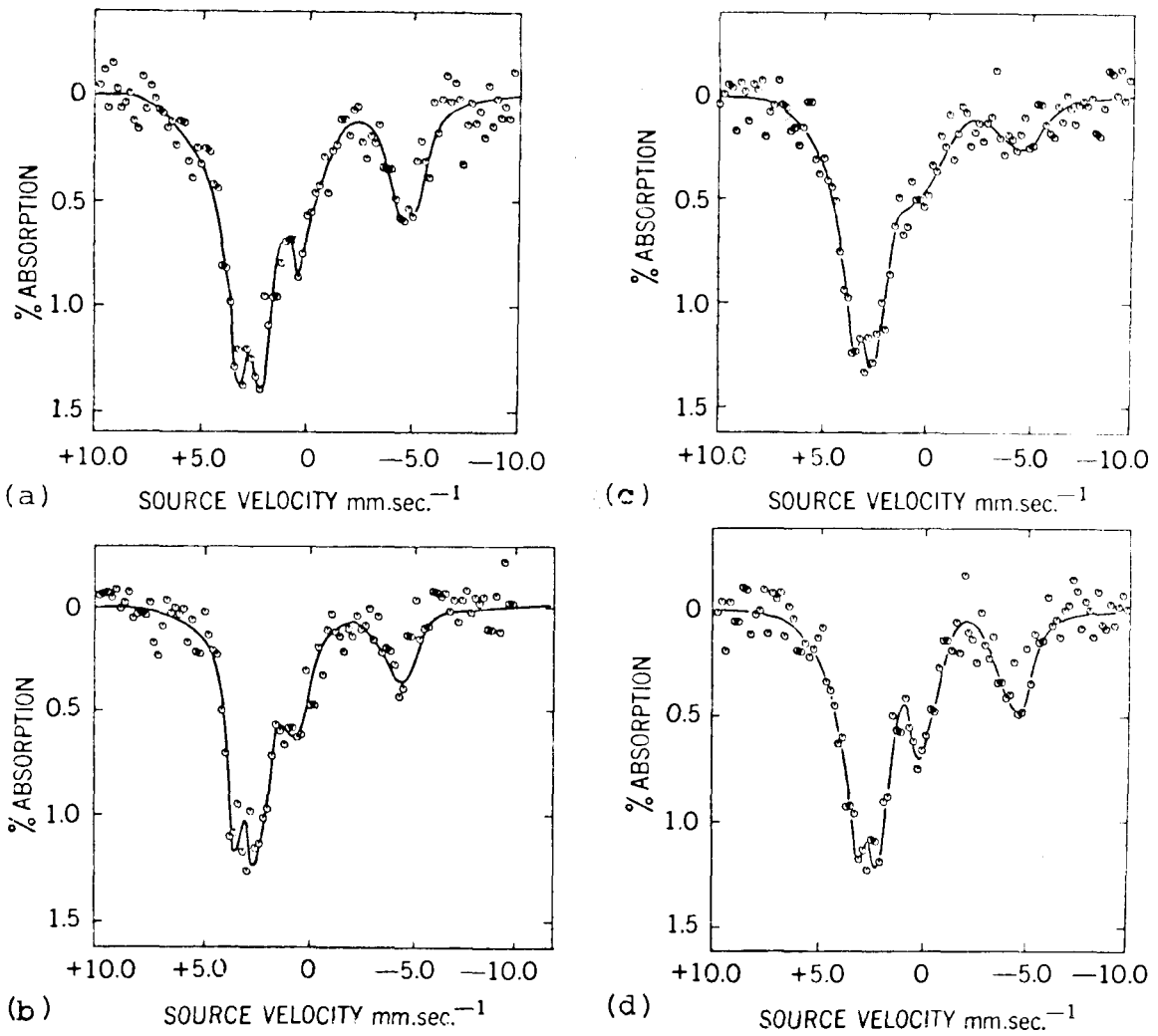

Figure 30 ^{129}I Mössbauer Emission Spectra Measured at 80°K. For a Na^{129}I Absorber vs. H$_6$^{129m}TeO$_6$ Source Thermally Annealed. The Spectra Were Measured (a) Before Thermal Annealing; (b) Source heated at 343°K. for 2 Hours; (c) Source heated at 373°K. for 2 Hours; and (d) Following Thermal Annealing After Radioactive Equilibrium had again been Reached at Room Temperature.

TABLE XI

THERMAL ANNEALING OF TELLURIUM RECOIL FRAGMENTS IN TELLURIC ACID

SAMPLE STUDIES	^{129}Te(VI)%	^{129}Te(IV)%
$H_6{}^{129m}TeO_6$		
Equilibrium at 373°K.	84±3	16±3
Equilibrium at 298°K.	51±3	49±3
Equilibrium at 80°K.	51±3	49±3
Equilibrium at 10°K.	56±3	44±3
Heated at 373°K., 2 Hours	74±3	26±3
Heated at 343°K., 2 Hours	66±3	34±3
$H_6{}^{128}TeO_6(n,\gamma)^{129}$Te-		
Heated at 373°K. for 10 minutes following the irradiation	71±3	29±3
Irradiated at 343°K.	59±3	41±3
Irradiated at 195°K.	34±3	66±3

obtained often had poor statistics. Nevertheless, as can be seen from Figures 29 and 30, annealing reactions were clearly observed between 298°K. and 373°K., leading to a decrease in all of the lines of the quadrupole split spectrum in the Te(IV) fraction, and an increase in the Te(VI) fraction. No annealing was observed between 10°K. and room temperature.

All of the experiments of Figure 30 were performed on one sample of $H_6{}^{129m}TeO_6$. Following an annealing study at one temperature, the sample was allowed to reach radioactive equilibrium at room temperature and was then heated at the new annealing temperature and the Mössbauer spectrum again recorded. It was found that cycles of annealing carried out in this way gave quite reproducible results, and the sample gave no evidence of macroscopic decomposition during these experiments. Moreover, following the heating at 373°K. and immediately recording the Mössbauer spectrum for 40 minutes, the sample was maintained at liquid nitrogen temperature and spectra recorded for one hour counting periods every hour. It was observed that the ^{129}Te(IV) fraction reappeared in the spectra, and this "regrowth" was characterised by the 69 minute half-life of the ^{129}Te daughter. This provided irrefutable evidence that the Te(IV) fragment was a product of molecular decomposition accompanying the isomeric transition.

It was important to establish whether the spectra of Figures 29 and 30 were evidence of a temperature dependence of the isomeric transition process itself, or whether they represented an annealing reaction in which stable Te(IV)

fragments formed in the crystal in the decay event were subsequently annealing to yield Te(VI) molecules. An experiment was therefore carried out in which the sample was allowed to reach transient equilibrium at room temperature over an 8 hour period and was then heated at 373°K. for 15 minutes. The spectrum was then immediately recorded at liquid N_2 temperature. The spectrum obtained was very similar to that for a sample allowed to reach transient equilibrium at 373°K. This is interpreted as evidence that the process occurring was a chemical reaction involving stabilised Te(IV) fragments in the crystal and that there was no temperature dependence of the isomeric transition process itself.

Similar experiments to the above were carried out on neutron irradiated samples of telluric acid. In Figure 31 are shown spectra for samples which were neutron irradiated at solid CO_2 temperature, 343°K., and for a sample heated at 373°K. for 10 minutes immediately following the irradiation prior to recording the spectrum. The distributions of ^{129}Te(IV) and ^{129}Te(VI) recoil fragments measured in these spectra are given in Table XI. These experiments clearly show that irradiation at 343°K. and annealing at 373°K. both resulted in a lower ^{129}Te(IV) fraction than irradiation at solid CO_2 temperature. A chemical reaction occurred at elevated temperatures leading to a decrease in the ^{129}Te(IV) fraction and an increase in the ^{129}Te(VI) fraction.

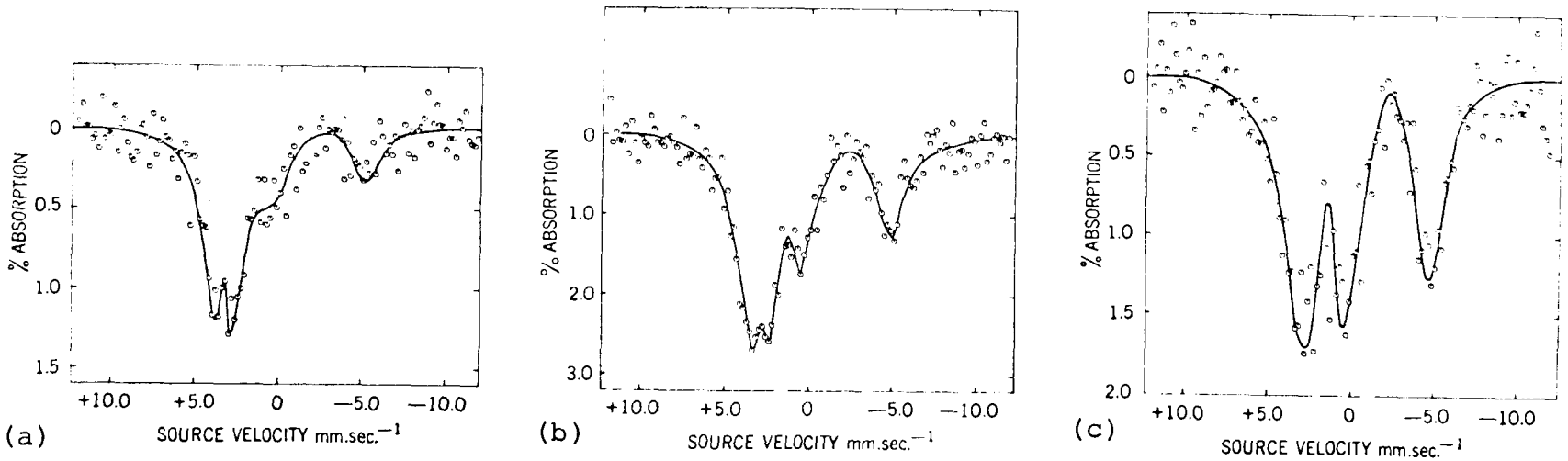

Figure 31 ^{129}I Mössbauer Emission Spectra Measured at 80°K. For a Na^{129}I Absorber vs. $H_6{}^{128}TeO_6$ $(n,\gamma)^{129}$Te Source Irradiated at Different Temperatures The Sources were (a) Reactor Irradiated at 343°K. Followed by Heating the Source for 10 Minutes at 373°K. Before the Spectrum Was Measured; (b) Reactor Irradiated at 343°K.; and (c) Reactor Irradiated at 195°K.

Other source compounds in which thermal annealing was investigated included $(H_2{}^{129m}TeO_4)_n$ and α-$^{129m}TeO_3$. However, no evidence was observed of thermal annealing processes occurring in these matricies, even at temperatures as high as 160°C. in $(H_2TeO_4)_n$ and 300°C. in α-TeO_3.

2. Discussion of Results

The same annealing reaction was observed both following isomeric transition and following the (n,γ) reaction in telluric acid. In the former case it was clearly shown that the annealing reaction was not dependent in any way on the previous thermal history of the sample.

All of the above annealing reactions were characterised by the same property; they led to the conversion of the Te(IV) fragment into the Te(VI) form in a single-step reaction in which no intermediate products were observed. Thus the reaction was not a sequential process and did not involve the step-wise addition of several oxygen atoms to the Te(IV) fragment. In the annealing reaction there was a very fundamental change in the nature of the bonding to the tellurium. In the Te(IV) fragment, the tellurium was bonded by pure p-bonds to the oxygens, while in the Te(VI) form the tellurium was employing sp^3d^2 hybrid orbitals.

One is left to conjecture as to the mechanism of the annealing reaction which occurs. A simple oxidation of the Te(IV) species may occur as:

$$TeO_3^{2-} \longrightarrow TeO_3 + 2e^-$$

or

$$TeO_3^{2-} + O \longrightarrow TeO_4^{2-}$$

However, it is difficult to see how, in the telluric acid matrix, this could lead to a six or four co-ordinate tellurium which would yield a very small quadrupole splitting on decay to ^{129}I.

On the basis of the known propensity of telluric acid to polymerise on heating, a quite plausable reaction path might be

$$^{129}TeO_3^{2-} + 2Te(OH)_6 \rightarrow (HO)_4TeO_2 \cdot {}^{129}Te(OH)_2 \cdot O_2Te(OH)_4 + 4H_2O + 2e^-$$

(adjacent molecules)

Such a reaction may occur within the unusual environment of the recoil site at temperatures considerably below that at which polymerisation normally occurs. However, if $(H_2TeO_4)_n$ was the product of annealing, the ^{129}I emission spectrum of the Te(VI) species in the lattice would be a combination of the quadrupole split spectrum of monoclinic $H_6{}^{129}TeO_6$, and the single line of the polymer. Although the somewhat poor resolution of the spectra in the annealing experiments does not necessarily mean that $(H_2{}^{129}TeO_4)_n$ was not present, perfectly acceptable and reproducible fits to these spectra

were obtained if only the presence of monoclinic $H_6{}^{129}TeO_6$ and $^{129}Te(IV)$ were assumed.

Another possible explanation of the annealing reaction is provided by Walton's[55] postulated explanation of bond-rupture and subsequent annealing. In the nuclear transformation the tellurium may break three of its Te-OH bonds, remaining bonded to the other three. The free -OH groups produced may remain at their original lattice sites because of the hydrogen bonding to adjacent -OH groups. This may be diagramatically represented as below:

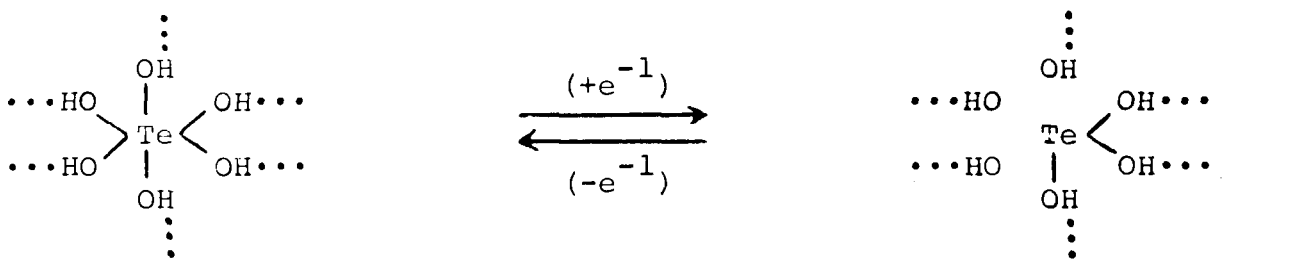

$^{129}Te(VI)$, sp^3d^2

$^{129}Te(IV)$, pure p(90° bonds)

$[Te(OH_3^+)$ complex]

The annealing process may then involve the oxidation of the tellurium back to Te(VI), with the reformation of the original, octahedrally disposed -OH bonds in a single-step process. The surrounding lattice then serves to constrain the positions of the initially bonded partners, and allows for the subsequent reformation of the parent molecule in a normal lattice site in the monoclinic lattice. Certainly in the annealing studies, the

product of the annealing reactions appeared to yield an ^{129}I Mössbauer spectrum with a small quadrupole splitting characteristic of the monoclinic lattice.

The above model emphasises one of the unusual features of the decomposition in the isomeric transition decay. Although the Auger charging process might be expected to produce high charge states on the tellurium, the daughter atom is stabilised in a reduced, Te(IV), state following bond rupture. The excitation in the decay leads to decomposition of the molecule, and subsequent rearrangement and relaxation processes reduce the daughter atom to the (IV) state. The decomposition product, in fact, acts as an electron trap in the crystal. On heating, the recoil atom is oxidised back to the Te(VI) state and this may correspond simply to the thermal ionisation of the defect lattice site. In the (IV) state, the tellurium has 2 non-bonding electrons in the 5s orbital and thus employs the empty 5p orbitals in bonding to the oxygens. On oxidation, the $5s^2$ electrons are lost and spd-type hybrid orbitals can now be formed to bond octahedrally to the surrounding ligand groups.

The reduction in charge state following the Auger cascade is not peculiar to this system and has previously been observed in Mössbauer studies for ^{57}Fe,[153,171] ^{119}Sn,[178-181] and ^{125}Te.[124,125] In all of these systems the decomposition product formed acts as an effective electron trap.

E. A Comparison With Radiochemical Results

A number of direct comparisons can be made between the results of the Mössbauer study reported above and radiochemical results of the previous chapter. In Table XII the main features of the Mössbauer and radiochemical results are briefly compared for both tellurium and iodine recoil atoms in telluric acid.

Considering first the results for tellurium recoil atoms, the radiochemical investigations provided only a simple description of the labelled products, observed following dissolution, in terms of the ^{129}Te(VI) and ^{129}Te(IV) oxidation states. The Mössbauer study, in contrast, allowed a more positive identification of the chemical form of the ^{129}Te recoil atoms present in the solid. The latter method thus showed that the ^{129}Te(VI) fraction was the monoclinic telluric acid molecule in an apparently undisturbed lattice site, and that the ^{129}Te(IV) fraction consisted of a single tellurium species in which the molecules have axial symmetry and in which the tellurium is bonded to three -OH or -O ligands with pure p-bonds. Moreover, where the radiochemical study showed only that similar Te(VI) and Te(IV) fragment distributions were formed following isomeric transition decay and following (n,γ) activation, the Mössbauer study clearly demonstrated that identical tellurium recoil fragments were produced in each transformation sequence. Nevertheless, it is apparent that, since the recoil product distribution in the solid

TABLE XII

A COMPARISON OF MÖSSBAUER AND RADIOCHEMICAL RESULTS FOR TELLURIUM AND IODINE RECOIL ATOMS IN TELLURIC ACID

Transformation	Temperature of Decay or Irradiation	Mössbauer Study		Radiochemical Study	
		Observed Recoil Products	Distribution in %	Observed Recoil Products	Distribution in %
$H_6{}^{129m}TeO_6 \xrightarrow{I.T.} {}^{129}Te$	298°K.	H_6TeO_6	53	Te(VI)	64
		$TeO_3{}^{-2}$	47	Te(IV)	36
$H_6{}^{129m}TeO_6 \xrightarrow{I.T.} {}^{129}Te$	373°K.	H_6TeO_6	84	Te(VI)	85
		$TeO_3{}^{2-}$	16	Te(IV)	15
$H_6{}^{128}TeO_6 \xrightarrow{(n,\gamma)} {}^{129}Te$	343°K.	H_6TeO_6	59	Te(VI)	56.3
		$TeO_3{}^{2-}$	41	Te(IV)	42.7
$H_6{}^{129}TeO_6 \xrightarrow{\beta^-} {}^{129}I$	80°K.	H_5IO_6	100	-	-
$H_6{}^{131m}TeO_6 \xrightarrow{\beta^-} {}^{131}I$	80°K. (dissolved at at room temperature)	-	-	IO_4^-	20
				IO_3^-	69
				I^-	11
$H_6{}^{131}TeO_6 \xrightarrow{\beta^-} {}^{131}I$	80°K. (dissolved at at room temperature)			IO_4^-	40
				IO_3^-	49
				I^-	11

in each of the above cases was in fact extremely simple, the radiochemical study gave a fairly accurate description of the processes occurring.

In examining the results of thermal annealing experiments in $H_6{}^{129m}TeO_6$, the radiochemical study showed only that the $^{129}Te(IV)$ fraction was in some way oxidised back into a ^{129}Te (VI) fraction, although the latter could not be positively identified as the parent telluric acid molecule. The Mössbauer work, however, clearly showed that the thermal annealing reaction was a single-step process in which the TeO_3^{2-} ion or $Te(OH)_3^+$ complex ion was probably converted back into a telluric acid molecule, again in an undisturbed monoclinic telluric acid lattice site. Moreover, it was found that the annealing process occurring in the reactor irradiated sample was exactly the same as in the ^{129m}Te-labelled sample.

The Mössbauer studies of the thermal annealing reactions also confirmed that these processes were independent of the thermal history of the sample, as had been previously demonstrated in the radiochemical study.

A quantitative comparison of the data obtained by the two techniques is not very meaningful, because the recoil-free fractions for the different tellurium products observed in the Mössbauer spectra may be different. However, it can be concluded that the results were in reasonable agreement.

Turning now to the chemical effects of β^--decay in

the production of iodine recoil atoms in tellurium compounds, it is clear that the two methods of study provided quite different information. The Mössbauer experiments showed that following β^--decay at liquid nitrogen or liquid helium temperatures in ^{129}Te-labelled telluric acid, the daughter ^{129}I remained bonded to the ligand -OH groups over a time long by comparison with the 16.8 nanosecond half-life of the Mössbauer transition. In comparison, in ^{131}Te-and ^{131m}Te-labelled telluric acid allowed to undergo β^--decay at 80°K., warmed to room temperature and dissolved up for radiochemical analysis, a spectrum of ^{131}I-labelled chemical products was observed which included I^-, IO_3^-, and IO_4^-. The internal conversion accompanying the decays in ^{131}Te and ^{131m}Te in some 18 per cent of events can not be the sole explanation for the observed product distribution.

Such differences in the results of the two types of experiment are also found in other tellurium compounds. Thus in TeO_2, the radiochemical method of analysis has shown that the $^{130}Te(n,\gamma)^{131}Te \xrightarrow{\beta^-} {}^{131}I$ transformation sequence[90,91] and $^{132}Te \xrightarrow{\beta^-} {}^{132}I$ decay[89] produces iodine recoil atoms in the three chemical forms of I^-, IO_3^-, and IO_4^-. However, in the present Mössbauer study the ^{129}I atoms in TeO_2 were in only one lattice environment, that of the parent tellurium, following neutron irradiation, internal conversion, and β^--decay.

There are two possible explanations for the radiochemical results, one being that the radioiodine-labelled product initially formed in the tellurium compound decomposes in the lattice at room temperature, and the other that chemical reactions occur during or following dissolution which yield the observed product distribution. It is also possible that a combination of these two processes may occur. Looking again at the results for telluric acid, there is evidence to support the proposal that the H_5IO_6 molecule must decompose in the $H_6{}^{131}TeO_6$ and $H_6{}^{131m}TeO_6$ lattice following the β^--decay event. Thus, if the solid was heated before dissolution and analysis, the distribution of ^{131}I activity between the forms I^-, IO_3^-, and IO_4^- subsequently observed in solution was found to change markedly. This then shows that the ^{131}I-labelled fragment product in the solid must undergo a chemical or physical change in the solid on heating.

In this instance it would be advantageous to be able to study the $^{129}Te \xrightarrow{\beta^-} {}^{129}I$ decay at, or near to, room temperature using the Mössbauer technique to see if in fact the H_5IO_6 molecule does fragment following the decay. Experiments were attempted in which the spectrum of $H_6{}^{129}TeO_6$ was recorded at 142°K. and 113°K., using slurries of n-pentane and isopentane with liquid nitrogen to maintain the source and absorber at these temperatures. Unfortunately however, no measurable resonance absorption was observed in these experiments.

In conclusion, it may be stated that Mössbauer spectroscopy provides a very powerful tool for studying recoil atoms produced by nuclear reactions or radioactive decay in solids. In the present investigation it allowed the identification of the primary chemical products of the nuclear transformations. For tellurium recoil atoms, the results obtained were very similar to those arrived at by the radiochemical method of analysis. In the case of iodine recoil atoms, however, this was not so and it is apparent that the radiochemical studies in that case only provided a picture of the chemical product distribution resulting from secondary processes occurring in the crystal or in solution.

The picture that emerges from the Mössbauer work is that simple β^--decay does not result in observable molecular fragmentation. The Auger charging process accompanying the internally converted isomeric transition does lead to decomposition in a large fraction of events. This process in a solid lattice, however, does not lead to a wide spectrum of chemical products or to the stabilisation of high charge states on the daughter tellurium atom, in contrast with the results of gas phase experiments.

REFERENCES

1. J.E. Willard, Ann. Rev. Nucl. Sci., 3, 193 (1953).

2. J.E. Willard, Ann. Rev.Phys. Chem., 6, 141 (1955).

3. G. Harbottle, Ann. Rev. Nucl. Sci., 15, 89 (1965).

4. S. Wexler, Actions Chimiques et Biologiques des Radiations, 8, 107 (1965).

5. H. Müller, Angew. Chem. International Edition, 6, 133 (1967).

6. A.G. Maddock and R. Wolfgang, Nuclear Chemistry, L. Yaafe, ed., (Academic Press, New York, 1968) II, p. 186.

7. Chemical Effects of Nuclear Transformations, Proc. Symp., Prague, October 24-27, 1960 (I.A.E.A., Vienna, 2 Vol., 1961).

8. Symp. Chemical Effects Associated with Nuclear Reactions and Radioactive Transformations, Vienna, December 7-11, 1964 (I.A.E.A., Vienna, 2 Vol., 1965).

9. J.H. Green and A.G. Maddock, Nature, 164, 788 (1949).

10. L.V. Groshev, A.M. Demidov, V.I. Pelekhov, L.L. Sokolovskii, G.A. Bartholomew, A. Doveika, E.M. Eastwood, and S. Monaro, "Compendium of Thermal Neutron Capture γ-Ray Measurements," Nuclear Data, A3, (4), (5) and (6), (1967); A5, (1), (2), (1968); A5, (3), (4), (1969).

11. J.W. Cobble and G.E. Boyd, J. Amer. Chem. Soc., 74, 1282 (1952).

12. C. Hsiung, H. Hsiung, A.A. Gordus, J. Chem. Phys., 34, 535 (1961).

13. H.C. Schweinler, Reference 7, I, p. 63.

14. B.B. Kinsey, Beta-and Gamma-Ray Spectroscopy, K. Siegbahn, ed. (Interscience Publishers, Inc., New York, 1955) p. 815.

15. F.R. Metgzer, Progr. Nucl. Phys., 7, 53 (1959).

16. M. Goldhaber and A.W. Sunyar, Reference 14, p. 463.

17. J. Cifka, Radiochimica Acta, 1, 125 (1963).

18. R.E. Segel, Phys. Rev., 113, 844 (1959).

19. S. Wexler and T.H. Davis, J. Chem. Phys., 20, 1688 (1952).

20. J.L. Thompson and W.W. Miller, J. Chem. Phys., 38, 2477 (1963).

21. S. Yosim and T.H. Davis, J. Phys. Chem., 56, 599 (1952).

22. J.A. Stone and W.L. Pillinger, Phys. Rev. Letters, 13, 200 (1964).

23. W. Triftshauser and P.P. Craig, Phys. Rev. Letters, 16, 1161 (1966).

24. M. Kaplan, J. Inorg. Nucl. Chem., 28, 331 (1966).

25. L. Grodzins, Ann. Rev.Nucl. Sci., 18, 291 (1968).

26. H.E.S. Burhop, The Auger Effect and Other Radiationless Transitions (Cambridge University Press, Cambridge, 1952).

27. I. Bergström and C. Nordling, Alpha-,Beta-, and Gamma-Ray Spectroscopy, K. Siegbahn, ed. (North-Holland Publishing Company, Amsterdam, 1966) p. 1523.

28. S. Wexler, Reference 4, p. 162.

29. F. Pleasonton and A.H. Snell, Proc. Roy. Soc. (London), A221, 141 (1957).

30. T.A. Carlson and R.M. White, J. Chem. Phys., 44, 4510 (1966).

31. T.A. Carlson and R.M. White, J. Chem. Phys., 48, 5191 (1968).

32. G.T. Seaborg, G. Friedlander and J.W. Kennedy, J. Amer. Chem. Soc., 62, 1309 (1940).

33. V.D. Nefedov, E.N. Sinotova and Shu-chen Sun, Radiokhimija, 4, 497 (1962).

34. R. Serber and H.S. Snyder, Phys. Rev., 87, 152 (1952).

35. T.A. Carlson, F. Pleasonton and C.H. Johnson, Phys. Rev., 129, 2220 (1963).

36. T.A. Carlson, Phys. Rev., 130, 2361 (1963).

37. T.A. Carlson, Phys. Rev., 131, 676 (1963).

38. A.H. Snell and F. Pleasonton, J. Phys. Chem., 62, 1377 (1958).

39. S. Wexler, G.R. Anderson and L.A. Singer, J. Chem. Phys., 32, 417 (1960).

40. T.A. Carlson and R.M. White, J. Chem. Phys., 39, 1748 (1963).

41. S. Wexler, J. Chem. Phys., 36, 1992 (1962).

42. F. Baumgartner, E.O, Fischer and U. Zahn, Chem. Berlin, 94, 2198 (1961).

43. F. Baumgartner, E.O. Fischer and P. Laubereau, Naturwissenschaften, 52, 560 (1965).

44. T. Andersen and A.B. Knutsen, J. Inorg. Nucl. Chem., 23, 191 (1961).

45. M. Genet, Radiochimica Acta, 12, 193 (1969).

46. G. Harbottle and N. Sutin, J. Phys. Chem., 62, 1344 (1958).

47. P.E. Yankwich, Canada J. Chem., 34, 301 (1956).

48. F. Seitz and J.S. Koehler, Solid State Physics, II, F. Seitz and D. Turnbull, ed. (Academic Press, New York, 1956).

49. H. Müller, J. Inorg. Nucl. Chem., 27, 1745 (1965).

50. H. Müller, Reference 8, II, p. 359.

51. J.B. Gibson, A.N. Goland, M. Milgram and G.H. Vineyard, Phys. Rev., 120, 1229 (1960).

52. G.H. Vineyard, Discuss. Faraday Soc., 31, 7 (1961).

53. J.A. Cairns and S.J. Thompson, Inorg. Nucl. Chem. Letters, 3, 107 (1967).

54. R.M. Hahn and J.E. Willard, J. Phys. Chem., 68, 2582 (1964).

55. G.N. Walton, Radiochimica Acta, 2, 108 (1964).

56. W.L. Brown, R.C. Fletcher and S. Machlup, Phys. Rev., 90, 709 (1953).

57. A.G. Maddock and M.M. de Maine, Canada J. Chem., 34, 275 (1956).

58. M.M. de Maine, A.G. Maddock and K. Taūgbôl, Disc. Faraday Soc., 23, 211 (1957).

59. R.C. Fletcher and W.L. Brown, Phys. Rev., 92, 585 and 591 (1953).

60. D.J. Apers, K.E. Collins, C.H. Collins, Y.F. Ghoos and P.C. Capron, Radiochimica Acta, 3, 18 (1964).

61. C.H. Collins, K.E. Collins, Y.F. Ghoos and D.J. Apers, Radiochimica Acta, 4, 211 (1965).

62. S. Kaucic and M Vlatkovic, Croat. Chim. Acta, 35, 305 (1963).

63. A.V. Bellido and D.R. Wiles, Radiochimica Acta, 12, 94 (1969); S. Khorana and D.R. Wiles, J. Inorg. Nucl. Chem., 31, 3387 (1969).

64. G.E. Boyd and Q.V. Larson, J. Amer. Chem. Soc., 92, 254 (1968).

65. T. Andersen and K. Olesen, Trans. Faraday Soc., 61, 781 (1965).

66. T. Andersen, H.E. Lundager Madsen and K. Olesen, Trans. Faraday Soc., 62, 2409 (1966).

67. T. Andersen, E. Christensen and K. Olesen, Trans. Faraday Soc., 62, 248 (1966).

68. K.E. Collins, Reference 8, I, p. 421.

69. T. Andersen and A.G. Maddock, Nature, 194, 371 (1962).

70. A.G. Maddock and H. Müller, Trans. Faraday Soc., 56, 509 (1960).

71. R.F.C. Claridge and A.G. Maddock, Trans. Faraday Soc., 57, 1392 (1961).

72. J.C. Machado, R.M. Machado and J.I. Vargas, Reference 8, II, p. 195.

73. K.E. Collins and G. Harbottle, Radiochimica Acta, 3, 21 and 29 (1964).

74. T. Andersen, L. Johansen and K. Olesen, Trans. Faraday Soc., 63. 1730 (1967).

75. C.H.W. Jones, Inorg. Nucl. Chem. Letters, 3, 363 (1967).

76. J. Shankar, K. Venkateswarlu and A. Nath, Reference 7, I, p. 309.

77. J. Shankar, S. Srivastava and R. Shankar, Reference 7, I, p. 393.

78. J. Shankar, V. Thomas and A. Nath, Reference 7, I, p. 383.

79. G. Harbottle and N. Sutin, Adv. Inorg. Nucl. Chem., 1, 267 (1959).

80. L.L. Williams, N. Sutin and J. Miller, J. Inorg. Nucl. Chem., 19,175 (1961).

81. V. Vand, Proc. Phys. Soc. (London), 55, 222 (1943).

82. W. Primak, Phys. Rev., 100, 1677 (1955).

83. K. Yoshihara and G. Harbottle, Radiochimica Acta, 1, 68 (1963).

84. C. Baba, K. Tanaka and K. Yoshihara, Bull. Chem. Soc. Japan, 36, 928 (1963).

85. G. Harbottle, B.L.N. Report 7135 (1963).

86. C.M. Lederer, J.M. Hollander and I. Perlman, Table of Isotopes, Sixth Edition (John Wiley and Sons, Inc., New York, 1968).

87. F.J. Keneshea and M. Kahn, J. Amer. Chem. Soc., 74, 5254 (1952).

88. A. Halpern and R. Sochacka, Reference 7,II, p.223, (1961).

89. Bro. C.J. Cummiskey, W.H. Hamill and R.R. Williams, J. Inorg. Nucl. Chem., 21, 205 (1961).

90. M. Bertet, Y. Chanut and R. Muxart, Radiochimica Acta, 2, 117 (1964).

91. L. Konrad, Radiochimica Acta, 3, 191 (1964).

92. Lj. Jacimovic, J. Stevovic and S.R. Veljkovic, J. Inorg. Nucl. Chem., 27, 29 (1965); Reference 8, II, p. 523.

93. C. Teofilovski, Bull. Boris. Kidrich Instit. Nucl. Sci., 17, 17 (1966).

94. J. Ortega, J. Inorg. Nucl. Chem., 28, 668 (1966).

95. T. Hashimoto, T. Tamai, R. Matsushita and Y. Kiso, Bull. Chem. Soc. Japan, 43, 1093 (1970).

96. A.H.W. Aten, G.K. Koch, G.A. Wesselink and A.M. de Roos, J. Amer. Chem. Soc., 79, 63 (1957).

97. J. Jach, H. Kawahara and G. Harbottle, J. Chromatography, 1, 501 (1958).

98. N.G. Zaitseva and L. Ven-Dzun, Radiochimija, 2, 614 (1960).

99. A.H.W. Aten, M. Lindner-Groen and L. Lindner, Reference 8, II, p. 125.

100. I. Dema and N.G. Zaitseva, Radiochimica Acta, 5, 113 (1966); Ibid., 5, 240 (1966).

101. A.V. Bellido, Radiochimica Acta, 7, 122 (1967).

102. G.A. Dupetit and A.H.W. Aten, Radiochimica Acta, 7, 165 (1967).

103. G.A. Dupetit, Radiochimica Acta, 7, 167 (1967).

104. G.E. Boyd and Q.V. Larson, J. Amer. Chem. Soc., 91, 4639 (1969).

105. Y.-C. Lin and D.R. Wiles, Radiochimica Acta, 13, 43 (1970).

106. G.T. Seaborg, G. Friedlander and J.W. Kennedy, J. Amer. Chem. Soc., 62, 1309 (1940).

107. R.R. Williams, J. Chem. Phys., 16, 513 (1948).

108. R.L. Hahn, J. Chem. Phys., 39, 3482 (1963); Ibid., 41, 1986 (1964).

109. D. Dancewicz and A. Halpern, Nature, 203, 145 (1964).

110. M. Bertet and R. Muxart, Reference 8, II, p. 13.

111. I.s. Kirin, V.M. Zaitsev and V.S. Gusel'nikov, Radiokhimija, 10, 354 (1968).

112. J. Stevovic and R. Muxart, Radiochimica Acta, 9, 76 (1968).

113. A. Halpern and D. Dancewicz, Radiochimica Acta, 11, 31 (1969).

114. R.L. Mössbauer, Soviet Phys. Uspekshi, 3, 866 (1961).

115. H. Lustig, Amer. J. Phys., 29, 1 (1961).

116. F.L. Shapiro, Soviet Phys. Uspekshi, 3, 881 (1961).

117. H. Frauenfelder, The Mössbauer Effect (W.A. Benjamin, Inc., New York, 1962).

118. Chemical Applications of Mössbauer Spectroscopy, V.I. Goldanskii and R.H. Herber, eds. (Academic Press, New York, 1968).

119. V.I. Goldanskii, The Mössbauer Effect and its Application in Chemistry (Consultants Bureau, New York, 1964).

120. The Mössbauer Effect and its Application in Chemistry, R.F. Gould, ed. (American Chemical Society Publications, Washington, D.C., 1967).

121. D.A. O'Connor, Nucl. Instr. Methods, 21, 318 (1963).

122. G.K. Wertheim, Mössbauer Effect: Principles and Applications (Academic Press, New York, 1964).

123. J.C. Slater, Quantum Theory and Atomic Structure, Vol. 2 (McGraw Hill, New York, 1960) p. 92.

124. C.E. Violet and R. Booth, Phys. Rev., 144, 225 (1966).

125. P. Jung and W. Triftshauser, Phys. Rev., 175, 512 (1968).

126. A.M. Babeshkin, E.V. Lamykin, V.A. Lebedev and An. N. Nesmeyanov, Vestn. Mosk. Univ. Khim.,11, 117 (1970).

127. R. Sanders and H. DeWaard, Phys. Rev., 146, 146 (1966).

128. S.L. Ruby and G.K. Shenoy, Phys. Rev., 186, 326 (1969).

129. D.A. Shirley, Rev. Phys. Chem., 20, 25 (1969).

130. M. Pasternak and S. Bukshpan, Phys. Rev., 163, 297 (1967).

131. R. Livingston and H. Zeldes, Phys. Rev., 90, 609 (1953).

132. S. Jha, R. Segnan and G. Lang, Phys. Rev., 128, 1160 (1962).

133. H. DeWaard, G. DePasquali and D. Hafemeister, Phys. Letters, 5, 217 (1963).

134. D. Hafemeister, G. DePasquali and H. DeWaard, Phys. Rev., 135, B1089 (1964).

135. K. Reddy, F. Barros and S. DeBenedetti, Phys. Letters, 20, 297 (1966).

136. Yu. S. Grushko, B.G. Lur'e and A.N. Murin, Soviet Phys., S.S., 11, 1733 (1970).

137. S. Jaswal, Phys. Letters, 19, 369 (1965).

138. W. Flygare and D. Hafemeister, J. Chem. Phys., 43, 789 (1965).

139. M. Pasternak and T. Sonnino, J. Chem. Phys., 48, 1997 and 2004 (1968).

140. S. Bukshpan, C. Goldstein, J. Sonnino and J. Shamir, J. Chem. Phys., 51, 3976 (1969).

141. M. Pasternak, A. Simopoulos and Y. Hazony, Phys. Rev., 140, A1892 (1965).

142. S. Bukshpan, C. Goldstein and T. Sonnino, J. Chem. Phys., 49, 5477 (1968).

143. T.P. Das and E.L. Hahn, Nuclear Quadrupole Resonance Spectroscopy, supplement 1 of Solid State Physics (Academic Press, New York, 1958).

144. R. Bersohn, J. Chem. Phys., 20, 1505 (1952).

145. M.H. Cohen, Phys. Rev., 96, 1278 (1954).

146. N. Bloemberger and P. Sorokin, Phys. Rev., 110, 865 (1958).

147. B.P. Dailey and C.H. Townes, J. Chem Phys., 23, 118 (1955).

148. W. Gordy and W. Thomas, J. Chem. Phys., 24, 439 (1956).

149. C.H. Townes and B.P. Dailey, J. Chem. Phys., 17, 782 (1949).

150. T.P. Das and E.L. Hahn, Reference 143, p. 140.

151. G.K. Wertheim, Phys. Rev., 124, 764 (1961).

152. P.C. Norem and G.K. Wertheim, J. Phys. Chem. Solids, 23, 1111 (1962).

153. G.K. Wertheim, W.R. Kingston and R.H. Herber, J. Chem. Phys., 37, 687 (1962).

154. G.K. Wertheim and R.H. Herber, J. Chem. Phys., 38, 2106 (1963).

155. J. G. Mullen, Phys. Rev., 131, 1410 (1963).

156. A.J. Bearden, P.L. Mattern and T.R. Hart, Rev. Mod. Phys., 36, 470 (1964).

157. Y.K. Lee, P.W. Keaton, E.T. Ritter and J.C. Walker, Phys. Rev. Letters, 14, 957 (1965).

158. D.A. Goldberg, P.W. Keaton, Y.K. Lee, L. Madansky and J.C. Walker, Phys. Rev. Letters, 15, 418 (1965).

159. G.K. Wertheim and H.J. Guggenheim, J. Chem. Phys., 42, 3873 (1965).

160. R. Ingalls and G. DePasquali, Phys. Letters, 15, 262 (1965).

161. V.G. Bhida and G.K. Shenoy, Phys. Rev., 143, 309 (1966).

162. C.J. Coston, R. Ingalls and H.G. Drickamer, Phys. Rev., 145, 409 (1966).

163. V.G. Bhida and G.J. Shenoy, Phys. Rev., 147, 306 (1966).

164. V.G. Bhida and M.S. Multani, Phys. Rev., 149 289 (1966).

165. R. Ingalls, C.J. Coston, G. DePasquali and H.G. Drickamer, J. Chem. Phys., 45, 1057 (1966).

166. J.M. Friedt and J.P. Adloff, Paper submitted at 4th International Hot-Atom Chemistry Symposium, Koyoto, Japan (October, 1967).

167. K.J. Ando, W. Kuendig, G. Constabaris and R.H. Lindquist, J. Phys. Chem. Solids, 28, 2291 (1967).

168. J. Fenger and K.E. Siekierska, Radiochimica Acta, 10, 172 (1968).

169. J.M. Friedt and L. Asch, Radiochimica Acta, 12, 208 (1969).

170. R. Jogannathan and H. Mathur, J. Inorg. Nucl, Chem., 31, 3363 (1969).

171. W. Triftshauser and D. Schroeer, Phys. Rev., 187, 491 (1969).

172. V.I. Belyakov, A.V. Kalyamin, B.G. Lur'e, L.A. Marshak, A.N. Murin and S.B. Tomilov, Fiz. Tverd. Tela, 11, 3600 (1969).

173. A.N. Murin, S.I. Bondarevskii and P.O. Seregin, Radiokhimija, 11, 474 (1969).

174. J.M. Friedt, J. Inog. Nucl. Chem., 32, 431 (1970).

175. K. Henning and K. Yung, Phys. Stat. Sol., 40, 365 (1970).

176. An. A. Nesmeyanov, A.M. Babeshkin, N.P. Kosev, A.A. Bekker and V.A. Lebedev, Reference 8, II, p. 419.

177. R.H. Herber and H.A. Stocker, Reference 8, II, p. 403.

178. P. Hannaford, C.J. Howard and J.W.G. Wignall, Phys. Letters, 19, 257 (1965).

179. An.N. Nesmeyanov, A.M. Babeshkin, A.A. Bekker and V. Fano, Radiokhimija, 8, 261 and 264 (1966).

180. A.M. Babeshkin, A.A. Bekker, An. N. Nesmeyanov, P.B. Fabrichnyi and K.V. Pokholok, Radiokhimija, 10, 752 (1968).

181. T. Andersen, "Experimental Investigations of Chemical Effects Associated with Nuclear Transformations in Some Inorganic Solids," Report of Institute of Chemistry, University of Aarhus, Denmark (1967).

182. A.M. Babeshkin, A.A. Bekker, E.N. Efrenov and An. N. Nesmeyanov, Vestu. Mosk, Univ., Khim., 24, 40 (1969).

183. H. Yoshida and R.H. Herber, Radiochimica Acta, 12, 14 (1969).

184. S.L. Ruby and R.E. Holland, Phys. Rev. Letters, 14, 591 (1965).

185. D.W. Hafemeister and E.B. Shera, Phys. Rev. Letters, 14, 593 (1965).

186. D. Seyboth, F.E. Obenshain and G. Czjzek, Phys. Rev. Letters, 14, 954 (1965).

187. V.A. Lebedev, A.M. Babeshkin, An. N. Nesmeyanov and E.V. Lamykin, Vestn. Mosk. Univ., Khim., 24, 45 (1969).

188. J.F. Ullrich, "^{125}Te Mössbauer Effect Study of Radiation Effects and Magnetic Hyperfine Interactions in Tellurium Compounds," Ph.D. Thesis, University of Michigan (1967).

189. A.G. Maddock, Private Communication.

190. G.J. Perlow and M.R. Perlow, J. Chem. Phys., 45, 2193 (1966).

191. G.J. Perlow and M.R. Perlow, Reference 8, II, p. 443.

192. M. Pasternak, Symp. Faraday Soc., 1, 119 (1967).

193. M. Pasternak and S. Bukshapan, Phys. Rev., 163, 297 (1967).

194. J. Fink and P. Kienle, Phys. Letters, 17, 326 (1965).

195. C.G. Jacobs and N. Hershkowitz, Phys. Rev. B, 1, 839 (1970).

196. P. Rother, F. Wagner and U. Zahn, Radiochimica Acta, 11, 203 (1969).

197. Y. Hazony and R.H. Herber, J. Inorg. Nucl. Chem., 31, 321 (1969).

198. A.R. Champion, R.W. Vaughan and G.H. Drickamer, J. Chem. Phys., 47, 2583 (1967).

199. A.R. Champion and G.H. Drickamer, J. Chem. Phys., 47, 2591 (1967).

200. L.F. Audrieth, Inorganic Synthesis Vol. III, 143 (1950).

201. R. Ripan, N. Calu and G. Tantu, Chem. Analyt. (Paris), 47, 299 (1965).

202. W.A. Dutton and W.C. Cooper, Chem. Rev., 66, 657 (1966).

203. J. Rosicky, J. Loub and J. Pavel, Zeit. Anorg. Allgem. Chem., 334, 312 (1965).

204. O.N. Breusov, O.T. Vorob'eva, N.A. Druz, T.V. Rozuma and B.N. Sobodeva, Izv. Adak. Nauk SSSR, Neorgan Materialy, 2, 308 (1966).

205. V.J. Loub, Zeit. Anorg. Allgem. Chem., 362, 98 (1968).

206. V.G. Jander and F. Kienbaum, Zeit. Anorg. Allgem. Chem., 316, 40 (1962).

207. N.E. Erickson and A.G. Maddock, J. Chem. Soc. (A), 1665 (1970).

208. H. Siebert, Zeit. Anorg. Allgem. Chem., 301, 11 (1959).

209. B.M. Gordon, J. Inorg. Nucl. Chem., 29, 287 (1967).

210. E. Montignie, Z. Anorg. Allgem. Chem., 252, 111 (1943).

211. F. Feher, Handbook of Preparative Inorganic Chemistry, Vol. I, G. Brauer, ed. (Academic Press, Inc., New York, 1963) p. 449.

212. J. Zemann, Z. Kristallography, 127, 319 (1968).

213. F. Feher, Reference 211, p. 444.

214. P.J. Hondra and Z. Jovic, J. Chem. Soc. (A), 600 (1968).

215. M.L. Unland, J. Chem. Phys., 49, 4514 (1968).

216. T.C. Gibb, R. Greatrex, N.N. Greenwood and A.C. Sarma, J. Chem. Soc. (A), 212 (1970).

217. K.W. Bagnall, Chemistry of Se, Te, Po (Elsevier Publishing Company, Amsterdam, 1966).

218. A.J. Stone, Cambridge, England; Program described in Appendix to G.M. Bancroft, A. G. Maddock, W.K. Ong and R.H. Prince, J. Chem. Soc. A, 1971 (1966).

219. C.E. Crouthamel, H.V. Meek, D.S. Martin and C,V, Banks, J. Amer. Chem. Soc., 71, 3031 (1949).

220. R. Livingston and H. Zeldes, J. Chem. Phys., 26, 351 (1957).

APPENDIX I

^{129}I MÖSSBAUER SPECTROSCOPY AS A TOOL FOR STUDYING STRUCTURE IN TELLURIUM COMPOUNDS

Until recently, ^{125}Te Mössbauer absorption spectroscopy was the only direct means for obtaining quadrupole coupling values from which structural information on tellurium compounds could be obtained. This work and the earlier work of Pasternak[193] has shown, however, that detailed structural information can be obtained using ^{129}I emission spectroscopy in which ^{129}Te-labelled tellurium compounds are used as Mössbauer sources and are measured against a standard single line ^{129}I absorber.

Where there are no chemical effects associated with the β^--decay event which populates the Mössbauer transition in ^{129}I in the tellurium source compound, the emission spectrum provides information about the bonding to the iodine atom in a lattice environment iso-structural and iso-electronic with that of the parent tellurium. Since the ^{129}I emission spectra have larger isomer shifts and quadrupole coupling constants, and exhibit narrower line widths than the corresponding ^{125}Te absorption spectra, the interpretation of the spectra should be considerably easier. Moreover, the 8 lines in the ^{129}I quadrupole split spectrum allow the direct determination of the sign of the electrostatic field gradient and the determination of the asymmetry parameter η. These parameters provide

further information about bonding and structure in the tellurium compounds.

To show the validity of using the ^{129}I emission spectra in studying the structure and bonding in tellurium compounds, we may first examine the ratio of the ^{125}Te absorption and ^{129}I emission isomer shifts, $\delta(^{125}Te)/\ \delta(^{129}I)$. From this ratio it is possible to determine the ratio in the change in size of the nuclei in these two Mössbauer transitions. Ruby and Shenoy[128] have measured the isomer shifts for a series of ^{125}Te and ^{129}I-labelled compounds using a standard absorption experiment. They found $\delta(^{125}Te)/\ \delta(^{129}I)$ to be 0.32, and the nuclear radius ratio, ρ, to be +0.31. However, Greenwood et al.[216] were critical of their analysis since it relied on the measurement of δ for tellurium and iodine compounds which in some instances were not iso-structural or iso-electronic. In the present work, the ^{125}Te and ^{129}I isomer shifts were compared for nuclei in the same lattice environments. The isomer shift plot was shown in Figure 21, and from the least squares fit

$$\delta(^{125}Te)/\ \delta(^{129}I) = .29 \pm .03$$

and thus $$\rho = .28 \pm .04$$

Thus the values obtained are in good agreement with those of Ruby and Shenoy, and the error in the determination of that work does not appear to have been significant.

A second parameter of interest is the ratio of the

quadrupole coupling constants for these two nuclei in the same environment. Pasternak and Bukshpan[193] have determined a value for this ratio for ^{125}Te and ^{129}I in equivalent lattice sites in orthorhombic TeO_2 and $Te(NO_3)_4$. From their work it was found that

$$\frac{q_{at}(^{125}Te)Q}{q_{at}(^{129}I)Q}\left(1+\frac{\eta^2}{3}\right)^{1/2} = .40$$

If the values of the present work are taken together with Bukshpan's values, it is found that the above ratio is equal to 0.45 ± .05, again in reasonable agreement with the previously reported value.

The importance of the quadrupole coupling ratio is that it emphasises that the ^{129}I spectra will exhibit much larger quadrupole splittings than the corresponding tellurium spectra. This is well illustrated by the case of monoclinic telluric acid. The ^{125}Te absorption spectrum is a single line. However, the ^{129}I emission spectrum is quadrupole split with a quadrupole coupling constant of $e^2qQ = 192 \pm 5$ Mc.sec.$^{-1}$ On the basis of the above quadrupole coupling ratio and the measured coupling constant for ^{129}I, a quadrupole splitting, $\Delta = \frac{1}{4}e^2qQ\left(1+\frac{\eta^2}{3}\right)^{1/2}$ for ^{125}Te of 1.67 ± .04 mm.sec.$^{-1}$ would be expected. This value is considerably smaller than the theoretical line width for ^{125}Te of 5.32 mm. sec.$^{-1}$, and thus a resolved quadrupole splitting is not observed in this instance.

The application of ^{129}I emission spectroscopy in studying bonding and structure may be best illustrated with reference to some examples.

Pasternak and Bukshpan[193] have previously reported the ^{129}I emission spectrum of orthorhombic TeO_2 while in the present work tetragonal TeO_2 has been studied. While the quadrupole coupling constants and asymmetry parameters are very similar for the two compounds, the isomer shifts of $1.52 \pm .01$ mm.sec.$^{-1}$ for orthorhombic and $2.74 \pm .14$ mm.sec.$^{-1}$ for tetragonal TeO_2 are significantly different. The difference may be explained by a difference in the s-character of the Te-O bonds in the two modifications.

If we assume, on the basis of the large isomer shift, that in tetragonal TeO_2 the bonding is pure p, involving no s-character, then we can calculate the number of holes in the 5p-shell of the daughter iodine, hp, using the expression

$$\delta = 1.5hp - 0.54 \text{ mm. sec.}^{-1} \qquad \text{(VI-4)}$$

This gives a value of hp = 2.2 for the tetragonal form.

The similar quadrupole coupling in the two crystal forms indicates the same value of Up, the p-electron deficit defined by

$$e^2q_{at}Q = -Up\ e^2q_{mol}Q \qquad \text{(VI-6)}$$

If we make the assumption that this, together with the known similarity in co-ordination and geometry, implies similar values for hp in the two modifications, then we can calculate the amount of s-character in the I-O bonds for ^{129}I produced in orthorhombic TeO_2, using the expression

$$\delta = -8.2\ hs + 1.5\ hp - 0.54 \qquad \text{(VI-5)}$$

From this we find that 0.04 s-electrons participate in each I-O bond, this being sufficient to lead to the observed difference in isomer shift from that of the tetragonal form.

The structures shown in Figure 9 for these two crystal modifications are consistent with the above discussion. In the tetragonal form the disposition of bonds must be very close to trigonal bi-pyramidal, but with the in-plane O-Te-O bond angles equal to 90°. This geometry

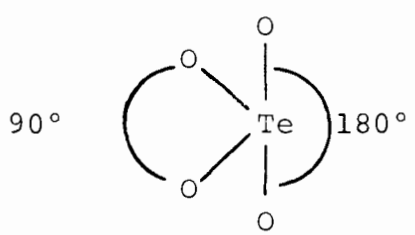

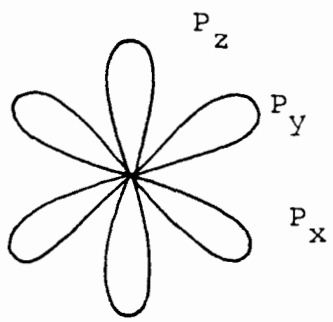

would arise from pure p bonding. In the orthorhombic form, however, the geometry is distorted from the pure p-orbital bond directions due to the presence of edge-bridging in the

polymeric structure. This distortion may arise from the participation of hybrid orbitals in bonding, with a small amount of s-character being involved.

Another study of some interest was that involving $(NH_4)_2TeCl_6$. In the decay of both ^{129}Te- and ^{129m}Te-labelled sources, the ^{129}I spectrum was a single line with a large positive isomer shift of δ = +6.03 mm.sec.$^{-1}$ This was interpreted as evidence for the formation of the ICl_6^- ion, and this is of some interest because compounds of this ion have not previously been synthesised. Experiments of this sort were first performed by Perlow,[191] the radioactive decay serving to synthesise a new molecule, while at the same time populating the Mössbauer transition which provides unique information about the bonding and structure in the new molecule.

The large positive isomer shift in the iodine spectrum in $(NH_4)_2TeCl_6$ indicates a very large $|\psi_s(0)|^2$. This may be explained by the removal of a large number of the 5p-electrons from the I^- configuration of the iodine into the bonding orbitals, the $5s^2$-electrons remaining localised on the iodine. Assuming this model for pure p-bonding, the value of hp may be calculated from the isomer shift and is found to be 4.4. This corresponds to the transfer of 0.73 electrons from the I^- configuration to the Cl ligand for each of the six I-Cl bonds. This value compares well with the values of $0.70e^-$ and $0.68e^-$ for each I-Cl

bond in ICl_2^- and ICl_4^- derived by Perlow,[190] and the values of $0.80e^-$ and $0.75e^-$ calculated recently by Ruby and Shenoy.[128]

The above analysis shows that the bonding in the postulated ICl_6^- ion is quite consistent with the previously proposed nature of the bonding in the known stable iodine-chlorine compounds. The analysis also shows that the linear relationship between isomer shift and hp holds out to a value of hp = 4.4, which is the largest value reported for an iodine compound.

The case of β-TeO_3 is also of interest here. In β-$^{129m}TeO_3$, one single line with an isomer shift corresponding to a value of hp = 5.36 was observed. This must correspond to an extraordinary tellurium parent and iodine daughter compound, in which almost all of the 5p-electrons have been totally removed, leading to a very high value of $|\psi_s(0)|^2$. At this time it is not at all clear what this molecule might be.

The above discussion illustrates the application of ^{129}I Mössbauer emission spectroscopy in studying the bonding and structure of tellurium compounds.